

Utah State University

DigitalCommons@USU

All Graduate Theses and Dissertations

Graduate Studies

5-2016

Crystallization Behavior of Waxes

Sarbojeet Jana
Utah State University

Follow this and additional works at: <https://digitalcommons.usu.edu/etd>



Part of the [Food Science Commons](#), and the [Nutrition Commons](#)

Recommended Citation

Jana, Sarbojeet, "Crystallization Behavior of Waxes" (2016). *All Graduate Theses and Dissertations*. 5088.
<https://digitalcommons.usu.edu/etd/5088>

This Dissertation is brought to you for free and open access by the Graduate Studies at DigitalCommons@USU. It has been accepted for inclusion in All Graduate Theses and Dissertations by an authorized administrator of DigitalCommons@USU. For more information, please contact digitalcommons@usu.edu.



CRYSTALLIZATION BEHAVIOR OF WAXES

by

Sarbojeet Jana

A dissertation submitted in partial fulfillment
of the requirements for the degree

of

DOCTOR OF PHILOSOPHY

in

Nutrition and Food Sciences

Approved:

Silvana Martini, Ph.D.
Major Professor

Marie K. Walsh, Ph.D.
Committee Member

Robert E. Ward, Ph.D.
Committee Member

Cheng-Wei Tom Chang, Ph.D.
Committee Member

Conly Hansen, Ph.D.
Committee Member

Mark McLellan, Ph.D.
Vice President for Research and
Dean of the School of Graduate Studies

UTAH STATE UNIVERSITY
Logan, Utah

2016

Copyright © Sarbojeet Jana 2016

All Rights Reserved

ABSTRACT

Crystallization Behavior of Waxes

by

Sarbojeet Jana, Doctor of Philosophy

Utah State University, 2016

Major Professor: Dr. Silvana Martini

Department: Nutrition, Dietetics, and Food Sciences

Crystallization behavior of different waxes such as beeswax (BW), paraffin wax (PW), ricebran wax (RBW), sunflower wax (SFW) was studied individually and in different oil solutions. Binary mixture at various proportions of the individual waxes was also explored in this study. Soybean oil is used in most of the study but olive, corn, sunflower, safflower, and canola oils were also explored. Lipid crystalline networks were characterized by several physical properties were such as melting profile, solid fat content, viscoelastic parameters, cooling rate, phase behavior, crystal morphology. High intensity ultrasound (HIU) was used to change processing conditions of lipid crystallization. Instruments used to analyze the physical characteristics were differential scanning calorimeter, nuclear magnetic resonance spectroscopy, rheometer, temperature controlled water-bath, turbiscan light scattering device, and polarized light microscopy. The use of high intensity ultrasound showed that HIU technology can be used to delay the phase separation in beeswax/ oil system (canola, corn, olive, safflower, sunflower and soybean oil). Crystal sizes were reduced in beeswax/oil system at 0.5 and 1% concentration with the application of HIU technology. A study on binary waxes showed

different phase behavior: eutectic behavior in BW/PW, SFW/PW, SFW/ BW, and RBW/BW; monotectic behavior in RBW/PW and continuous solid solution in RBW/SFW. Binary waxes in oil system (2.5% binary waxes) showed different physical properties when a range of binary blends were analyzed. Phase diagrams using iso-solid lines in binary wax/oil study show similarity when binary waxes without oil were studied using melting profile data. From all the above study it is understood that the physical properties of wax/oil systems are affected not only by the concentration and type of wax used, but also by the type of oil and application of HIU which induces wax crystallization and retards phase separation in wax/oil systems. Studies performed on all the topics suggest that understanding wax crystallization could help develop product formulation in food, pharmaceuticals, cosmetics, medicine and other industries.

(198 pages)

PUBLIC ABSTRACT

Crystallization Behavior of Waxes

Sarbojeet Jana

Partially hydrogenated oil (PHO) has no longer GRAS status. However, PHO is one of the important ingredients in bakery and confectionary industry and therefore the food industry is seeking for an alternative fat to replace PHO. Waxes have shown promise to fulfill that demand because of its easy availability and cheap in price. Waxes with high melting points ($> 40\text{ }^{\circ}\text{C}$) help in the crystallization process when mixed with low melting point oils. A crystalline network is formed in this wax/oil crystallization process where liquid oil is entrapped in wax crystal network. A new material is formed which is neither completely solid nor completely liquid; it's called semisolid material. This wax/oil semisolid material is formed physically; there are no chemical processes or treatments involved. This material has a potential use in the lipid industry due to its resemblance to the properties of commercial margarine or similar lipids. BW has shown softer crystalline network formation compared to SFW and RBW. It is understood that presence of higher wax ester in SFW and RBW leads to stronger crystalline material formation. Blending waxes of different chemical composition (e.g. BW: wax ester, hydrocarbon, fatty acids, di-esters, hydroxyl esters. RBW: 100% wax ester) shows differences in physical characteristics at different blending proportions. HIU technology helps in delaying phase separation of crystals in low concentration (0.5 and 1% wt. basis) of wax/oil system. Our overall wax crystallization study has shown that there are different physical characteristics of wax/oil semi-solid system based on different

parameters and processing conditions such as wax concentration, wax and oil type, cooling rate, storage temperature, high intensity ultrasound. The hypothesis of this dissertation is that chemical composition of waxes and vegetable oils and also processing conditions affect wax crystallization and physical properties of wax/oil materials.

This dissertation is dedicated to my parents and sister

ACKNOWLEDGMENTS

I am so grateful to Dr. Martini and without whom my PhD would not have been successful. Her ideology, inspiration and impeccable credentials helped me improvise my absolute best in professional life as well as my personal life.

I am so thankful to all of my committee members, Dr. Marie Walsh, Dr. Robert Ward, Dr. Tom Chang, and Dr. Conly Hansen for being supportive and without which, it would have been hardly conducive to getting my PhD. Help and appreciation from my fellow lab mates Yubin Ye, Jiwon Lee, Jeta Kadamne is cordially appreciated. Encouragement and assistance in my entire doctoral program from my parents and other graduate friends would not be forgotten.

Sarbojeet Jana

CONTENTS

| | Page |
|---|------|
| ABSTRACT | iii |
| PUBLIC ABSTRACT | v |
| ACKNOWLEDGMENTS | viii |
| LIST OF TABLES | x |
| LIST OF FIGURES | xi |
| LIST OF ABBREVIATIONS | xvi |
| CHAPTER | |
| 1. INTRODUCTION..... | 1 |
| 2. LITERATURE REVIEW | 9 |
| 3. PHASE SEPARATION IN 0.5% BINARY WAX BLEND IN SOYBEAN OIL..... | 53 |
| 4. EFFECT OF HIGH INTENSITY ULTRASOUND AND COOLING RATE ON THE CRYSTALLIZATION BEHAVIOR OF BEESWAX IN EDIBLE OILS | 65 |
| 5. VISCOELASTIC PROPERTIES OF WAX/OIL CRYSTALLINE NETWORKS | 99 |
| 6. PHASE BEHAVIOR OF BINARY BLENDS OF FOUR DIFFERENT WAXES..... | 107 |
| 7. PHYSICAL CHARACTERIZATION OF CRYSTALLINE NETWORKS FORMED BY BINARY BLENDS OF WAXES IN SOYBEAN OIL | 142 |
| 8. CONCLUSION | 171 |

| | |
|------------------------|-----|
| APPENDICES | 176 |
| CURRICULUM VITAE | 180 |

LIST OF TABLES

| Table | Page |
|---|------|
| 2-1. Wax/oil organogel application in Foods | 12 |
| 3-1. Binary wax blend preparation in different proportions | 55 |
| 4-1. Fatty acid composition of the oils used in this research. Mean values are standard deviation of 2 replicates are reported. Fatty acids present at levels below 0.5% are not reported | 82 |
| 4-2. Onset (T_{on}) and peak (T_p) temperatures of crystals obtained from 0.5% BW and 1% BW crystallized in different edible oils (canola, corn, olive, safflower, sunflower, and soybean) at 0.1 °C/min without and with HIU after 7 days at 25 °C. Mean values and standard deviation of 2 independent runs are reported. NS means that T_{on} or T_p within each BW/oil samples are not significantly different ($\alpha = 0.05$). * means $p < 0.05$; ** means $p < 0.01$, *** means $p < 0.001$ | 94 |
| 6-1. The Mean, Median, and Range of Percentage Agreement Scores for Hank's and Adult Behaviors during the Intervention | 111 |
| 7-1. Melting temperatures (T_p , °C) of binary mixtures used in this study, as reported by Jana and Martini 2016. Two melting values indicate two melting peaks observed..... | 155 |

LIST OF FIGURES

| Figure | Page |
|---|------|
| 1-1. Left top: n-alkane; Left bottom: long chain aliphatic ester; Right top: free fatty acid; Right bottom: aliphatic alcohol | 2 |
| 2-1. Types of phase behaviors observed in materials a: continuous solid solution; b: eutectic; c: monotectic; d: peritectic | 18 |
| 2-2. Crystallization of palm oil after 24 h at 36 °C in solid fat tubes: With 270 W 60 s (left) and without HIU | 30 |
| 3-1. Vial pictures of 0.5% (wt. basis) of BW/PW binary blends (0-100% wt. basis) in SBO stored at 25 °C in an incubator after 7 days..... | 58 |
| 3-2. Vial pictures of 0.5% (wt. basis) of RBW/BW binary blends (0-100% wt. basis) in SBO stored at 25 °C in an incubator after 7 days..... | 59 |
| 3-3. Vial pictures of 0.5% (wt. basis) of RBW/PW binary blends (0-100% wt. basis) in SBO stored at 25 °C in an incubator after 7 days..... | 60 |
| 3-4. Vial pictures of 0.5% (wt. basis) of SFW/BW binary blends (0-100% wt. basis) in SBO stored at 25 °C in an incubator after 7 days..... | 61 |
| 3-5. Vial pictures of 0.5% (wt. basis) of SFW/PW binary blends (0-100% wt. basis) in SBO stored at 25 °C in an incubator after 7 days..... | 62 |
| 3-6. Vial pictures of 0.5% (wt. basis) of RBW/SFW binary blends (0-100% wt. basis) in SBO stored at 25 °C in an incubator after 7 days..... | 63 |
| 4-1. Transmission measurements of 0.5% BW in soybean oil crystallized at 25 °C for 7 days using different cooling rates (0.1, 1 and 10 °C/min) without (left column) and with (right column) HIU. Figures A and B = 10 °C/min, Figures C and D = 1 °C/min, Figures E and F = 0.1 °C/min. Transmission measurements were performed at the bottom of the tube (5-10 mm from the bottom, filled circles), at the middle of the tube (17.5-22.5 mm, filled squares), and at the top of the tube (30-35 mm, filled triangles).The arrow (right column) indicates the moment at which HIU was applied. 100% transmission of light indicates there is no turbidity and 0% transmission indicates that the assay tubes are completely turbid..... | 74 |
| 4-2. Morphology of crystals obtained when 0.5% BW in SBO is crystallized at 25 °C for 7 days at different cooling rates (0.1, 1 and 10 °C/min) without (left column) and with (right column) HIU. Crystal pictures | |

- were taken at 20X magnification under Polarized Light Microscopy.
The white bar corresponds to 50 μm 75
- 4-3. Transmission measurements of 1% BW in soybean oil crystallized at 25 °C for 7 days using different cooling rates (0.1, 1 and 10 °C/min) without (left column) and with (right column) HIU. Figures A and B = 10 °C/min, Figures C and D = 1 °C/min, Figures E and F = 0.1 °C/min. Transmission measurements were performed at the bottom of the tube (5-10 mm from the bottom, filled circles), at the middle of the tube (17.5-22.5 mm, filled squares), and at the top of the tube (30-35 mm, filled triangles). The arrow (right column) indicates the moment at which HIU was applied. 100% transmission of light indicates there is no turbidity and 0% transmission indicates that the assay tubes are completely turbid.....79
- 4-4. Morphology of crystals obtained when 1% BW in SBO is crystallized at 25 °C for 7 days at different cooling rates (0.1, 1 and 10 °C/min) without (left column) and with (right column) HIU. Crystal pictures were taken at 20X magnification under Polarized Light Microscopy. The white bar corresponds to 50 μm 80
- 4-5. Transmission measurements of 0.5% BW in different edible oils crystallized at 25 °C for 7 days using slow cooling rate 0.1 °C/min without (left column) and with (right column) HIU. Figures A and B = canola oil, Figures C and D = corn oil, Figures E and F = olive oil, Figures G and H = safflower oil, Figures I and J = sunflower oil. The arrow shows the time of HIU application i.e.; 300 min after starting the experiment.....84
- 4-6. Transmission measurements of 0.5% BW in different edible oils crystallized at 25 °C for 7 days using slow cooling rate 0.1 °C/min without (left column) and with (right column) HIU. Figures A and B = canola oil, Figures C and D = corn oil, Figures E and F = olive oil, Figures G and H = safflower oil, Figures I and J = sunflower oil. The arrow shows the time of HIU application i.e.; 300 min after starting the experiment.....86
- 4-7. Morphology of crystals obtained when 0.5% BW is crystallized in different edible oils at slow cooling rate (0.1 °C/min) without (left column) and with (right column) HIU after 7 days of storage at 25 °C. Figures A and B = canola oil, Figures C and D = corn oil, Figures E and F = olive oil, Figures G and H = safflower oil, Figures I and J = sunflower oil. Crystal pictures were taken at 20X magnification under Polarized Light Microscopy. The white bar corresponds to 50 μm 91

- 4-8. Morphology of crystals obtained when 1% BW is crystallized in different edible oils at slow cooling rate (0.1 °C/min) without (left column) and with (right column) HIU after 7 days of storage at 25 °C. Figures A and B = canola oil, Figures C and D = corn oil, Figures E and F = olive oil, Figures G and H = safflower oil, Figures I and J = sunflower oil. Crystal pictures were taken at 20X magnification under Polarized Light Microscopy.
The white bar corresponds to 50 μm 92
- 4-9. Mean crystal area (μm^2) of crystals obtained when 0.5% (A) and 1% (B) BW is crystallized in different vegetable oils (canola, corn, olive, safflower, sunflower, and soybean) at 0.1 °C/min after 7 days of storage at 25 °C. Mean values and standard errors are reported. * $p < 0.05$, ** $p < 0.01$, *** $p < 0.001$, NS means non-significant ($\alpha = 0.05$)93
- 5-1. Viscoelastic properties of wax/oil systems crystallized at 1, 2.5, 5, and 10% concentrations (a-d, respectively) after 24 h incubation at 25°C. Within each wax concentration, same letters indicate that values are not significantly different ($\alpha = 0.05$)104
- 6-1. DSC melting profile of binary blends of waxes. Melting profiles for BW/PW, RBW/PW, SFW/PW, SFW/RBW, SFW/BW, and RBW/BW are shown in a, b, c, d, e, and f, respectively. From the bottom to the top lines represent the melting behavior of binary wax mixtures at 10% interval increases of the first component. The first line from the bottom represents the DSC melting profile of the second wax component of the blend (100%) and the top line represents the melting profile of the first wax component of the blend (100%). The dotted line represents 50% of the binary wax blend. Peaks associated with each wax type are indicated with different symbols116
- 6-2. Pseudo-phase diagrams of binary wax blends for BW/PW, RBW/PW, SFW/PW, SFW/RBW, SFW/BW, and RBW/BW in a, b, c, d, e, and f, respectively. The line formed by T_p values (open squares) is called the liquidus line above which everything is liquid. The line formed by T_{on} values (filled circle) is called the solidus line below which everything is solid. There is an intermediate phase formed inside liquidus and solidus line where solid and liquid phases are in equilibrium120
- 6-3. Crystal morphology of binary blends of waxes crystallized at 25 °C (20X magnification) at slow cooling rate (0.5 °C/min).

- The first column shows crystals obtained for 0% of the first wax component. Increasing levels (20, 80 and 100%) of the first component of the mixture is shown in the second, third, and fourth columns, respectively. White bar indicates 50 μ m.....125
- 6-4. Crystal morphology of binary blends of waxes crystallized at 50° C (20X magnification) at slow cooling rate (0.5° C/min). The first column shows crystals obtained for 0% of the first wax component. Increasing levels (20, 80 and 100%) of the first component of the mixture is shown in the second, third, and fourth columns, respectively. White bar indicates 50 μ m.....129
- 6-5. Box-counting fractal dimension (D_b) values obtained for samples crystallized at (a) 25 °C and (b) 50 °C. Columns with the same letter are no significantly different ($\alpha = 0.05$)131
- 7-1. DSC melting profile of 2.5% (wt. basis) binary wax in soybean oil (SBO). Binary wax proportions of 0, 20, 50, 80 and 100% are tested. The first melting curve from the top indicates 0% of the first component in the wax mixture and the bottom curve indicates 100% of the first component in the wax mixture. The 3rd line from the top indicates the 50% of the binary wax. Melting profile of SFW/BW, RBW/BW, and RBW/SFW in SBO are shown in A, B, and C respectively151
- 7-2. Peak melting temperature (T_p), onset melting temperature (T_{on}) and melting enthalpy values are reported in A, B, and C respectively in proportions of 0, 20, 50, 80 and 100%. Columns with same letters indicate that values are not significantly different ($\alpha = 0.05$).....154
- 7-3. Comparison of theoretical (black circle symbol) and experimental (black square symbol) enthalpies for binary wax blends in SBO. The dotted line indicates the linear regression line for experimental enthalpy points. Theoretical and experimental enthalpies of SFW/BW, RBW/BW and RBW/SFW blends in SBO are shown in A, B, and C respectively. Confidence interval (95%) for the experimental data is shown in light dotted hyperbolic lines.....158
- 7-4. Solid Fat Content (SFC) as a function of crystallization temperature for binary wax mixtures in SBO are plotted from temperature-controlled pulse-NMR data. SFC of SFW/BW, RBW/BW, and RBW/SFW blends in SBO are shown in A, B, and C respectively160

- 7-5. Iso-solid lines for the binary mixtures in SBO are drawn using interpolation method from SFC data in Figure 4. Iso-solid lines represent same solid fat content at 0.5, 1, and 1.5%. Iso-solid diagrams of SFW/BW, RBW/BW and RBW/SFW in SBO are shown in A, B, and C respectively.....162
- 7-6. Viscoelastic parameters such as storage modulus (G') and loss modulus (G'') measured at 25 °C after 24 h incubation in a water-bath. Y-axis is represented in \log_{10} scale. Columns with same letters indicate that there is no significance difference among others ($\alpha = 0.05$).....164
- 7-7. Crystal Morphology of 2.5% binary wax in SBO oil at 20X magnification at 25 °C after 24h of sample incubation in a water-bath. All the binary wax in SBO system crystals are arranged from 0% to 100%. White bar indicates 50 μm165
- 7-8. Fractal dimension (D_b) of the crystals is analyzed using Box-plot counting technique at different concentrations at 25 °C. Columns with same letters indicate that there is no significance difference among others ($\alpha = 0.05$).....167

LIST OF ABBREVIATIONS

| | |
|--|--|
| AOCS, American Oil Chemists' Society | RBW, Rice Bran Wax |
| ANOVA, Analysis of Variance | SAFO, Safflower Oil |
| BW, Beeswax | SBO, Soybean Oil |
| CAO, Canola Oil | SFC, Solid Fat Content |
| CO, Corn Oil | SFO, Sunflower Oil |
| DSC, Differential Scanning Calorimetry | SFW, Sunflower Wax |
| G', Storage modulus | TAG, Triacylglycerol |
| G'', Loss modulus | T _c , Crystallization temperature |
| ΔH, Change in Enthalpy | T _{on} , Onset temperature |
| HIU, High Intensity Ultrasound | T _p , Peak temperature |
| NMR, Nuclear magnetic Resonance | |
| OO, Olive Oil | |
| PLM, Polarized Light Microscopy | |
| PW, Paraffin Wax | |

CHAPTER 1

INTRODUCTION

Waxes are classified as lipids because they are non-polar and soluble in organic solvents. Throughout time, waxes have been utilized in various applications: candles, cosmetic products (i.e. lipstick, mascara, moisturizing creams and sunscreens), dental science, rubber tire formulations, dehydrating cheese and food waxing and coating. Waxes are ideal components for these applications since they have high melting points and they self-assemble at room temperature to form crystalline materials. Most wax studies have been performed on paraffin wax (PW) which is composed by a complex composition of hydrocarbons. Paraffin wax is obtained from crude oils where it crystallizes at low temperature where the temperature of the external environment is below the cloud point temperature. Research groups within the world of oil refinery have studied paraffin wax crystallization in great detail [1, 2], but the crystallization behavior of vegetable waxes has not been studied thoroughly. Animal and vegetable waxes have been used as natural, solvent-free and economic sources to replace non-soluble polymers in the pharmaceutical and cosmetic industries. Waxes such as sunflower wax (SFW), beeswax (BW) and rice bran wax (RBW) in particular have gained attention within the food industries given the natural origin of these materials and the possibility of including them in clean-label products. During crystallization, various molecular rearrangements may occur. Such rearrangements result in differing crystalline material properties, such as hardness, viscoelasticity and encapsulation efficiency. Wax composition is particularly complex due to the presence of many different types of molecules. It has been noted that crystalline network formations differ in physical characteristics, depending on the type of

wax being studied. PW is composed of high molecular weight n-alkanes. RBW consists of long chain aliphatic esters. SFW and BW include a mixture of n-alkanes, esters, free fatty acids and aliphatic alcohols. Figure 1-1 represents examples of these classes of molecules present in waxes. The type and content of each of these molecules also leads to differing melting temperatures—90, 85, 74 and 68 °C in RBW, SFW, BW and PW, respectively.

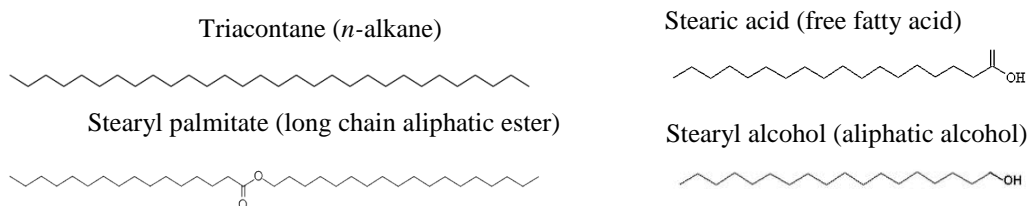


Figure 1-1. Left top: n-alkane; Left bottom: long chain aliphatic ester; Right top: free fatty acid; Right bottom: aliphatic alcohol

No scientific research clearly describes how different molecules in waxes co-crystallize when super-cooled to form crystals. None have discussed the potentially major role inter-molecular forces such as van der Waals forces, hydrogen bonds and London dispersion forces could play in co-crystallization of waxes. Phase diagrams can be used to understand the phase behavior of a system and to evaluate how molecules interact during the crystallization process. A phase diagram shows each phase (solid, liquid, or gas) of the materials studied at equilibrium as a function of temperature, composition and sometimes pressure. This diagram helps to determine total amount of material that can be crystallized under any given condition. Mixtures of pure triacylglycerols [3, 4, 5], fatty

acids [6, 7] and monoacylglycerols [8] were studied using phase diagrams, while pseudo-phase diagrams were reported for confectionery fats, such as cocoa butter and anhydrous milk fat [9, 10].

In 2015, the FDA announced that partially hydrogenated oils with a high content of trans-fats would no longer have GRAS (Generally Recognized as Safe) status [11]. To transform liquid oil to solid at room temperature (25 °C) without hydrogenation, the wax/oil oleogel concept has recently gained popularity. When high wax concentrations (2.5, 5, 10, 15%) are used, a strong crystalline network is formed, with properties similar to those observed in edible shortenings. This resulting material is usually called an oleogel or organogel [12]. Its crystalline network creates a system that is not free-flowing, and hence, an oleogel is neither solid nor liquid and it is considered a semi-solid. It is, therefore, important to understand the crystallization behavior of waxes in order to better predict the physical and functional properties of the oleogels that they form. Previous research on candelilla wax has shown that when this wax is crystallized at low concentrations (1%), some degree of phase separation (crystal sedimentation) is observed, limiting its use as an oleogelator [13]. When higher wax concentrations are used, oleogels or organogels [14] are formed. Research [6] has shown that a wax's chemical composition acts as a leading predictor of the changes in physical properties of wax/oil system. The physical properties of waxes, including hardness, viscoelasticity, smoothness and encapsulation efficiency, are driven by each wax's molecular composition and the molecular interactions that occur during crystallization. As high melting point materials ($T_m = 50\text{--}80\text{ }^\circ\text{C}$) with low solubility in vegetable oils, waxes

crystallize rapidly when placed at room temperature. Even when present at an extremely low concentration (i.e. 0.1%) waxes in oil can generate a crystalline material. The formation of oleogels using natural waxes was first reported by the Toro-Vazquez group [15-21], which used candelilla wax to form an oleogel in safflower oil. Those research groups have analyzed the physical characteristics of wax/oil systems by using varying wax and oil combinations.

Based on the current knowledge related to wax crystallization the overall goal of this dissertation is to cast light on the roles that molecular entities present in waxes, the types of oil used and processing conditions affect wax crystallization and the physical properties of the materials obtained thereby.

Hypothesis

Chemical composition of waxes and vegetable oils and processing conditions affect wax crystallization and the physical properties of the materials obtained.

The specific objectives to test the hypothesis are:

Objective 1:

Objective 1a: Evaluate the crystallization behavior of beeswax (BW) in different vegetable oils (canola, corn, olive, safflower, sunflower and soybean oil), as affected by cooling rate (0.1, 1, and 10°C/min) and wax concentration (0.5 and 1%)

Objective 1b: Evaluate the effect of high-intensity ultrasound on wax crystallization and phase separation.

Objective 2:

Characterize the viscoelastic properties of three waxes of different chemical composition (sunflower oil wax, beeswax and paraffin wax) in different vegetable oils (soybean, canola, corn, sunflower, safflower and olive oil) at concentrations relevant for food applications (1, 2.5, 5, and 10%).

Objective 3:

Study phase behavior of binary systems using blends of four waxes: paraffin wax/beeswax (PW/BW), paraffin wax/rice bran wax (PW/RBW), paraffin wax/sunflower wax (PW/SFW), rice bran wax/beeswax (RBW/BW), rice bran wax/sunflower wax (RBW/SFW) and sunflower wax/beeswax (SFW/BW) in different proportions, from 0-100% in 10% intervals.

Objective 4:

Study the physical characterization of crystalline networks formed by the binary blends of waxes (2.5% of SFW/BW, RBW/BW and RBW/SFW) in soybean oil.

References

1. Rhodes, F.H.; Mason, C.W.; Sutton, W.R. Crystallization of Paraffin Wax. *Ind. Eng. Chem.*, 1927, 19 (8), pp 935–938.
2. Edwards, R.T. Crystal Habit of Paraffin wax. *Ind. Eng. Chem.*, 1957, 49 (4), pp 750–757.

3. Knoester M, De Bruijne P, Van Den Tempel M (1972) The solid–liquid equilibrium of binary mixtures of triglycerides with palmitic and stearic chains. *Chem Phys Lipids* 9:309–319.
4. Takeuchi M, Ueno S, Flöter E, Sato K (2002) Binary phase behavior of 1, 3-distearoyl-2-oleoyl-sn-glycerol (SOS) and 1, 3-distearoyl-2-linoleoyl-sn-glycerol (SLS). *J Am Oil Chem Soc* 79:627–632.
5. Takeuchi M, Ueno S, Sato K (2003) Synchrotron radiation SAXS/WAXS study of polymorph-dependent phase behavior of binary mixtures of saturated monoacid triacylglycerols. *Cryst Growth Des* 3:369–374.
6. Hwang HS, Kim S, Singh M, Winkler-Moser JK, Liu SX (2012) Organogel formation of soybean oil with waxes. *J Am Oil Chem Soc* 89:639–647.
7. Koch JR, Hable GJ, Wrangell L (1938) Melting point studies of binary and trinary mixtures of commercial waxes. *Ind Eng Chem Anal Ed* 10:166–168.
8. Craven RJ, Lenki RW (2011) Binary phase behavior of diacid 1, 3-diacylglycerols. *J Am Oil Chem Soc* 88:1125–1134.
9. Timms RE (1984) Phase behavior of fats and their mixtures. *Prog Lipid Res* 23:1–38.
10. Timms RE (1981) Phase behavior of fats and mixtures of fats. Oral Presentation at Palm Oil Research Institute of Malaysia.
11. The FDA takes step to remove artificial trans fats in processed foods. Last Access: July 9th 2015.

<http://www.fda.gov/NewsEvents/Newsroom/PressAnnouncements/ucm451237.htm>).

12. Dassanayake, L. S.; Kodali, D. R.; Ueno, S. Formation of oleogels based on edible lipid materials. *Curr. Opin. Colloid Interface Sci.* 2011, 16, 432–439.
13. Toro-Vazquez, J. F.; Morales-Rueda, J. A.; Dibildox-Alvarado, E.; Charo-Alonso, M.; Alonzo-Macias, M.; Gonzalez-Chavez, M. M. Thermal and textural properties of organogels developed by candelilla wax in safflower oil. *J. Am. Oil Chem. Soc.* 2007, 84, 989–1000.
14. Dassanayake, L. S.; Kodali, D. R.; Ueno, S. Formation of oleogels based on edible lipid materials. *Curr. Opin. Colloid Interface Sci.* 2011, 16, 432–439.
15. Toro-Vazquez, J. F.; Morales-Rueda, J. A.; Dibildox-Alvarado, E.; Charo-Alonso, M.; Alonzo-Macias, M.; Gonzalez-Chavez, M. M. Thermal and textural properties of organogels developed by candelilla wax in safflower oil. *J. Am. Oil Chem. Soc.* 2007, 84, 989–1000.
16. Morales-Rueda, J. A.; Dibildox-Alvarado, E.; Charo-Alonso, M. A.; Toro-Vazquez, J. F. Rheological properties of candelilla wax and dotriacontane organogels measured with a true-gap system. *J. Am. Oil Chem. Soc.* 2009, 86, 765–772.
17. Morales-Rueda, J. A.; Dibildox-Alvarado, E.; Charo-Alonso, M. A.; Weiss, R. G.; Toro-Vazquez, J. F. Thermo-mechanical properties of candelilla wax and

- dotriacontane organogels in safflower oil. *Eur. J. Lipid Sci. Technol.* 2009, 111, 207–215.
18. Toro-Vazquez, J. F.; Alonzo-Macias, M.; Dibilidox-Alvarado, E.; Charo-Alonso, M. A. The effect of tripalmitin crystallization on the thermomechanical properties of candelilla wax organogels. *Food Biophys.* 2009, 4, 199–212.
19. Toro-Vazquez, J. F.; Morales-Rueda, J.; Mallia, V. A.; Weiss, R. G. Relationship between molecular structure and thermo-mechanical properties of candelilla wax and amides derived from (R)-12hydroxystearic acid as gelators of safflower oil. *Food Biophys.* 2010, 5, 193–202.
20. Chopin-Doroteo, M.; Morales-Rueda, J. A.; Dibilidox-Alvarado, E.; Charo-Alonso, M. A.; de la Peña-Gil, A.; Toro-Vazquez, J. F. The effect of shearing in the thermo-mechanical properties of candelilla wax and candelilla wax-tripalmitin organogels. *Food Biophys.* 2011, 6, 359–376.
21. Alvarez-Mitre, F. M.; Morales-Rueda, J. A.; Dibilidox-Alvarado, E.; Charo-Alonso, M. A.; Toro-Vazquez, J. F. Shearing as a variable to engineer the rheology of candelilla wax organogels. *Food Res. Int.* 2012, 49, 580–587.

CHAPTER 2

LITERATURE REVIEW

Introduction

The literature review will provide an overview of the recent trends in wax crystallization mostly related to wax/oil systems. The basic lipid crystallization behavior and functional properties will be discussed.

Removal of partially hydrogenated oil from foods

Most vegetable oils such as soybean, safflower, canola, corn are liquids at room temperature (25 °C). Those oils can be transformed by partial hydrogenation into a semi-solid at room temperature. Solid or semi-solid fats are popular among food producers since they provide better functional properties to foods. However, due to the negative health effects of *trans*-fats and the elimination of GRAS status by the FDA (2015), scientists are exploring new technologies and processes that can make liquid oil solid at room temperature without the ill presence of *trans*-fat. Gelation has gained popularity due to its solid-fat functionality, where a low molecular weight compound can self-assemble upon cooling and form a crystalline network that will entrap oil, so that the system will behave as a semi-solid material. According to Humphrey et al. [1], oleogels are semi-solid materials where a gelling molecule dissolved in a liquid phase aggregates by self-assembly or crystallization. When the liquid is an organic solvent, the gel is called organogel. Similarly, if the liquid is oil, the gel is called oleogel. The solid component or gelling molecule is often referred to as the gelator. In the study of wax/oil systems, the

commonly used term is oleogel and in these systems, wax is the solid-like component or gelator that arrests the free flow of oil.

There are two major routes used to structure organic solvents and especially edible oils [2, 3]. The first technique uses a dispersed foreign phase such as small inert particles, crystallized solids, or separated droplets to form a network that entraps oil. The second technique includes self-assembly molecular interactions, generally observed with low-molecular weight organogelators. These molecular interactions include covalent, electrostatic, steric, van der Waals, or hydrogen-bonding. Several compounds [4] can be used for oil gelation such as waxes, fatty acids [5], fatty alcohols [6], mono- and diacylglycerols [7], ceramides [8], 12-hydroxystearic acid [9-12], and binary systems such as β -sitosterol + oryzanol [13], fatty acids + fatty alcohol, lecithin + sorbitol esters [14] and even polymer ethyl cellulose [15]. Crystallization behavior of fatty acids is the main oil structuring route for the gel formation, but aggregation of tubules [16] is also another method to form gel. Bot et al. [16] have shown that a binary mixture of γ -oryzanol + β -sitosterol can self-assemble to form tubules, and the tubules then aggregate to form transparent gel in triglyceride oils [17]. The structuring of oil involves crystallization of lipids and thus phase changes are a major concern. Wright et al. emphasized the importance of phase behavior when dealing with crystallization of lipids. Previous studies with different molecular compounds have shown that low molecular weight compounds (LMW) [18] are the best to be used as gelators.

Recent studies confirm that acute post prandial [19] and long-term serum triacylglycerol levels are directly connected to the type of fat in diet [20]. It is therefore

needed to normalize or decrease serum-free fatty acid levels to reduce the risk for chronic diseases [21]. Substitution of saturated and *trans*-fats by edible liquid oils may decrease the incidence of many of these chronic diseases [21, 22]. Hughes et al. [23] showed that mean post prandial serum triacylglycerol levels are significantly lower for organogel than for butter and margarine, but that canola oil shows a small increase. The same trend is observed for mean post prandial serum-free fatty acid levels. The same group of researchers [23] also found that a binary mixture of sitosterol and oryzanol (< 2% in weight basis) in edible oils and organogels demonstrated the ability to protect part of their components through the early stages of the human digestive process. These new studies show the potential of using oleogels as healthier lipid sources and should also be engaged in further evaluation of the nutritional potential of organogels.

Different types of wax-oleogel depending on wax and oil

Waxes have been used in pharmaceutical, cosmetic, and food industries [24-28] due to the ability to self-assemble at room temperature to form crystalline materials. The physical properties of waxes such as hardness, viscoelasticity, smoothness, and encapsulation efficiency are driven by the molecular compositions and molecular interactions that occur during crystallization. In particular, the food industry has traditionally used waxes such as candelilla wax as edible coatings to improve shelf life of fruits and vegetables [29]. In addition, waxes such as carnauba, candelilla, beeswax, paraffin, montan, and various hydrocarbon waxes have been used to formulate ionic and non-ionic micro-emulsions to be used as edible coatings [30]. Other uses of natural waxes

include the use of jojoba wax as a food additive [31] and of carnauba wax to microencapsulate flavors [32].

Natural waxes are composed of several different molecular entities, such as esters of long-chain aliphatic alcohols and long-chain fatty acids, n-alkanes, free fatty acids, and free long-chain alcohols. Table 2-1 shows recent studies that evaluate food applications of wax/oil systems. All these studies have used wax/oil blends to replace margarine-type ingredients in a food product.

Table 2-1. Wax/oil organogel application in Foods:

| No. | Citations | Formulation | Food Product Use |
|------------|--------------------|---|---------------------------------------|
| 1 | Yilmaz et al. [45] | Sunflower wax (3%, 7% and 10%) + Olive oil And Beeswax (3%, 7% and 10%) + Olive oil | Breakfast Margarine |
| 2 | Botega et. al [46] | Rice bran wax (10%) + Sunflower oil | Solid Fat in Ice cream |
| 3 | Jang et al. [47] | Candelilla wax (3 – 6%) + Canola oil | Shortening in Baked goods |
| 4 | Patel et al. [48] | Shellac (2%) + Sunflower oil And emulsion in 20% water | Spreads, chocolate paste and cakes |
| 5 | Yilmaz et al. [49] | Sunflower wax + hazelnut oil | Cookies |

| And Beeswax + hazelnut oil | | | |
|----------------------------|--------------------|--------------------------------------|-----------------------------------|
| 6 | Öğütçü et al. [50] | Carnauba wax (3%) + Virgin Olive oil | Breakfast margarine-like products |

For example, rice bran wax is composed almost 100% esters, whereas beeswax is composed of esters, n-alkanes, diesters, and free acids. Crystallization of paraffin wax in crude oil pipeline is a common phenomenon in the petroleum industry. This phenomenon gave birth to the idea that saturated hydrocarbons can form a gel with other hydrophobic solvents [33]. Then scientists in the food industry began making food grade oils (e.g., safflower oil, soybean oil, olive oil, etc.) as a semi-solid system at room temperature by incorporating food grade waxes such as beeswax, candelilla wax, or carnauba wax. Toro-Vazquez et al. [34] studied candelilla wax (2% wt. basis) in safflower oil; Dassanayake et al. [35] studied rice bran wax in olive oil, rice bran wax and carnauba wax in liquid oils [olive oil and salad oil (canola: soy bean oil = 50:50)]; Hwang et al. [36] studied sunflower wax in soybean oil, and similar wax-based organogels have been studied as well [37-44]. All these studies involved different wax/oil combinations and focused on major physical characteristics of gelation properties, e.g., cooling rate, thermal properties of wax and oil, microstructure, solid fat content, rheological properties, and storage temperature. In general, these wax-based organogel studies showed that gelation occurred when at least 2.5 - 10% wt. basis of waxes in oil is used. When higher wax concentrations are used, a stronger crystalline network is formed with properties similar to those observed in edible shortenings. However, there are still concerns about the organoleptic

properties of these materials, such as waxy mouth feel, when dealing with these high concentrations of waxes in oils. It is not possible to understand the gelation properties by only analyzing one characteristic. One must study all the properties combined to get an overall picture how these semi-solid systems work. In the future, a mathematical modelling of different wax/oil systems could help interpret a better system for any specific product formulation.

Phase behavior of lipids and their blends

Phase behavior refers to a phase change in a material with respect to temperature or pressure. Phase diagrams are plots that shows phase equilibrium of any particular substance under specific thermodynamic conditions such as temperature, pressure, volume, or mass [51]. This plot helps formulate different products irrespective of the field of research. In lipid science, a phase diagram is always needed to formulate products like chocolate using cocoa butter, milk fat, cocoa butter replacers and cocoa butter substitutes [52]. Phase diagrams are constructed for pure components but when the components are not categorized as pure, such as natural fats the same phase diagram is usually referred to as pseudo-phase diagram. With the rapid growth of research engaged in wax/oil system study, pseudo-phase diagrams could depict a clear picture in identifying crystallization behavior of wax blends.

Pseudo-phase diagrams have become an important tool in the confectionery industry for identifying fats that are compatible with cocoa butter and it will not form eutectics [5, 13]. A eutectic system describes a homogeneous mixture of different chemical

constituents where there is a mutual freezing point. That point is called as eutectic point and a eutectic point describes a unique temperature for solidus and liquidus lines.

Eutectic formation between fats and cocoa butter result in a softer material that significantly affects product quality and shelf life. Wright et al. [53] studied preliminary phase behavior of vegetable oil-based organogel using ricinoleic acid (12-hydroxy-9-trans-octadecenoic acid, REA); and they showed different phases such as fat-like, non-transparent gel, thick liquid and liquid. Chen et al. [54] had shown DSC phase diagram of monoglycerides-C18/hazelnut oil system. Experimental phase diagram of a blend of two lipid molecules can be drawn from the melting behavior of the material by calculating melting onset (T_{on}) and peak temperatures (T_p). These values are usually plotted against composition. A common practice in the lipid industry is to mix different fats to obtain shortenings with specific physical and functional properties.

Therefore, it is more useful to study phase transition of mixtures of bulk fats rather than pure molecules. These diagrams can be also plotted using iso-solid lines where temperatures at which the samples have the same solid fat content (SFC) are plotted against composition.

Different types of phase behaviors exist depending on the melting points of molecules. These types of behaviors include monotectic, eutectic, peritectic, and continuous solid solution system (Figure 2-1). A continuous solid solution is formed when two pure components have similar melting points. Figure 2-1 shows the types of phase behaviors observed in materials, where A = pure component, B = another pure component (\neq A) that melts at a higher temperature than A, L = liquid solution, S = solid

solution, S_A = solid solution rich in component A, S_B = solid solution rich in component B, Liquidus Line = the temperature boundary line above which a component is completely liquid (L). This line is also interpreted as the maximum thermodynamic equilibrium temperature at which crystals can co-exist. Finally, the solidus line is the temperature boundary line below which a component is completely solid (S). Figure 2-1a shows a phase diagram describing a solid solution system of two pure components. When A and B are mixed in different proportions, they co-crystallize forming a solid solution where the composition of the solid obtained does not vary with changes in the compositions of the components. This is the simplest phase diagram. L + S indicates the solid and liquid coexistence with respect to the composition. In this case, none of the components can crystallize as a pure component and a freezing point depression is not observed.

Figure 2-1b shows a typical phase diagram for components that display eutectic behavior. The section of the diagram that contains $L+S_A$ indicates a zone where a liquid is in equilibrium with a solid solution rich in component A. Similarly, $L+S_B$ means that the liquid is in equilibrium with a solid rich in component B.

When two different components with different chemical compositions are mixed, two different liquidus lines are formed and the eutectic point is where those two liquidus lines meet each other. This point is also considered the result of mutual freezing point depression between two components [58]. This phase diagram also shows a horizontal line touching the eutectic point which is called the eutectic boundary line. This eutectic boundary line signifies the mutual solidus line for both the components. The interesting

thing about the eutectic point is that the solid and liquid phase of both components comes to one single temperature at corresponding composition mixtures of the components.

Figure 2-1c shows a phase diagram of two components that show a monotectic behavior. Generally, this type of behavior is observed if there is a big difference in melting temperatures of the two pure components. In this system, when the binary liquid is cooled, the solid portion of the higher melting component starts crystallizing (S_B). If the cooling is continued, the liquid solution will be maximally enriched with S_B , so S_B becomes predominant in the binary liquid solution.

Figure 2-1d shows the phase diagram of a peritectic system. This type of behavior is very rare and complex but exists mostly in mixed saturated and unsaturated systems [56]. This system looks like a eutectic system with the formations of $L+S_A$ and $L+S_B$, and with S_A+S_B below the eutectic boundary line (as in Figure 2-1b), but in this case there is no eutectic point.

Solid solutions were reported by Timms [56] for binary TAGs (triacylglycerol): POSt/StOSt and StStSt/StStE where P: palmitic acid, O: oleic acid, St: stearic acid, E: elaidic acid. In general, monotectic systems are formed when the melting/boiling points of the binary system are higher than the melting/boiling points of any of the pure components. Timms et al. [56] reported that TAGs (PPP/ StOSt and PPP/POP) with melting points that differ by 20°C show a monotectic behavior. In the eutectic system, the melting/ boiling point of the system is lower than that of the individual pure components in the solution. In this system, eutectic point shows the same temperature for the solidus

and liquidus line. A similar eutectic behavior was observed in most stable β forms of LLL/MMM TAG binary system reported by Takeuchi et al. [57] and in PPP/StStSt, POST/POP and StOSt/StStO reported by Timms [56] (where L: lauric acid, M: myristic acid, P: palmitic acid, St: stearic acid and O: oleic acid). Peritectic systems are formed when a binary system melts and forms another solid instead of its liquid form. This type of phase behavior generally occurs in a system with a saturated and unsaturated mixture, where at least one TAG has two unsaturated fatty acids [56].

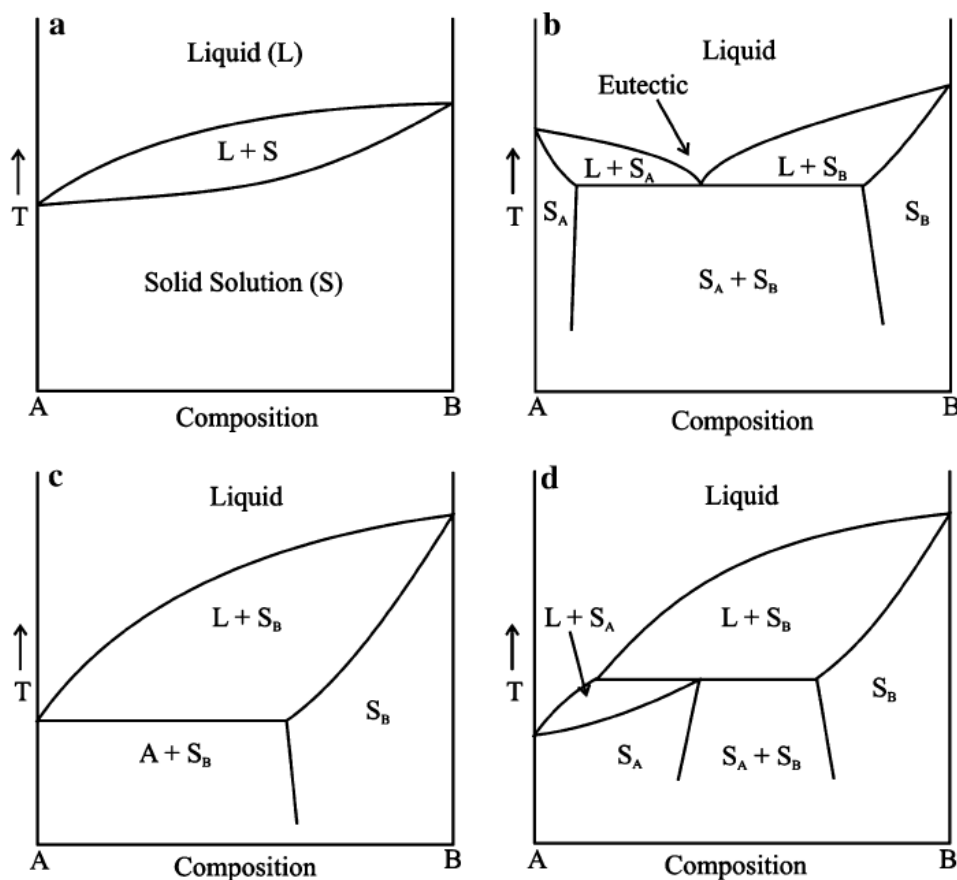


Figure 2-1. Types of phase behaviors observed in materials a: continuous solid solution; b: eutectic; c: monotectic; d: peritectic [59]

The phase behavior of the TAGs in the blend is affected by the crystallization behavior, which in turn depends on the solubility effects of the lipid mixture.

Lipid crystallization

Waxes are high melting point materials ($T_m = 50\text{--}80\text{ }^\circ\text{C}$) and have low solubility in vegetable oils and therefore crystallize rapidly when placed at room temperature. The crystallization behavior and the functional properties of the wax materials and oil type differ significantly due to their different chemical compositions. Crystallization is an important process in lipid-containing foods. The lipid crystal network formation and the size and shape of different lipid crystals determine the physical and functional properties of foods to be developed. For example, a lipid that crystallizes forming smaller crystals leads to harder texture. There are different parameters and conditions driving these structure formations. Lipid crystal structures depend on the type of the lipid, fatty acid distribution, lipid molecule types and purity, as well as crystallization conditions such as temperature, rate of cooling, shear, presence of seeds and solvent. When a TAG molecule crystallizes, the chains align side by side to maximize the interaction of van der Waal forces. In the industry, different physical conditions are mainly maintained to achieve better crystallization. Lipid crystallization is mainly comprised of three steps: super-cooling or super-saturation, nucleation, and crystal growth.

Super-saturation and super-cooling are the two driving forces of crystallization. The difference in isothermal crystallization temperature (T_c) and melting temperature (T_m) is defined as super-cooling ($\Delta T = T_m - T_c$). When T_m is constant in a lipid system as T_c

decreases a high super-cooling is achieved which in turn speeds crystallization. To obtain super-saturation $[\ln(C/C_s)]$, the concentration (C) of the solution should be greater than the saturation concentration (C_s). As either of these driving forces increase, the rate of nucleation increases and the induction time decreases. Induction time is defined as the time required for the first detectable nucleus formation in any solution. The metastable region is an area where stable confrontation of molecules is not formed due to Brownian effects. The energy of interaction among triacylglycerol molecules should be greater than the kinetic energy of the molecules at their melting temperatures to overcome Brownian effects, thus crossing the metastable zone. As super-cooling is increased, stable nuclei are formed at its specific critical size.

The second phase of crystallization, nucleation is classified as either primary or secondary nucleation. Primary nucleation involves a homogeneous or heterogeneous mechanism. Homogeneous nucleation is the formation of a crystal lattice structure based on the accumulation of molecules into a stable shape and size. Heterogeneous nucleation involves a foreign impurity promoting the formation of the nucleus. Secondary nucleation is also called contact nucleation because the nuclei formation occurs because of contact between a crystal and something else, such as another crystal, a stirrer or a solid wall. After nucleation has occurred crystals continue to grow as long as the driving force remains in the system. Crystal growth is affected by the diffusion of TAGs from the bulk solution across a boundary layer, and by the incorporation of TAGs into the crystal lattice of an existing crystal. There are a number of factors governing TAG crystal growth: the degree of super-cooling (driving force), rate of molecular diffusion to the crystal surface

and the time required for TAG molecules to fit into growing crystal lattice. The crystal growth rate and mechanism depends on the nature of the crystal melting interface and structure of the crystal surface [60]. There is a linear relationship between continuous growth and super-saturation (driving force) of the system [60, 61]. Layered growth models (two-dimensional nucleation and spiral growth) are more predominant than smoother surface growth [60, 62]. Martini et al. [63] studied the crystallization behavior of sunflower oil and wax system. They found there is an increase in onset temperature (T_{on}) as T_c increases due to low super-cooling temperature in both fast (20 °C/min) and slow (1 °C/min) cooling systems. This group also found that super-saturation played an important role in wax in oil (sunflower) crystallization. In the overall study, they pointed out that wax crystallization is affected by different experimental parameters such as T_c and cooling rate, and also wax concentration of the sample. With the advent of oleogel research, wax/oil system crystallization should be studied further.

Techniques to characterize physical properties of lipids

Lipid crystalline networks can be characterized by several physical properties such as melting temperature and melting behavior, crystal size, solid fat content, texture, and elasticity. Studying different melting point temperatures gives an overview of the melting behavior of the lipid system. Crystal morphology study provides information on the final crystal size and shapes formed and how this would lead to organoleptic properties in the end food products. Solid fat content (SFC) data provides information about the amount of the sample that is solid at a specific temperature and therefore can be used to measure the melting behavior of the sample. For example, SFC is used to measure the melting

behavior of chocolate at mouth temperature. Rheology measurements provide information about the viscoelasticity of the sample. When dealing with a semi-solid lipid system, turbidity is another property which is observed as well as phase separation due to crystal sedimentation. Processing time and temperature are the prime factors in any experiments in lipid systems, as well as storage temperature and time. Cooling rate is another important experimental variable that must be controlled since it has a direct impact on crystal size and structure. Therefore, it is recommended to verify all the data from different experiments to study any lipid system and connecting all the data with each other. For example, rheology data is connected with crystal morphology. Presented below are some of the recent studies that evaluate these physical properties in TAGs and waxes.

Melting behavior

Lipids are complex materials since they are formed by several hundreds of triacylglycerols (TAGs). Therefore, they crystallize and melt over a wide range of temperatures. While there is no singular melting temperature for these lipids, in general the melting behavior can be quantified by calculating the onset and peak temperature of the melting process [64]. The study of lipids' melting behavior helps us understand some of their functional properties. Differential scanning calorimetry (DSC) is widely used in research laboratories to study the thermal behavior of lipids. The main parameters analyzed by DSC curves are peak temperature (T_p), onset temperature (T_{on}), and enthalpy (ΔH). DSC crystallization curve is influenced by the chemical composition of the sample, and the melting curve is influenced by the initial crystalline state [65]. Melting curve data

is mostly used to interpret thermal profile data of most TAGs [66-70]. The principle of DSC analysis is based on determining heat flow through a sample by simultaneous measurements through a sample pan and an empty reference pan. Melting profile study helps interpret different aspects of the data but most commonly, the amount of solids formed through the melting enthalpy values, phase transition (solid and liquid form) of the crystal network formed as a function of temperature during melting, different temperature of melting of the lipid network, and polymorphism [71-74]. DSC has been used to study the melting behavior of several wax/oil systems. Dassanayake et al. [35] studied melting profiles of ricebran wax, carbauba wax and candellila wax in different oils. Hwang et al. [36] studied melting profiles of sunflower wax, candellila wax and rice bran wax in soybean oil. When studying melting profile of waxes, it is observed that some waxes have more than one melting temperature [75]. The presence of several melting peaks can be explained by looking at the waxes' chemical composition. While pure components are characterized by a single melting point, waxes are complex materials formed by several molecular entities, allowing them to melt over a range of temperatures. Therefore, melting profile study is a required experiment when analyzing wax or wax/oil systems.

Crystal morphology

The texture of any lipid product depends on the microscopic crystal morphology of the finished product. Sensory attributes of lipid-based foods such as spread-ability, mouth feel, and hardness are predetermined by the morphology lipid crystals among other factors [76-79]. The morphology of lipid crystals represents a crystal in a two-

dimensional network (X-Y axis). Fractal dimension technique is often used to quantify the microstructure of lipid crystal networks [80]. Analysis of crystal microstructure provides information about crystal size, number of crystallites, and total crystalline mass [81]. Polarized light microscopy and electron microscopy are mainly used for this two-dimensional morphology study. Crystal morphology depends on different processing conditions of lipids such as cooling rate [82], crystallization temperature [83], high intensity ultrasound [84] or high pressure treatment [85]. Higher agitation and faster cooling rate help form smaller crystals, while larger crystals with broader crystal size distribution are formed at higher crystallization temperature [86]. High intensity ultrasound or high pressure treatment also helps form smaller crystals [84, 85]. Several studies have shown that wax morphology is affected by the type of wax used, the type of oil used and processing conditions. Martini et al. [63] concluded that crystal morphology is affected by T_c and cooling rate, depending on the wax concentration of the sample. Blake et al. [87] showed that 2% of rice bran wax, sunflower wax and candelilla wax in peanut oil forms pallet-like crystal morphology. While Dassanayake et al. [35] reported that rice bran wax in olive and salad oil showed needle-like morphology. Beeswax in rice bran oil shows spherulite type crystal morphology, as reported by Doan et al. [88].

Solid fat content

Solid fat content (SFC) is defined as one of the characteristics of fat which measures percentage of solid parts in fat at different temperatures. SFC can be used to study the compatibility of fats by determining the changes in the percentage of solids at different fat proportions [89, 90]. SFC gives a better understanding of fat crystals when consumed

in mouth and how it melts overtime with the mouth temperature. It provides details about the sensory and organoleptic properties of lipid-based products such as general appearance of the product, ease of packing, spread-ability, oil exudation [91]. In a solid or semi-solid fat sample, SFC is measured based on the ratio of the number of detected protons in solid fat over the total number of detected protons in both solid and liquid phases. NMR is widely used to measure SFC, although there are some new technologies such as ultrasonic spectroscopy and NMR mobile universal surface explorer [92]. An oil with a steeper SFC profile as a function of temperature has a very narrow plastic range; a lipid system with a flat SFC profile has a wide plastic range [93]. SFC profiles are used to design pseudo-phase diagrams using iso-solid lines [94]. Karabulut et al. [95] studied SFC with respect to temperature when comparing the physical properties of fully hydrogenated palm oil stearin (FHPOS), palm oil stearin (POS), canola oil (CO) and cottonseed oil (CSO) mixed in various ratios (w/w). They found that SFCs of the interesterified blends decrease compared to the starting blends, and the interesterified products showed softer rheology than starting blends. When analyzing the physical properties of any lipid system, solid fat content study is recommended for different interpretation.

Viscoelastic properties

Rheology measurements are used as a tool to determine viscoelastic parameters of lipid-based ingredients and final products. These are also helpful for quality control in manufacturing processes, such as mixing, pumping, stirring, filling, and sterilization [97, 98]. Viscoelastic behavior is well described by stress-strain curve where it shows that

viscoelastic materials return to their original shape even after the deforming force been removed.

Three rheological parameters are generally analyzed: storage modulus (G'), loss modulus (G'') and $\tan\delta$ (G''/G'). The term “viscoelastic properties” generally refers to the measurement of these parameters in an oscillatory rheometer. Storage modulus (G') is used to describe the elastic characteristic (solid-like) of a material, meaning that the higher the G' value, the more solid-like behavior is observed. Loss modulus (G'') is used to describe the viscous (liquid-like) behavior of a material, meaning that the higher the G'' value, the more liquid-like behavior is observed. The term $\tan\delta$ represents the ratio of G'' to G' .

$$\tan\delta = G''/G'$$

The domain range of the parameter ($\tan\delta$) varies from infinity (in a perfect liquid system when G' is close to zero) to a very small value (i.e., a high viscosity system) [99].

Viscoelastic properties are dependent on different factors such as cooling and agitation rates, crystallization temperature, chemical composition, and time of storage. Slow cooling rate and decreased agitation rate show higher G' and G'' in lipid samples. Ojijo et al. [100] studied rheological properties of olive oil/monoglyceride gel network. They found that high cooling rate leads to low G' values and that G' increases as monoglyceride content increases. Liang et al. [101] showed that rheological properties were highly correlated with the various quantitative microstructural parameters, with the exception of the fractal dimension by the PCM (particle-counting method) in a model

lipid system (low melting sunflower oil and high melting palm oil mixture). Doan et al. [88] found that rice bran wax, carnauba wax, beeswax, sunflower wax and candelilla wax in rice bran oil have better gelling properties because of higher G' values than G'' in all cases.

Turbidity

Turbidity is the study of transparency, where the liquid phase loses its transparency due to suspended solids. Lecithin organogel with water forms a semisolid non-transparent phase as described by Mezzasalma et al. [102] and similar results have been reported by others [103-107]. Phase separation, or lipid crystal sedimentation, is the phenomenon by which liquid and solid phases separate over time. Hwang et al. [108, 109] described phase separation when organogels of different waxes (sunflower wax, ricebran wax, paraffin wax, and candelilla wax) with soybean oil were studied at different processing conditions (cooling rate, storage temperature, melting temperature). Similar results were reported by Toro-Vazquez et al. [110] when they studied candelilla wax in safflower oil organogel. In the case of wax in oil organogel, phase separation is greatly affected by the concentration of wax, cooling rate, storage temperature and even molecular composition discussed by Patel et al. [111]. They proposed that there could be a link between macroscopic flow/deformation response of gels and microscopic interaction between crystalline aggregates. When samples crystallize, they create a certain amount of turbidity, showing a decrease in the transmission of light. Researchers measure transmission of light through the samples with TurbiScan equipment, and data are

analyzed using computer software (Turbisoft version 1.2.1). This equipment is used to analyze destabilization mechanism of concentrated media.

Processing conditions commonly used to change physical properties of lipids.

Lipid, also has characteristics of physical properties such as mouthfeel, texture, and appearance. The physical properties are dependent on processing conditions such as cooling rate, agitation in the crystallization process, melting temperature, and storage temperature. Novel processing techniques such as high intensity ultrasound can be used to change the processing conditions; which in turn change the physical properties of lipid.

Cooling rate and storage

Changes in physical properties such as crystal morphology can be observed during storage of margarine [112]. Storage temperature and time affect the rheological and morphological properties of the lipid crystal as reported by Toro-Vazquez et al. [113] and Morales-Rueda et al. [114] because they observed that organogel crystals aggregated as a function of storage time, a process that resulted in an increase in organogel hardness. Cooling rate can also affect physical properties of lipids such as crystal size and shape. Hwang et al. [115] concluded that slow cooling rate leads to bigger crystal size compared to fast cooling rate and similar results were confirmed by others [116-120].

High-intensity ultrasound (HIU) use in lipid crystallization

HIU has been used in several fields such as pharmaceutical and chemical [121-134] to structure colloidal particles and provide better delivery systems. HIU has also been

used in the food industry in several processes such as drying, mixing, homogenization and extraction [135-138]. The first solution used for ultrasound application was thio-sulphate solution in 1927. This leads to further research in sono-crystallization in different material systems. Studies have shown that that sono-crystallization can be used to change some physical characteristics of lipids such as texture, viscoelasticity and crystal size [139-142]. Some researchers suggest that the propagation and interaction of sound waves alters the physical and chemical properties of materials [143]. A recent lipid study by Lee et al. [144] confirms that HIU effect does not cause major chemical changes such as oxidation stability (peroxide value measurement). Similar research on sunflower oil suggests that there are no changes in fatty acid composition due to HIU [145]. Thus, the application of HIU in the lipid crystallization study is mainly based on the changes in physical characteristics. Patrick et al. [146] studied the effect of HIU on the crystal structure of palm oil and Ye et al. [148] applied HIU in a commercial shortening to change the crystal microstructure of the system and similar studies were done by other scholars [149-154]. Figure 2-2 shows a study on turbidity where HIU was applied to palm oil in which Chen et al. [147] concluded that HIU delays phase separation. Morphological study on the crystal structures has shown that the crystals in HIU-treated samples are smaller than those not treated with HIU. That study also confirmed that storage temperature has a direct impact on the phase separation.

Overall, this literature review provides a background to understand the rationale behind this research. Phase separation is a problem in creating semi-solids using wax/oil

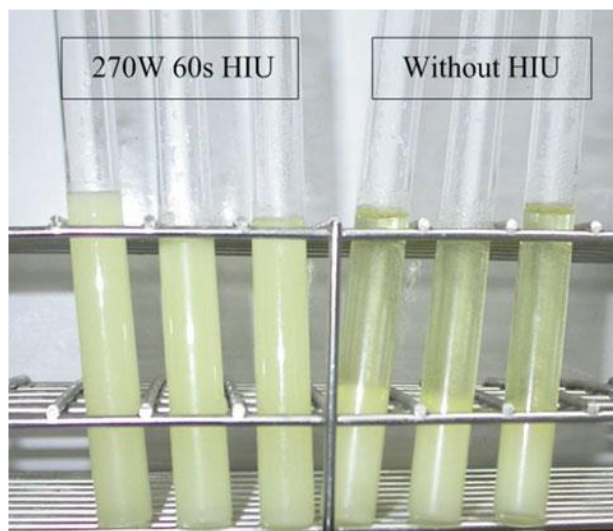


Figure 2-2. Crystallization of palm oil after 24 h at 36 °C in solid fat tubes: With 270 W 60 s (left) and without HIU (right). Phase separation (solid and liquid phase) is observed in the case of without HIU samples [147].

systems with low concentrations of wax. This problem could be solved by using HIU as this technique has shown great promise in palm oil crystallization. It could also be interesting to explore if processing conditions such as cooling rate and storage temperature impact HIU treated samples. In addition, it is not clear if wax/oil systems behave similarly irrespective of oils used. Systematic studies should be performed keeping one type of wax constant and changing the oil types. Similarly, studies should also be done to determine if different waxes change the crystallization behavior when the oil is kept constant. Lastly, evaluation of crystallization behavior of wax mixtures should be performed to optimize the use of these systems in lipid-based product formulation.

References

1. Humphrey, K.L.; Narine, S.S. In *Fat Crystal Networks*; Marangoni, AG; Eds; Marcel Dekker. New York. 2005. Chapter 3, pp 83-90.
2. Perneti, M; Van Malssen, K.F; Flöter, E; Bot, A. Structuring of edible oils by alternatives to crystalline fat. *Current Opinion in Colloid and Interface Science*, 12 (2007), pp. 221–231.
3. Perneti, M; Van Malssen, K.F; Kalnin, D; Flöter, E. Structuring edible oil with lecithin and sorbitan tri-stearate. *Food Hydrocolloids*, 21 (2007), pp. 855–861.
4. Flöter, E. Structuring oils without highly saturated fats – how far are we? *Eur. J. Lipid Sci. Technol.* 2012, 114, 983 – 984.
5. Daniel, J; Rajasekharan, R. Organogelation of plant oils and hydrocarbons by long-chain saturated FA, fatty alcohols, wax esters, and dicarboxylic acids. *Journal of the American Oil Chemists Society*, 80 (2003), pp. 417–421.
6. Murdan, S; Gregoriadis, G; Florence, A. T. Novel sorbitan monostearate organogels. *Journal of Pharmaceutical Sciences*, 88 (6) (1999), pp. 608–614.
7. Rogers, M.A. (2011) Ceramide Oleogels. In: Marangoni AG, Garti N (eds) *Edible oleogels: structure and health implications*. AOCS Press, Urbana, pp 221–234.
8. Rogers, M.A; Smith, A.K; Wright, A.J; Marangoni, A.G. (2007) A novel cryo-SEM technique for imaging vegetable oil based organogels. *J Am Oil Chem Soc* 84(10):899-906.

9. Terech, P; Weiss, R.G. (1997) Low molecular mass gelators of organic liquids and the properties of their gels. *Chem. Rev.* 97:3133–3159.
10. Rogers, M.A; Wright, A.J; Marangoni, A.G. (2008a) Engineering the oil binding capacity and crystallinity of self-assembled fibrillar networks of 12-hydroxystearic acid in edible oils. *Soft Matter* 4:1483–1490.
11. Rogers, M.A; Marangoni; A.G. (2008b) Non-isothermal nucleation and crystallization of 12-hydroxystearic acid in vegetable oils. *Cryst Growth Des* 8:4596–4601.
12. Perneti, M; Van Malssen, K.F; Flöter, E; Bot, A. (2007a) Structuring of edible oils by alternatives to crystalline fat. *Curr. Opin. Colloid Interface Sci.* 12:221–231.
13. Perneti M, van Malssen KF, Kalnin D, Flöter E (2007) Structuring edible oil with lecithin and sorbitan tri-stearate. *Food Hydrocolloids* 21:855–861.
14. Zetzl AK, Marangoni AG, Barbut S (2012) Mechanical properties of ethylcellulose oleogels and their potential for saturated fat reduction in frankfurters. *Food Funct.* 3:327-337. DOI: 10.1039/c2fo10202a.
15. Perneti, M., van Malssen, K.F., Flöter, E. and Bot, A. ‘Structuring of edible oils by alternatives to crystalline fat’, *Current Opinion in Colloid and Interface Science*, 12, 221-231 (2007b).

16. Bot, A., den Adel, R. and Roijers, E.C. 'Fibrils of γ -oryzanol + β -sitosterol in edible oil organogels', *Journal of the American Oil Chemists' Society*, 85, 1127-1134 (2008).
17. Wright, Marangoni (2006) Formation, structure, and rheological properties of ricinelaidic acid-vegetable oil organogels. *J Am Oil Chem Soc* 83:497–503.
18. Te´rech, P; Weiss, R.G. (1997) Low molecular mass gelators of organic liquids and the properties of their gels. *Chem Rev* 97:3133–3159.
19. Harte, A.L; Varma,M.C; Tripathi, G; McGee, K.C; Al-Daghri, N.M; Al-Attas, O.S; Sabico, S; O'Hare, J.P; Ceriello, A; Saravanan, P; Kumar, S; McTernan, P.G. High fat intake leads to acute postprandial exposure to circulating endotoxin in type 2 diabetic subjects. *Diabetes Care*. 2012 vol. 35 no. 2 375-382.
20. Mozaffarian, D; Katan, M.B; Ascherio, A; Stampfer, M.J; Willett, W.C. Trans Fatty Acids and Cardiovascular Disease. *N Engl J Med* 2006; 354:1601-1613.
21. Boden, G; Carnell, L.H. Nutritional effects of fat on carbohydrate metabolism. *Best Practice and Research Clinical Endocrinology and Metabolism*, 17 (2003), pp. 399–410.
22. Woodside, J.V; Kromhout, D. Fatty acids and CHD. *Proceedings of the Nutrition Society*, 64 (2005), pp. 554–564.

23. Hughes, N. E; Marangoni, A.G; Wright, A.J; Rogers, M.A; Rush, J.W.E.
Potential food applications of edible oil organogels. Trends in Food Science &
Technology 20 (2009) 470-480.
24. Hughes, N.E; Marangoni, A.G; Wright, A. J; Rogers. M.A; Rush, J.W.E.
Potential food applications of edible oil organogels. 2009. Trends in Food Science &
Technology 20: 470-480.
25. Hwang, K.S; Singh, M; Bakota, E.L; Winkler-Moser, J.K; Kim, S; Liu, S.X.
Margarine from Organogels of Plant Wax and Soybean Oil. 2013. J Am Oil Chem
Soc. 90:1705–1712.
26. Aguilar, F; Crebelli, R; Dusemund, B; Galtier, P; Gott, D; Gundert-Remy, U;
König, J; Lambré, C; Leblanc, J.C; Mortensen, A; Mosesso, P; Parent-Massin, D;
Stankovic, I; Tobback, P; Waalkens-Berendsen, I; Woutersen, R.A; Wright, M.
Scientific Opinion on the re-evaluation of carnauba wax (E 903) as a food additive.
2012. EFSA Journal. 10(10): 2880.
27. Russell, L.W; Welch; A.E. Analysis of lipsticks. 1984. Forensic Science
International. Vol. 25, Issue 2, Pages 105–116.
28. Kato, Y; Sunada, H; Yonezawa, Y; Ishino, R. Sustained Release Mechanisms of
Wax Matrix System for Controlled Release. 1994. Chem. Pharm. Bull. 42(8): 1646-
1650.

29. Pompa, SS; Molina, RR; Carbó, A.F.A; Galindo, AS; Garza, H; Cantú, DJ; Aguilar, CN. Edible film based on candelilla wax to improve the shelf life and quality of avocado. 2009. *Food Research International* 42. 511–515.
30. Hagenmajer, R.D. Wax microemulsion formulations used as fruit coatings. 1998. *Florida State Horticultural Society* 111: 251-255.
31. Tada, A; Jin, Z.L; Sugimoto, N; Sato, K; Yamazaki, T; Tanamoto, K. Analysis of the Constituents in Jojoba Wax Used as a Food Additive by LC/MS/MS. 2005. *J. Food Hyg. Soc. Japan* Vol. 46, No. 5.
32. Milanovic, J; Manojlovic, V; Levic, S; Rajic, N; Nedovic, V, Bugarski, V. Microencapsulation of Flavors in Carnauba Wax. 2010. *Sensors* 10: 901-912; doi: 10.3390/s100100901. ISSN 1424-8220 www.mdpi.com/journal/sensors.
33. Srivastava, S.P; Saxena, A.K; Tandon, R.S; Shekher, V. (1997) Measurement and prediction of solubility of petroleum waxes in organic solvents. *Fuel* 76:625–630.
34. Toro-Vazquez, J.F; Morales-Rueda, J.A; Dibildox-Alvarado, E; Charo'-Alonso, M; Alonzo-Macias, M; Gonza'lez-Cha'vez, M.M. (2007) Thermal and textural properties of organogels developed by candelilla wax in safflower oil. *J Am Oil Chem Soc* 84:989–1000.
35. Dassanayake LSK, Kodali DR, Ueno S, Sato K (2009) Physical properties of rice bran wax in bulk and organogels. *J Am Oil Chem Soc* 86:1163–1173.

36. Hwang, H.S; Kim, S; Singh, M; Winkler-Moser, J.K; Liu, S.X. Organogel Formation of Soybean Oil with Waxes. *J Am Oil Chem Soc* (2012) 89:639–647.
37. Yilmaz, E.; Öğütçü, M. Properties and stability of hazelnut oil organogels with beeswax and monoglyceride. *J. Am. Oil Chem. Soc.* 2014, 91, 1007–1017.
38. Dassanayake, L. S.; Kodali, D. R.; Ueno, S. Formation of oleogels based on edible lipid materials. *Curr. Opin. Colloid Interface Sci.* 2011, 16, 432–439.
39. Blake, A. I.; Co, E. D.; Marangoni, A. G. Structure and physical properties of plan wax crystal networks and their relationship to oil binding capacity. *J. Am. Oil Chem. Soc.* 2014, 91, 885–903.
40. Hwang, H. S.; Kim, S.; Singh, M.; Winkler-Moser, J. K.; Liu, S. X. Organogel formation of soybean oil with waxes. *J. Am. Oil Chem. Soc.* 2012, 89, 639–647.
41. Chopin-Doroteo, M.; Morales-Rueda, J. A.; Dibilidox-Alvarado, E.; Charo-Alonso, M. A.; de la Peña-Gil, A.; Toro-Vazquez, J. F. The effect of shearing in the thermo-mechanical properties of candelilla wax and candelilla wax-tripalmitin organogels. *Food Biophys.* 2011, 6, 359–376.
42. Alvarez-Mitre, F. M.; Morales-Rueda, J. A.; Dibilidox-Alvarado, E.; Charo-Alonso, M. A.; Toro-Vazquez, J. F. Shearing as a variable to engineer the rheology of candelilla wax organogels. *Food Res. Int.* 2012, 49, 580–587.
43. Toro-Vazquez, J. F.; Morales-Rueda, J.; Mallia, V. A.; Weiss, R. G. Relationship between molecular structure and thermo-mechanical properties of candelilla wax and

amides derived from (R)-12- hydroxystearic acid as gelators of safflower oil. *Food Biophys.* 2010, 5, 193–202.

44. Morales-Rueda, J. A.; Dibilidox-Alvarado, E.; Charo-Alonso, M. A.; Toro-Vazquez, J. F. Rheological properties of candelilla wax and dotriacontane organogels measured with a true-gap system. *J. Am. Oil Chem. Soc.* 2009, 86, 765–772.

45. Yilmaz, E; Öğütçü, M. Comparative Analysis of Olive Oil Organogels Containing Beeswax and Sunflower Wax with Breakfast Margarine. 2014. *Journal of Food Science.* Vol 79, Nr. 9.

46. Botega, D. C. J; Marangoni, A.G; Smith, A.K; Goff, H.D. The Potential Application of Rice Bran Wax Oleogel to Replace Solid Fat and Enhance Unsaturated Fat Content in Ice Cream. 2013. *Journal of Food Science.* Vol. 78, Nr. 9.

47. Jang. A; Bae, W; Hwang, H.S; Lee, H.G, Lee, S. Evaluation of canola oil oleogels with candelilla wax as an alternative to shortening in baked goods. 2015. *Food Chemistry* 187: 525–529.

48. Patel, A.R; Rajarethinem, P. S; Gredowska, A; Turhan, O; Lesaffer, A; De Vos, W.H; Van de Walle, D; Dewettinck, K. Edible applications of shellac oleogels: spreads, chocolate paste and cakes. 2014. *Food Funct.*, 2014, 5, 645–652.

49. Yilmaz, E; Öğütçü, M. The texture, sensory properties and stability of cookies prepared with wax oleogels. *Food Funct.*, 2015,6, 1194-1204.

50. Ögütçü, M; Yilmaz, E. Oleogels of virgin olive oil with carnauba wax and monoglyceride as spreadable products. doi: <http://dx.doi.org/10.3989/gya.0349141>. (<http://grasasyaceites.revistas.csic.es/index.php/grasasyaceites/article/view/1505/1599>).
51. Humphrey, K.L.; Narine, S.S. In *Fat Crystal Networks*; Marangoni, AG; Eds; Marcel Dekker. New York. 2005. Chapter 3, pp 83-90.
52. Timms, R. E. "Phase behavior of fats and mixtures of fats", Oral Presentation at Palm Oil Research Institute of Malaysia, 2nd June (1981).
53. Wright, A.J.; Marangoni, A.G. Formation, Structure, and Rheological Properties of Ricinelaidic Acid–Vegetable Oil Organogels. *J. Am. Oil Chem. Soc.* 2006, 6, 497-503.
54. Chen, C.H.; Damme, I, V.; Terentjev, E.M. Phase behavior of C18 monoglyceride in hydrophobic solutions. *Soft Matter*, 2009, 5, 432-439.
55. Craven, R.J.; Lenki, R.W. Binary Phase Behavior of Diacid 1, 3-Diacylglycerols. *J Am Oil Chem Soc* (2011) 88:1125–1134.
56. Timms, R.E. Phase behavior of fats and their mixtures. 1984. *Prog Lipid Res* 23:1–38.
57. Takeuchi, M.; Ueno, S.; Sato, K. Synchrotron Radiation SAXS/WAXS Study of Polymorph-Dependent Phase Behavior of Binary Mixtures of Saturated Monoacid Triacylglycerols. *Cryst. Growth Des.* 2003, 3, 369-374.

58. White, M.A. Properties of Materials. 1999. Oxford University Press, New York.
59. Craven, R.J.; Lenki, R.W. Binary Phase Behavior of Diacid 1, 3-Diacylglycerols. *J Am Oil Chem Soc* (2011) 88:1125–1134.
60. Garside, J. General Principles of crystallization. In: Food Structure and Behavior; food and technology: a series of monographs. Blanshard, J.M.W.; Lillford, P. Eds. London: Academic Press, 1978:35 – 49.
61. Larsson, K. The crystal structure of β - form of trilaurin. *Arkiv Kemi* 1964; 23: 1-15.
62. Boistelle, R. Fundamentals of nucleation and crystal growth. In: Crystallization and polymorphism of fats and fatty acids. Garti, N.; Sato, K, Eds. New York: Marcel Dekker, 1988:133 – 178.
63. Martini, S.; Añon, M, C. Crystallization of sunflower oil waxes. *JAOCS*, Vol. 80, no. 6 (2003)
64. Md. Ali, A.R.; Dimick, P.S. Thermal Analysis of Palm Mid- Fraction, Cocoa Butter and Milk Fat Blends by Differential Scanning Calorimetry, *Ibid.* 71:299–302 (1994).
65. Tan, C.P.; and Man, Y.B. Che. Quantitative Differential Scanning Calorimetric Analysis for Determining Total Polar Compounds in Heated Oils, *Ibid.* 76:1047–1057 (1999).

66. Dunn RO, Bagby MO (1995) Low-temperature properties of triglyceride-based diesel fuels: transesterified methyl esters and petroleum middle distillate/ester blends. *J Am Oil Chem Soc* 72:895–904.
67. Dunn, R.O. (1999) Thermal analysis of alternative diesel fuels from vegetable oils. *J Am Oil Chem Soc* 76:109–115.
68. Lee, I.; Johnson, L.A.; Hammond, E.G. (1995) Use of branched-chain esters to reduce the crystallization temperature of biodiesel. *J Am Oil Chem Soc* 72:1155–1160.
69. Foglia, T.A.; Nelson, L.A.; Dunn, R.O.; Marmer, W.N. (1997) Low-temperature properties of alkyl esters of tallow and grease. *J Am Oil Chem Soc* 74:951–955.
70. Wu, W.H.; Foglia, T.A.; Marmer, W.N; Dunn, R.O; Goering, C.E; Briggs, T.E. (1998) Low temperature property and engine performance evaluation of ethyl and isopropyl esters of tallow and grease. *J Am Oil Chem Soc* 75:1173–1178.
71. Timms, R. E., Physical-Properties of Blends of Milk-Fat with Beef Tallow and Beef Tallow Fractions. *Aust J Dairy Technol* 1979, 34, 60-65.
72. Lohman, M. H.; Hartel, R. W., Effect of Milk-Fat Fractions on Fat Bloom in Dark Chocolate. *J Am Oil Chem Soc* 1994, 71, 267-276.
73. Ten Grotenhuis, E.; van Aken, G. A.; van Malssen, K. F.; Schenk, H., Polymorphism of milk fat studied by differential scanning calorimetry and real-time X-ray powder diffraction. *J Am Oil Chem Soc* 1999, 76, 1031-1039.

74. Suzuki, M.; Ogaki, T.; Sato, K., Crystallization and Transformation Mechanisms of Alpha,Beta-Polymorphs and Gamma-Polymorphs of Ultra-Pure Oleic-Acid. *J Am Oil Chem Soc* 1985, 62, 1600-1604.
75. Kotsiomiti, E; McCabe J.F. (1997) Experimental wax mixtures for dental use. *Journal of Oral Rehabilitation*. 97 24; 517-52.
76. Heertje, I., Microstructural Studies in Fat Research, *Food Struct.* 12:77–94 (1993).
77. Heertje, I.; Leunis, M., Measurement of shape and size of fat crystals by electron microscopy. *Food Sci Technol-Leb* 1997, 30, 141-146.
78. Marangoni, A.G., and D. Rousseau, Is Plastic Fat Rheology Governed by the Fractal Nature of the Fat Crystal Network? *J. Am. Oil Chem. Soc.* 73:991–994 (1996).
79. Pothiraj, C; Zuñiga, R; Simonin, H; Chevallier, S; Le-Bail, A. Methodology assessment on melting and texture properties of spread during ageing and impact of sample size on the representativeness of the results. *Journal of Stored Products and Postharvest Research* Vol. 3(10), pp. 137 – 144, 16 May, 2012.
80. Marangoni, AG. The nature of fractality in fat crystal networks. *Trends Food Sci. Technol.* 2002, 13, 37–47.
81. Campos, R. In *Fat Crystal Networks*; Marangoni, AG; Eds; Marcel Dekker. New York. 2005. Chapter 9, pp 319.

82. Martini, S.; Herrera, M. L.; Hartel, R. W., Effect of cooling rate on crystallization behavior of milk fat fraction/sunflower oil blends. *J Am Oil Chem Soc* 2002, 79, 1055-1062.
83. Martini, S.; Herrera, M. L.; Hartel, R. W., Effect of processing conditions on microstructure of milk fat fraction/sunflower oil blends. *J Am Oil Chem Soc* 2002, 79, 1063-1068.
84. Ye, Y; Wagh, A; Martini, S. Using High Intensity Ultrasound as a Tool To Change the Functional Properties of Interesterified Soybean Oil. *J. Agric. Food Chem.*, 2011, 59 (19), 10712–10722.
85. Zulkurnain, M; Maleky, F; Balasubramaniam, V.M. 2015. Effects of High Pressure Treatment on Structure and Physical Properties of Fat Blends of Fully Hydrogenated Soybean Oil. AOCs 106th Annual Meeting, Orlando, FL, May 3-6th.
86. Herrera, M. L.; Hartel, R. W., Effect of processing conditions on physical properties of a milk fat model system: Microstructure. *J Am Oil Chem Soc* 2000, 77, 1197-1204.
87. Blake, A.I.; Marangoni, A.G. Plant wax crystals display platelet-like morphology. *Food Structure*, Vol 3, 30-34.
88. Doan, C.D.; Walle, D.V.; Dewettinck, K.; Patel, A.R. Evaluating the Oil-Gelling Properties of Natural Waxes in Rice Bran Oil: Rheological, Thermal, and Microstructural Study. *J Am Oil Chem Soc* (2015) 92:801–811.

89. Noor Lida, H.M.D; Sundram, K; Siew, W.L; Aminah, A; Mamot, S. (2002) *J Am Oil Chem Soc* 79:1138–1143.
90. Noor Lida, H.M.D; Ali, A.R. (1998) *J Am Oil Chem Soc* 75:1625–1631.
91. Krawczyk, G.R; Buliga, G.S; Bertrand, D.T; Humpreys, W.M. Reviewing the Technology of Low-Fat Spreads, *INFORM* 7:635–639 (1996).
92. Martini, S; Herrera, M.L; Marangoni, A. New Technologies to Determine Solid Fat Content On-line. *Journal of the American Oil Chemists' Society* 2005, Volume 82, Issue 5, pp 313-317.
93. Chrysam, M. M., Table spreads and shortenings. In *Bailey's industrial oil and fat products*, Applewhite, T. H., Ed. John Wiley and Sons: New York, 1985; Vol. 3, pp 41-125.
94. Humphrey, K.L; Narine, S.S. In *Fat Crystal Networks*; Marangoni, AG; Eds; Marcel Dekker. New York. 2005. Chapter 3, pp 95-103.
95. Karabulut, I; Turan, S; Ergin, G. Effects of chemical interesterification on solid fat content and slip melting point of fat/oil blends. *Eur Food Res Technol* (2004) 218:224–229.
96. Martini, S; Herrera, M.L; Hartel, R.W. Effect of Cooling Rate on Crystallization Behavior of Milk Fat Fraction/Sunflower Oil Blends. *JAACS*, Vol. 79, (2002), 11, 1055-1062.

97. Davis, S.S. Viscoelastic properties of pharmaceutical semisolids. I. Ointment bases. *J. Pharm. Sci.*, 58 (4) (1969), pp. 412–418.
98. Barry, B.W. *Drugs and the Pharmaceutical Sciences, Dermatological Formulations-Percutaneous Absorption, Rheology of Dermatological Vehicles*, 18, Marcel Dekker, New York (1983), pp. 351–396, chapter 7. Ferraris, V. A. H. C. F., *Guide to Rheological Nomenclature: Measurements in Ceramic Particulate Systems*. In Commerce, U. S. D. o., Ed. National Institute of Standards and Technology: 2001.
99. Herrera, M. L.; Hartel, R. W., Effect of processing conditions on physical properties of a milk fat model system: Rheology. *J Am Oil Chem Soc* 2000, 77, 1189-1195.
100. Ojijo, N. K.O; Neeman, I; Eger, S; Shimoni, E. Effects of monoglyceride content, cooling rate and shear on the rheological properties of olive oil/monoglyceride gel networks. *J Sci Food Agric* 84:1585–1593 (online: 2004).
101. Liang, B; Shi, Y; Hartel, R.W. Correlation of Rheological and Microstructural Properties in a Model Lipid System. *J Am Oil Chem Soc* (2008) 85:397–404.
102. Mezzasalma, S.A; Koper, G.J.M; Shchipunov, Y.A. Lecithin organogel as a binary blend of monodisperse polymer-like micelles. *Langmuir*. 2000; 16:10564-10565.

103. Capitani, D; Segre, A.L; Dreher, F; Walde, P; Luisi, P.L. Multinuclear NMR investigation of phosphatidylcholine organogels. *J Phys Chem.* 1996; 100:15211-15217.
104. Walde, P; Giuliani, A.M; Boicelli, C.A; Luisi, P.L. Phospholipid-based reverse micelles. *Chem Phys Lipids.* 1990; 53:265-288.
105. Shumilina, E.V; Khromova, Y; Shchipunov, Y.A. A study of the structure of lecithin organic gels by Fourier-transform IR spectroscopy. *Zhurnal Fizicheskoi Khimii.* 2000; 74:1210-1219.
106. Cirkel, P; Koper, G.J.M. The structure of lecithin organogels. *Proceedings of Conference on Colloid Chemistry: Memoriam Aladar Buzagh; September 23-26, 1996; Budapest, Hungary, Hungarian Chemical Society; 1996; 36-39.*
107. Shchipunov, Y.A. Lecithin organogel: a micellar system with unique properties. *Colloids Surf A Physicochemical and Engineering Aspects.* 2001; 183-185:541-554.
108. Hwang, H. S.; Kim, S.; Singh, M.; Winkler-Moser, J. K.; Liu, S. X. Organogel formation of soybean oil with waxes. *J. Am. Oil Chem. Soc.* 2012, 89, 639–647.
109. Hwang, H. S.; Singh, M.; Bakota, E. L.; Winkler-Moser, J. K.; Kim, S.; Liu, S. X. Margarine from Organogels of plant wax and soybean oil. *J. Am. Oil Chem. Soc.* 2013, 90, 1705–1712.
110. Toro-Vazquez, J. F.; Morales-Rueda, J. A.; Dibildox-Alvarado, E.; Charo-Alonso, M.; Alonzo-Macias, M.; Gonzalez-Chavez, M. M. Thermal and textural

properties of organogels developed by candelilla wax in safflower oil. *J. Am. Oil Chem. Soc.* 2007, 84, 989–1000.

111. Patel, A.R; Babaahmadi, M; Lesaffer, A; Dewettinck, K. Rheological Profiling of Organogels Prepared at Critical Gelling Concentrations of Natural Waxes in a Triacylglycerol Solvent. *J. Agric. Food Chem.* 2015, 63, 4862–4869.

112. Zhang, H; Jacobsen, C; Adler-Nissen, J. (2005). Storage stability study of margarines produced from enzymatically interesterified fats compared to margarines produced by conventional methods. I. Physical properties. *Euro. J. Lipid Sci. Technol.*, 107(7-8), 530 - 539.

113. Toro-Vazquez JF, Morales-Rueda JA, Dibildox-Alvarado E, Charo´-Alonso M, Alonzo-Macias M, Gonza´lez-Cha´vez MM (2007) Thermal and textural properties of organogels developed by candelilla wax in safflower oil. *J Am Oil Chem Soc* 84:989–1000.

114. Morales-Rueda JA, Dibildox-Alvarado E, Charo´-Alonso MA, Toro-Vazquez JF (2009) Rheological properties of candelilla wax and dotriacontane organogels measured with a true-gap system. *J Am Oil Chem Soc* 86:765–772.

115. Hwang, H. S.; Kim, S.; Singh, M.; Winkler-Moser, J. K.; Liu, S. X. Organogel formation of soybean oil with waxes. *J. Am. Oil Chem. Soc.* 2012, 89, 639–647.

116. Daniel Co, E; Marangoni, A.G. Organogels: An Alternative Edible Oil-Structuring Method. *J Am Oil Chem Soc* (2012) 89:749–780.

117. Morales-Rueda, J. A.; Dibildox-Alvarado, E.; Charo-Alonso, M.; Weiss, R. G.; Toro-Vazquez, J. F. Thermo-mechanical properties of candelilla wax and dotriacontane organogels in safflower oil. *Eur. J. Lipid Sci. Technol.* 2009, 111, 207–215.
118. Wang, R.; Liu, X. Y.; Xiong, J.; Li, J. Real-time observation of fiber network formation in molecular organogel: Supersaturation dependent microstructure and its related rheological property. *J. Phys. Chem. B* 2006, 110, 7275–7280.
119. Moniruzzaman, M.; Sundararajan, P. R. Low molecular weight organogels based on long-chain carbamates. *Langmuir* 2005, 21, 3802–3807.
120. Lam, R.; Pederson, T.; Quaroni, L.; Rogers, M. A. A molecular insight into the nature of crystallographic mismatches in selfassembled fibrillar networks under non-isothermal crystallization conditions. *Soft Matter* 2010, 6, 404–408.
121. DeCastro, M.D.L; Priego-Capote, F. (2007) Ultrasound-assisted crystallization (sonocrystallization). *Ultrason Sonochem* 14(6):717–724.
122. Krishna, M.V; Babu, J.R; Latha, P.V.M; Sankar, D.G. (2007) Sonocrystallization: for better pharmaceutical crystals. *Asian J Chem* 19(2):1369–1374.
123. Miyasaka, E; Ebihara, S; Hirasawa, I. (2006) Investigation of primary nucleation phenomena of acetylsalicylic acid crystals induced by ultrasonic irradiation—

- ultrasonic energy needed to activate primary nucleation. *J Cryst Growth* 295(1):97–101.
124. Louhi-Kultanen, M; Karjalainen, M; Rantanen, J; Huhtanen, M; Kallas, J. (2006) Crystallization of glycine with ultrasound. *Int J Pharm* 320(1–2):23–29.
125. Manish, M; Harshal, J; Anant, P. (2005) Melt sonocrystallization of ibuprofen: effect on crystal properties. *Eur J Pharm Sci* 25(1):41–48.
126. Mansour AR, Takrouri KJ (2007) A new technology for the crystallization of Dead Sea potassium chloride. *Chem Eng Commun* 194(6):803–810.
127. Bucar, D.K; MacGillivray, L.R. (2007) Preparation and reactivity of nanocrystalline cocrystals formed via sonocrystallization. *J Am Chem Soc* 129(1):32–33.
128. Paradkar, A; Maheshwari, M; Kamble, R; Grimsey, I; York, P. (2006) Design and evaluation of celecoxib porous particles using melt sonocrystallization. *Pharm Res* 23(6):1395–1400.
129. Li, H; Li, H.R; Guo, Z.C; Liu, Y. (2006). The application of power ultrasound to reaction crystallization. *Ultrason Sonochem* 13(4):359–363.
130. Li, H; Wang, J.K; Bao, Y; Guo, Z.C; Zhang, M.Y. (2003) Rapid sonocrystallization in the salting-out process. *J Cryst Growth* 247(1–2):192–198.

131. Ruecroft, G; Hipkiss, D; Ly, T; Maxted, N; Cains, P.W. (2005) Sonocrystallization: the use of ultrasound for improved industrial crystallization. *Org Process Res Dev* 9(6):923–932.
132. Oldenburg, K; Pooler, D; Scudder, K; Lipinski, C; Kelly, M. (2005) High throughput sonication: evaluation for compound solubilization. *Comb Chem High Throughput Screen* 8(6):499–512.
133. Kaerger, J.S; Price, R. (2004) Processing of spherical crystalline particles via a novel solution atomization and crystallization by sonication (SAXS) technique. *Pharm Res* 21(2):372–381.
134. Cain, P.W; Martin, P.D; Price, C.J. (1998). The use of ultrasound in industrial chemical synthesis and crystallization. 1. Applications to synthetic chemistry. *Org Process Res Dev* 2(1):34–48.
135. Fairbanks, H.V. Drying powdered coal with the aid of ultrasound *Powder Technology*, 40 (1–3) (2001), pp. 257–264.
136. Mason, T. Industrial sonochemistry: potential and practicality *Ultrasonics*, 30 (3) (1992), pp. 192–196.
137. Mason, T.J; Paniwnyka, L; Lorimera, J.P. The uses of ultrasound in food technology *Ultrasonics Sonochemistry*, 3 (3) (1996), pp. S253–S260.
138. Povey, M.J.W. Ultrasonics of food *Contemporary Physics*, 39 (6) (1998), pp. 467–478.

139. Sato, K; Bayés-García, L; Calvet, T; Cuevas-Diarte, M, À; Ueno, S. External factors affecting polymorphic crystallization of lipids. *Eur. J. Lipid Sci. Technol.* 2013, 115, 1224– 1238.
140. Sato, K; Ueno, S. Crystallization, transformation and microstructures of polymorphic fats in colloidal dispersion states. *Current Opinion in Colloid & Interface Science* 16 (2011) 384–390.
141. Martini, S; Suzuki, A. H; Hartel, R.W. Effect of High Intensity Ultrasound on Crystallization Behavior of Anhydrous Milk Fat. *J Am Oil Chem Soc* (2008) 85:621–628.
142. Martini, S. High intensity ultrasound as a novel technology to change the physical properties of lipids. 248th National Meeting of the American-Chemical-Society (ACS), Volume: 248.
143. Mason, T; Lorimer, J. *Sonochemistry: Theory, applications and uses of ultrasound in chemistry.* Ellis Horwood Limited, Chichester (1988).
144. Lee, J; Ye, Y; Martini, S. Physicochemical and Oxidative Changes in Sonicated Interesterified Soybean Oil. *J Am Oil Chem Soc* (2015) 92:305–308.
145. Chemat, F; Grondin, I; Costes, P; Moutoussamy, L; Sing, A.S.C; Smadja, J. High power ultrasound effects on lipid oxidation of refined sunflower oil. *Ultrasonics Sonochemistry* 11 (2004) 281–285.

146. Patrick, M; Blindt, R; Janssen, J. The effect of ultrasonic intensity on the crystal structure of palm oil. *Ultrasonics Sonochemistry* 11 (2004) 251–255.
147. Chen, F; Zhang, H; Sun, X; Wang, X; Xu, X. Effects of Ultrasonic Parameters on the Crystallization Behavior of Palm Oil. *J Am Oil Chem Soc* (2013) 90:941–949.
148. Ye, Y; Tan, C. Y; Kim, D.A; Martini, S. Application of High Intensity Ultrasound to a Zero-trans Shortening During Temperature Cycling at Different Cooling Rates. *J Am Oil Chem Soc* (2014) 91:1155–1169.
149. Martini, S.; Suzuki, A.H.; Hartel, R.W. Effect of High Intensity Ultrasound on Crystallization Behavior of Anhydrous Milk Fat. *J Am Oil Chem Soc* (2008) 85:621–628.
150. Ye, Y.; Wagh, A.; Martini, S. Using High Intensity Ultrasound as a Tool To Change the Functional Properties of Interesterified Soybean Oil. *J. Agric. Food Chem.*, 2011, 59 (19), pp 10712–10722.
151. Wagh, A.; Walsh, M.K.; Martini, S. Effect of Lactose Monolaurate and High Intensity Ultrasound on Crystallization Behavior of Anhydrous Milk Fat. *J Am Oil Chem Soc* (2008) 90:977–987.
152. Martini, S.; Tejeda-Pichardo, R.; Ye, Y.; Padilla, S.G.; Shen, F.K; Doyle, T. Bubble and Crystal Formation in Lipid Systems During High-Intensity Insonation. *J Am Oil Chem Soc* (2008) 89:1921–1928.

153. Ye, Y.; Tan, C.Y.; Kim, D.A.; Martini, S. Application of High Intensity Ultrasound to a Zero-trans Shortening During Temperature Cycling at Different Cooling Rates. *J Am Oil Chem Soc* (2008) 91:1155–1169.

154. Ye, Y.; Martini, S. Application of High-Intensity Ultrasound to Palm Oil in a Continuous System. *J. Agric. Food Chem.*, 2015, 63 (1), pp 319–327

CHAPTER 3

PHASE SEPARATION IN 0.5% BINARY WAX BLEND IN SOYBEAN OIL

Abstract

The objective of this research is to investigate phase separation in wax/oil systems at room temperature (25 °C). A binary wax system from 0-100% was used in a 10% increment. Beeswax (BW), paraffin waxes (PW), rice bran wax (RBW), and sunflower wax (SFW) was used to form the binary wax blends. The binary wax to oil ratio used was 0.5: 99.5 (% wt. basis) in the vials. Results showed that binary wax containing BW has majority of phase separation in the vials. Wax-ester rich waxes such as RBW and SFW showed a less trend towards crystals' sedimentation in the vials. It is also studied that wax amount less than 1% in oil solution can form a firm crystal network but more emphasis is needed on the chemical composition of the waxes and also oil.

Introduction

Wax concentration plays a major role in crystalline network formation in oil. High wax concentration (> 1-2 % wt. basis) helps form strong crystalline networks. Toro-Vazquez et al. [1] observed phase separation in 1% candelilla wax in sunflower oil when stored at 25 °C for 7 days. Similar phase separation with candelilla wax was reported by Hwang et al. [2] when this group worked on 2-6% of candelilla wax in soybean oil. If a wax concentration below 1% is used a loose crystal network formation leads to sedimentation of wax crystals in the oil and to a consequent phase separation. Therefore, the objective of this research is to find out if any crystal sedimentation happens at room

temperature (25 °C) in 0.5% of wax blends in soybean oil. In this experiment binary waxes were used to make wax in oil system. Different proportions of waxes were prepared in this fashion: 'Z%' = 'X%' + 'Y%'. X = 1st wax component, Y = 2nd wax component, and Z = Binary wax.

Materials and methods

Binary systems were prepared by mixing these waxes (PW/BW, PW/RBW, PW/SFW, RBW/BW, RBW/SFW, and SFW/ BW) in different proportions from 0 to 100 % in 10 % increments. The binary systems were prepared by placing specific amounts of the waxes in 17 × 60-mm² (8 ml) vials to reach 1 g of solids. Approximately 7 ml of hexane was added to the vial, which was then closed with an appropriate lid. Vials were placed in a sonication water bath for 5–10 min and on a vortex mixer for 1–2 min to allow for complete dissolution of the waxes in the hexane. The vial lids were then loosened, and the vials placed under the airflow of a thin-wall fume hood for 1 week to evaporate the hexane. The remaining solid was ground into powder and utilized for the binary wax (0.5% wt. basis) in soybean oil vial experiment where 11 set of vials for each binary blend (in different proportions Table 3-1) were used in replicates. The vials were stored in an incubator at 25 °C for 7 days. The vial pictures were taken after 7 days.

Results and discussion

Wax/oil system phase separation study was conducted in a closed vial at 25 °C for 7 days. High melting wax crystals entraps low melting oil in wax/oil system forming a turbid solution or a semi-solid system. When the amount of wax is increased in the oil the

oil entrapping capacity increases in general. In this experiment amount of individual wax was decreased by forming a binary wax blend keeping the total wax concentration 0.5% (wt. basis). As Toro-Vazquez et al. [1] and Hwang et al. [2] mentioned that individual wax concentration plays a major role in phase separation; it is interesting to investigate if it applies in binary waxes too and at a concentration below 1%.

Table 3-1.Binary wax blend preparation in different proportions

| X (%) | Y (%) | Z (%) |
|-------|-------|-------|
| 0 | 100 | 100 |
| 10 | 90 | 100 |
| 20 | 80 | 100 |
| 30 | 70 | 100 |
| 40 | 60 | 100 |
| 50 | 50 | 100 |
| 60 | 40 | 100 |
| 70 | 30 | 100 |
| 80 | 20 | 100 |
| 90 | 10 | 100 |
| 100 | 0 | 100 |

Figure 3-1 shows vial pictures of 0.5% BW/PW wax in soybean oil system. In Figure 3-1, it is observed that only 100% BW shows phase separation. 10% of PW

addition in 90% BW shows no crystals sedimentation. Similarly, all the other proportions having PW show no phase separation. It is also interesting to note that 60% - 90% all the systems show a turbid solution.

Figure 3-2 shows vial pictures of 0.5% RBW/BW wax in soybean oil system. 50-80% of the RBW/BW blends show a turbid solution where turbidity increased from top to bottom. 90 and 100% of RBW/BW pictures show no liquid phase as compared to other wax proportions. This is interesting to compare with other above pictures because wax concentration is same (0.5% wt. basis) in all the cases. 90 and 100% RBW/BW blends form a stronger crystalline network forming a semisolid material (at 25 °C) where there is no complete liquid oil phase (soybean oil at 25 °C) or solid phase (wax blends at 25 °C).

Figure 3-3 shows vial pictures of 0.5% RBW/PW wax in soybean oil system. A little addition of RBW in PW from 10% shows turbid solution. It is noticed that from 20% to 100% the turbidity of the solutions increases in an ascending order. This also suggests that the crystal network formation becomes stronger in that order. This trend could be attributed to the very nature of their melting point (M.P.) and chemical compositions [RBW (M.P. 80 °C): 100% wax ester, PW (M.P. 60 °C): 100% hydrocarbon]. From Figure 3-2 and Figure 3-3, it is observed that presence of RBW forms stronger crystalline network formation at 0.5% total wax concentration in soybean oil.

Figure 3-4 shows vial pictures of 0.5% SFW/BW wax in soybean oil system. In this Figure 3-4, 0, 10 and 50% of the wax blends show phase separation.

From 20% to 100% SFW/BW blends show gradual increase of crystal network formation except 50%. A little amount (20%) of SFW addition in BW shows stronger crystal network. This trend is similar with RBW as SFW has similar melting point as 75 °C and having 66% of wax ester presence in total chemical composition.

Figure 3-5 shows vial pictures of 0.5% SFW/PW wax in soybean oil system. 10, 20 and 30% of the solutions show very less and loose crystal network formation. From 40% to 100% SFW/PW shows a gradual increase in strong crystalline network formation. This trend is similar as Figure 3-3.

Figure 3-6 shows vial pictures of 0.5% RBW/SFW wax in soybean oil system. Almost all the blends show no phase separation. All the blends form strong crystalline network leading to the best wax/oil system comparing all the above discussed systems.

Conclusion

Although low wax concentration is a major cause of phase separation due to loose crystal network formation, the chemical compositions and melting points are also another indicator of phase separation in wax oil system. High wax ester composition in waxes (RBW, SFW) increases the strong crystal network formation. It is therefore possible to use 0.5% wax in soybean oil to create a semisolid material where phase separation can be avoided. It is seen that BW in all binary systems leads to more phase separation. It is therefore necessary to apply novel processing techniques to check the sedimentation of the crystals in the oil solution.

Figure 3-1. Vial pictures of 0.5% (wt. basis) of BW/PW binary blends (0-100% wt. basis) in SBO stored at 25 °C in an incubator after 7 days

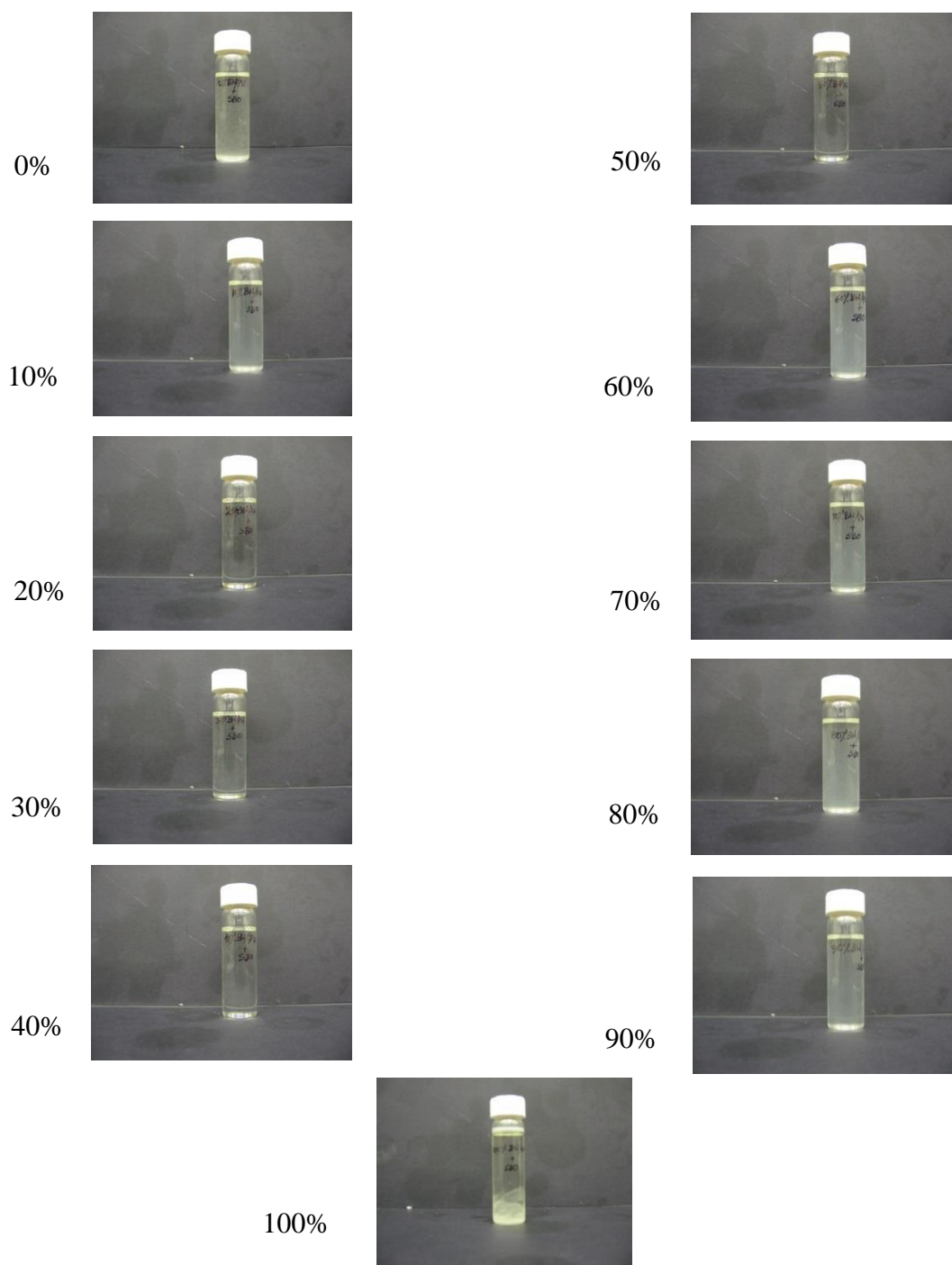


Figure 3-2. Vial pictures of 0.5% (wt. basis) of RBW/BW binary blends (0-100% wt. basis) in SBO stored at 25 °C in an incubator after 7 days

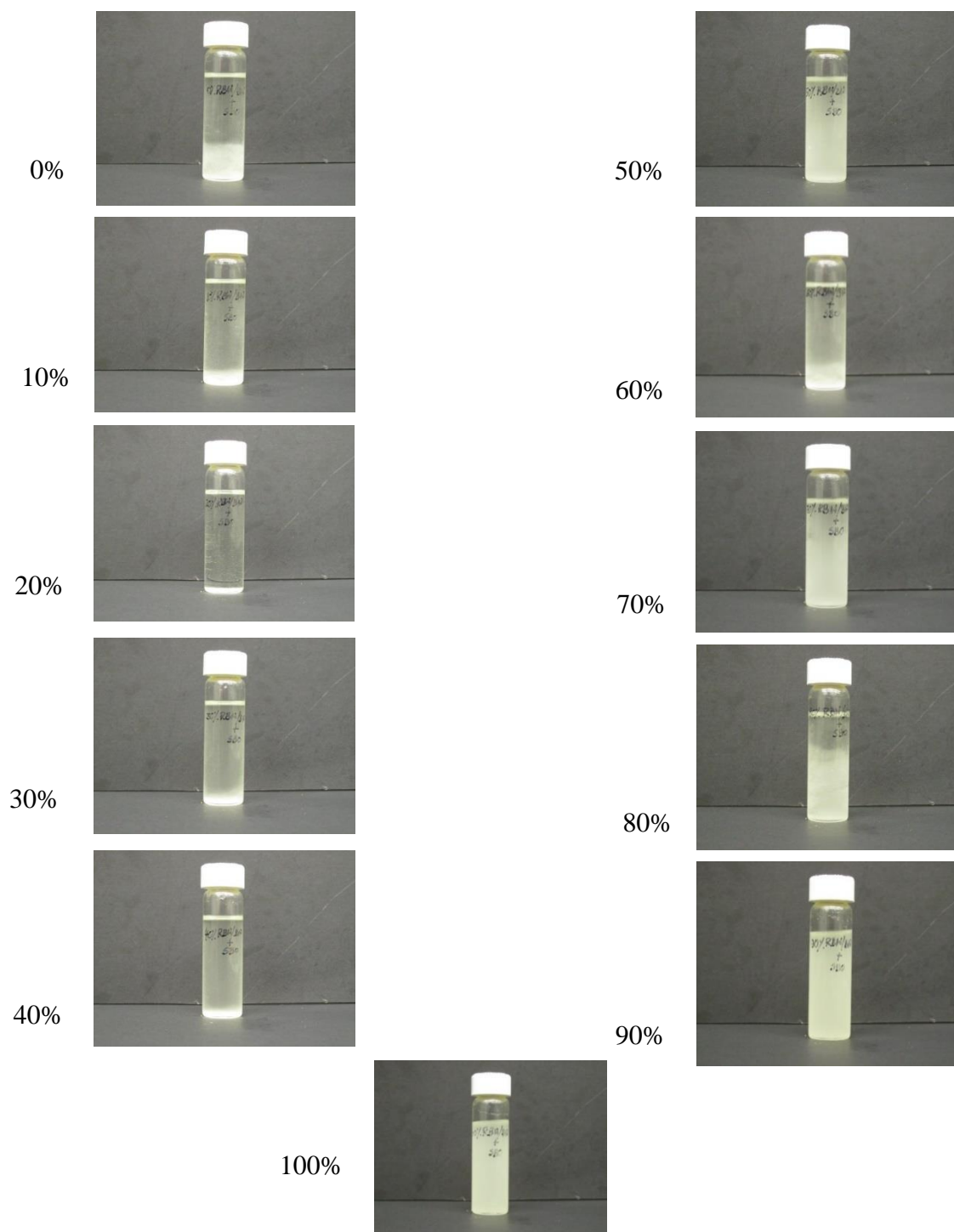


Figure 3-3. Vial pictures of 0.5% (wt. basis) of RBW/PW binary blends (0-100% wt. basis) in SBO stored at 25 °C in an incubator after 7 days

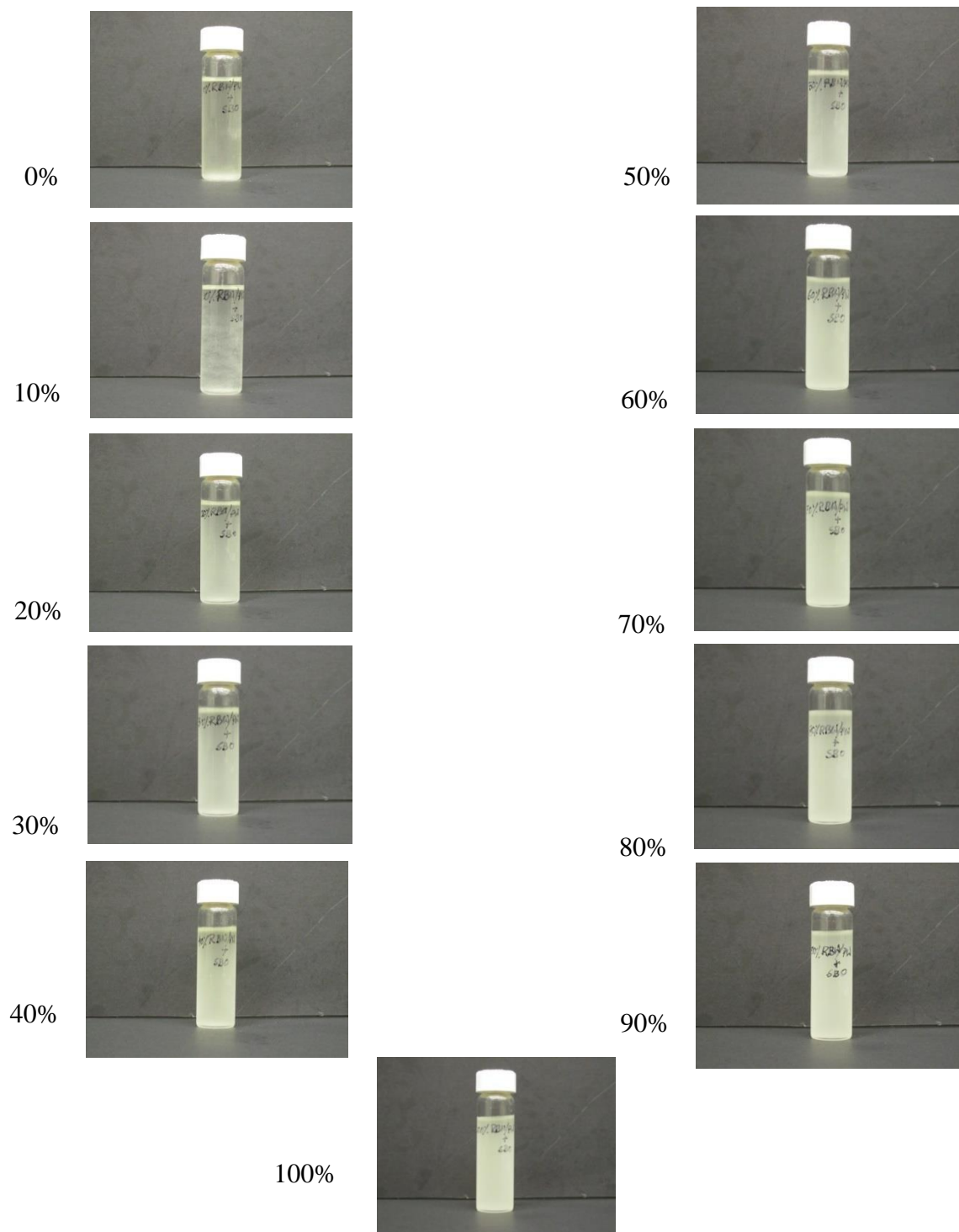


Figure 3-4. Vial pictures of 0.5% (wt. basis) of SFW/BW binary blends (0-100% wt. basis) in SBO stored at 25 °C in an incubator after 7 days

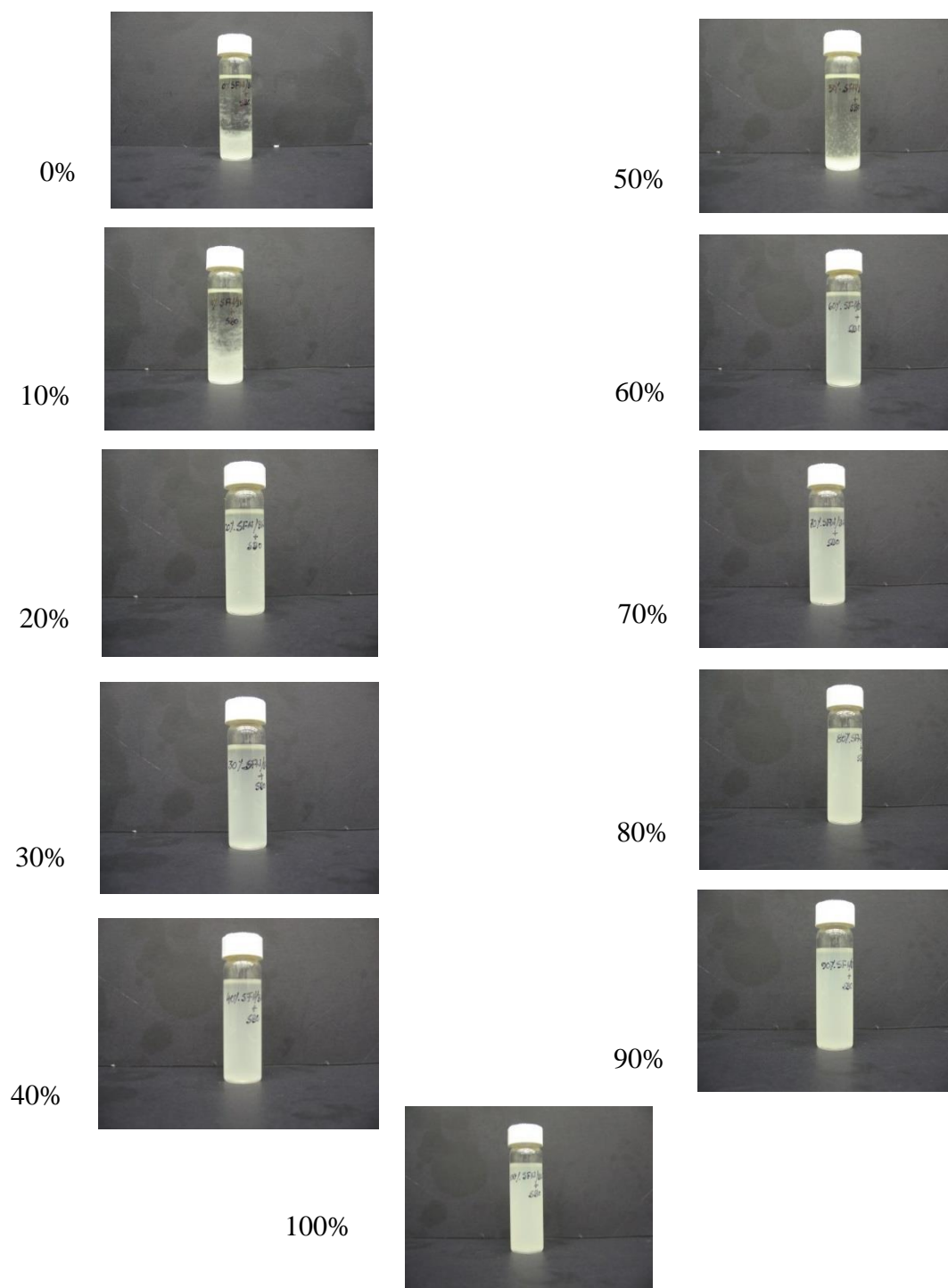


Figure 3-5. Vial pictures of 0.5% (wt. basis) of SFW/PW binary blends (0-100% wt. basis) in SBO stored at 25 °C in an incubator after 7 days

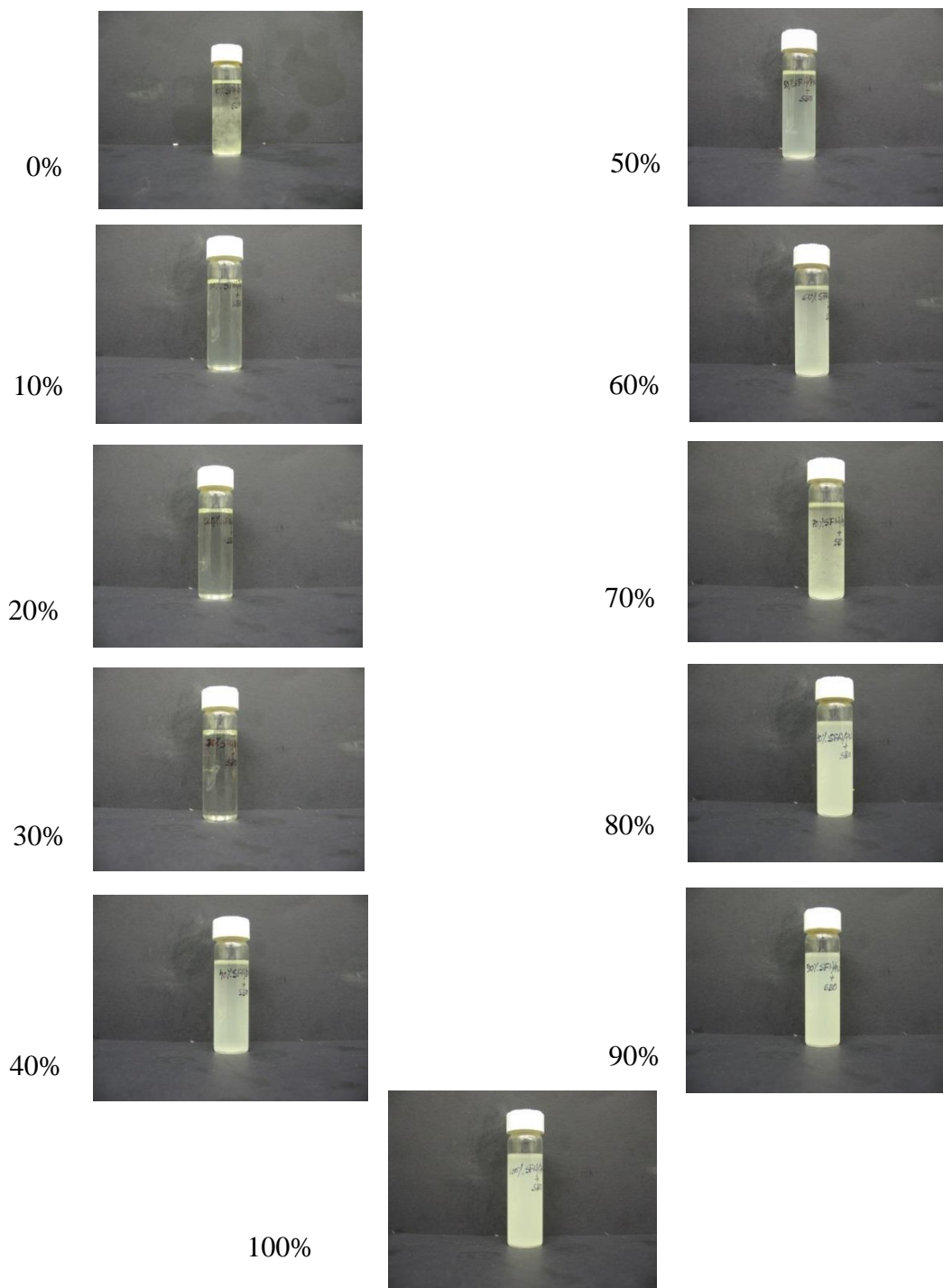
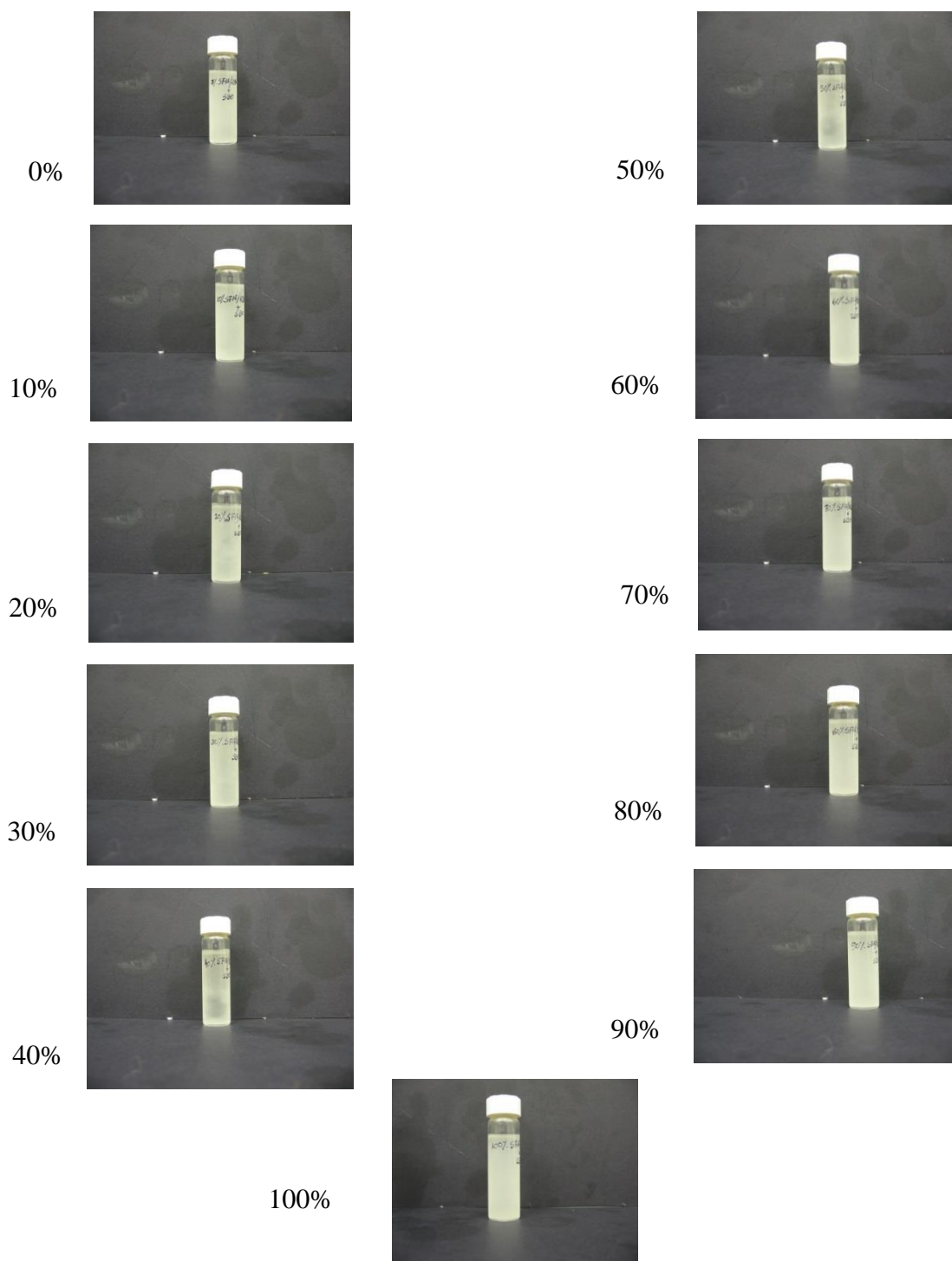


Figure 3-6. Vial pictures of 0.5% (wt. basis) of RBW/SFW binary blends (0-100% wt. basis) in SBO stored at 25 °C in an incubator after 7 days



When a trend in turbidity (increasing in ascending order or vice-versa) is not followed such as 50% SFW/BW, there is needed further analysis of phase diagram study for binary waxes alone.

References

1. Toro-Vazquez, J. F.; Morales-Rueda, J. A.; Dibildox-Alvarado, E.; Charo-Alonso, M.; Alonzo-Macias, M.; Gonzalez-Chavez, M. M. Thermal and textural properties of organogels developed by candelilla wax in safflower oil. *J. Am. Oil Chem. Soc.* 2007, 84, 989–1000.
2. Hwang, H. S.; Singh, M.; Bakota, E. L.; Winkler-Moser, J. K.; Kim, S.; Liu, S. X. Margarine from Organogels of plant wax and soybean oil. *J. Am. Oil Chem. Soc.* 2013, 90, 1705–1712.

CHAPTER 4

EFFECT OF HIGH INTENSITY ULTRASOUND AND COOLING RATE ON THE CRYSTALLIZATION BEHAVIOR OF BEESWAX IN EDIBLE OILS¹

Abstract

The objective of this study was to evaluate the effect of wax concentration (0.5 and 1%), cooling rate (0.1, 1, and 10 °C/min), and high-intensity ultrasound (HIU) on the crystallization behavior of beeswax (BW) in six different edible oils. Samples were crystallized at 25 °C with and without HIU. Crystal sizes and morphologies and melting profiles were measured by microscopy and differential scanning calorimetry, respectively, after 7 days of incubation. Higher wax concentrations resulted in faster crystallization and more turbidity. Phase separation was observed due to crystals' sedimentation when samples were crystallized at slow cooling rates. Results showed that HIU induced the crystallization of 0.5% BW samples and delayed phase separation in sunflower, olive, soybean, and corn oils. Similar effects were observed in 1% samples where HIU delayed phase separation in canola, soybean, olive, and safflower oils.

¹ Reprinted with permission from (Jana, S.; Martini, S. Effect of High-Intensity Ultrasound and Cooling Rate on the Crystallization Behavior of Beeswax in Edible Oils. *J. Agric. Food Chem.*, 2014, 62 (41), pp 10192–10202) © American Chemical Society (2014)

Introduction

Wax crystallization has become a topic of interest among food scientists for the past decade due to its facilitation of the formation of edible oleogels with the potential to be used as *trans*-fat and saturated fat replacers. Oleogels are semisolid materials composed of a self-assembled gelator and liquid oil. Molecular interactions established by the gelator result in the formation of a network that entraps liquid oil. Several gelators have been evaluated such as polyphenols,¹ sitosterol and oryzanol,² medium-chain sugar amphiphiles,³ and waxes.⁴ In particular, natural waxes such as beeswax (BW), sunflower wax, candelilla wax, and rice bran wax have been studied.⁵⁻¹⁸ Natural waxes are composed of several different molecular entities such as esters of long-chain aliphatic alcohols and long-chain fatty acids, n-alkanes, free fatty acids, and free long-chain alcohols. For example, rice bran wax is composed almost 100% by esters, whereas BW is composed of esters, n-alkanes, diesters, and free acids.¹⁴ Waxes are high melting point materials ($T_m = 50-80$ °C) and have low solubility in vegetable oils and therefore crystallize rapidly when placed at room temperature. Concentration as low as 0.1% of wax in oil can generate crystalline material. When higher wax concentrations are used, a stronger crystalline network is formed with properties similar to those observed in edible shortenings. This material is usually called an oleogel or organogel.¹⁸

The formation of oleogels using natural waxes was first reported by Toro-Vazquez's group,⁵⁻¹¹ who used candelilla wax to form an oleogel in safflower oil. This group of researchers characterized candelilla wax/safflower oil organogels in terms of rheological and thermal behavior and crystalline structure and also evaluated the interaction between

candelilla wax molecules and other high melting point molecules such as tripalmitin⁸ and 12-hydroxystearic acid.⁹ This research on candelilla waxes triggered interest in other natural waxes such as rice bran wax and carnauba wax^{12,13,16} and sunflower wax and beeswax.^{14,15} This body of literature agrees upon the fact that the rheological and thermal properties of oleogels are driven by the crystallization behavior of the wax, which in turn is affected by the molecular composition of the wax, the type of oil phase used, and processing conditions such as shear, temperature, and cooling rate. It is therefore important to understand the crystallization behavior of waxes to better predict the physical and functional properties of the oleogels that they form. Previous research on candelilla wax has shown that when this wax is crystallized at low concentrations (1%), some degree of phase separation (crystal sedimentation) is observed, limiting its use as an oleogelator.⁵ Preliminary research in our laboratory has shown that BW has a similar behavior and that this phase separation might be affected also by the type of oil used and by other processing conditions such as cooling rate. Beeswax is approved as GRAS (generally recognized as safe)¹⁹ and is natural, easily available, and cheaper than other waxes.

Therefore, the objective of this study was to evaluate the crystallization behavior of BW in different vegetable oils (canola, corn, olive, safflower, sunflower, and soybean oil) as affected by cooling rate (0.1, 1, and 10 °C/min) and wax concentration (0.5 and 1%) and to evaluate if high-intensity ultrasound affects the degree of phase separation observed. This research will increase our understanding of how oil composition and processing conditions affect BW crystallization with the ultimate purpose of finding new

processing conditions and materials that can be used to replace *trans*-fats and saturated fats in foods.

Materials and methods

Materials and Sample Preparation:

All of the oils were purchased from a local supermarket. Kroger pure canola oil, Kroger pure corn oil, Great Value pure olive oil, high-oleic All Natural Louana pure safflower oil, high-oleic Antoine & Muse imported pure sunflower oil, and Pure Wesson soybean oil were used in our experiments. Beeswax was supplied by Koster Keunen, Inc. BW is composed of wax esters (35%, mainly C50), hydroxyl esters (24%, mainly ester of 15- hydroxypalmitic acid and C24–C34 alcohols), hydrocarbon (14%), diesters (12%), free acids (12%), and unidentified compounds (6%).¹⁴ Samples of 0.5 and 1% BW in vegetable oils were used. Three different cooling rates were evaluated (0.1, 1, and 10 °C/min) to represent slow, medium, and fast cooling rates. BW was mixed with the oils and heated to 100 °C in an oven to allow for complete melting and dissolution of the wax in the oil. Samples were kept at 100 °C for at least 30 min, and then 5 g of the melted samples was placed in customized tubes for transmission measurements (see section below) and placed again in the oven to ensure that no wax crystallized during the filling of the tubes.

Fatty Acid Compositions in Different Oils:

Fatty acid compositions of the oils were determined as described by Ye et al.²⁰ using a gas chromatograph (Shimadzu 2010) equipped with a flame ionization detector (Shimadzu, Columbia, MD, USA).

Cooling Rate Measurement:

After the samples had been kept in the oven for 30 min, samples were cooled from 60 to 25 °C using the three different cooling rates previously mentioned. Slower cooling rates (0.1 and 1 °C/min) were achieved using a programmable water bath (Lauda Ecoline Staredition (Delran, NJ, USA). The fast cooling rate (10 °C/min) was achieved by placing the hot samples in a water bath (VWR, model 1160S (Buffalo Grove, IL, USA), that was pre-set at the crystallization temperature (25 °C).

High-Intensity Ultrasound (HIU):

HIU operating at a frequency of 20 kHz was applied to the samples using a 2 mm probe (part 4423, Qsonica Sonicators, Newtown, CT, USA) with a vibration amplitude of 180 µm for 10 s, which resulted in a power level of 10 W. To achieve maximum efficiency of the ultrasound waves, HIU was applied in the presence of crystals;²⁰ therefore, HIU was applied at 300, 20, and 1.5 min for the 0.5% BW samples cooled at 0.1, 1, and 10 °C/min cooling rates, respectively. HIU was applied at 300, 15, and 1.5 min for 1% BW cooled at 0.1, 1, and 10 °C/min cooling rates, respectively.

Transmission Measurement:

The crystallization behavior of the samples was followed by measuring the transmission of light through the samples. When samples crystallize, they create a certain amount of turbidity, showing a decrease in the transmission of light. Transmission of light through the samples was taken with TurbiScan equipment (Turbiscan Classic, MA2000, L'Union, France), and data were analyzed using computer software (Turbisoft version 1.2.1). Melted samples (5 g) were placed in the TurbiScan tubes reaching a height of 40 ± 0.5 mm, and transmission was measured as a function of time. Transmission of the tubes was measured at three different levels, 5–10 mm (bottom), 17.5–22.5 mm (middle), and 30–35 mm (top), respectively, from the bottom of the tubes. TurbiScan data were taken on a daily basis for 7 days, from the start of the experiment. Details regarding the operation of TurbiScan can be found in Martini and Tippetts.²¹

Crystal Morphology:

After 1 week of storage in an incubator at 25 °C, crystals present in the samples were evaluated. Samples were taken from the middle of the tube when no phase separation was observed and from the bottom when phase separation was observed. Crystal morphology was analyzed at different cooling rates at different concentrations of BW in different oils crystallized with and without the use of HIU. The crystals were observed using a polarized light microscope (Olympus BX41, Olympus Optical Co., Tokyo, Japan). A small amount of sample containing crystals was placed on a glass microscope slide and covered gently with a glass cover slip. Digital images of the

polarized specimens were captured using Lumenera's Infinity 2 (Lumenera Corp., Nepean, Canada). Approximately 10 pictures of each sample and crystallization run were taken to obtain approximately 200 crystals. These pictures were used to measure crystal sizes using ImageJ 1.42q (Wayne Rasband, National Institutes of Health, USA).

Differential Scanning Calorimetry (DSC):

The melting profile of the different samples crystallized at 25 °C for 7 days was measured using DSC (TA Instruments DSC model Q20 1963 with RCS cooling system, New Castle, DE, USA). Samples were centrifuged at 25 °C at 3000g for 30 min to separate the crystals from the oil and achieve higher resolution in the DSC. The DSC baseline and temperature were calibrated with a pure indium standard. Approximately 10 mg of crystals was placed in Tzero aluminum pans, covered and sealed with Tzero aluminum lids. The samples were heated from 25 to 100 °C with a ramp of 5 °C/min to analyze the melting profile of the samples. TA Universal Analysis software was used to analyze the onset and peak temperatures.

Statistics:

Samples were crystallized in triplicate. From each crystallization run, transmission measurements were taken in quintuplicate and DSC measurements were taken in duplicate. TurbiScan data were reported using GraphPad Prism6 software (Graphpad Software, San Diego, CA, USA). Crystal sizes were analyzed using Microsoft Office Excel 2010 (Microsoft Corp., Redmond, WA, USA). Statistical analysis was performed using two-way ANOVA test using GraphPad Prism6 software.

Results and discussion

Effect of Cooling Rate, Wax Concentration, and HIU on BW Crystallization:

Figure 4-1 shows transmission measurements of 0.5% BW in soybean oil crystallized to 25 °C for 7 days using three different cooling rates (0.1, 1, and 10 °C/min). The x-axis denotes time of storage at 25 °C, and the y-axis is the percentage of transmission through the wax/oil sample. Transmission counts were taken at the bottom, middle, and top of the tube to evaluate if crystallization occurs in a homogeneous manner throughout the tube. As expected, samples crystallized more quickly when cooled at the fast cooling rate (10 °C/min) and reached a minimum value of approximately 25% transmission after 7 h (Figure 4-1A) at 25 °C. When samples were crystallized at 1 °C/min (Figure 4-1C), values of transmission similar to the ones observed for the sample crystallized at 10 °C/min were obtained. However, when the sample was crystallized at 1 °C/min, slighter higher values of transmission were observed after 1 day (1440 min) at 25 °C at the middle and top of the tube compared to the transmission values obtained at the bottom of the tube. This indicates that some degree of phase separation occurs under these conditions when the sample gets less turbid over time due to crystal sedimentation. This effect is even more significant when samples are cooled at 0.1 °C/min (Figure 4-1E), when a significant phase separation is observed after the first day of storage at 25 °C (note the significant increase in transmission in Figure 4-1E), and a high transmission value (~100%) is observed after 3 days (4320 min), suggesting that the tube is completely clear after 3 days of storage and that the crystals have sedimented at the

bottom of the tube (lower than 5 mm from the bottom). Therefore, it is evident that the cooling rate has a direct influence on the phase separation of the wax in oil mixture.

HIU was used in these samples to evaluate if this processing tool could help in stabilizing crystal networks and therefore delay phase separation. When HIU was applied in samples crystallized at the fast cooling rate, higher transmission values (27 ± 7 and $65 \pm 6\%$ for samples crystallized without and with HIU, respectively) were observed (Figure 4-1B), suggesting that HIU delays wax crystallization under these conditions. Figure 4-1D shows that HIU slightly delays phase separation when samples were cooled at $1 \text{ }^\circ\text{C}/\text{min}$ because transmission values obtained at the bottom, middle, and top of the tube are similar. This can be observed by comparing transmission values reported in panels C and D of Figure 4-1 at 30–35 mm (35 ± 5 and $28 \pm 10\%$, respectively). A significant delay in phase separation is observed for samples crystallized at the slow cooling rate and with HIU application. No phase separation was observed at the bottom of the tube, and significantly lower transmission values were observed in the middle and top of the tubes (Figure 4-1F) compared to the same sample crystallized without the use of HIU (Figure 4-1E). These data suggest that HIU can help in the stabilization of a crystalline network to avoid phase separation, especially when samples are processed using slow cooling rates.

To understand the results reported in Figure 4-1, the morphology of the crystals was evaluated using polarized light microscopy after storage. Figure 4-2 shows the morphology of crystals obtained for the 0.5% BW samples crystallized in soybean oil at different cooling rates (0.1, 1, and $10 \text{ }^\circ\text{C}/\text{min}$) with and without the use of HIU.

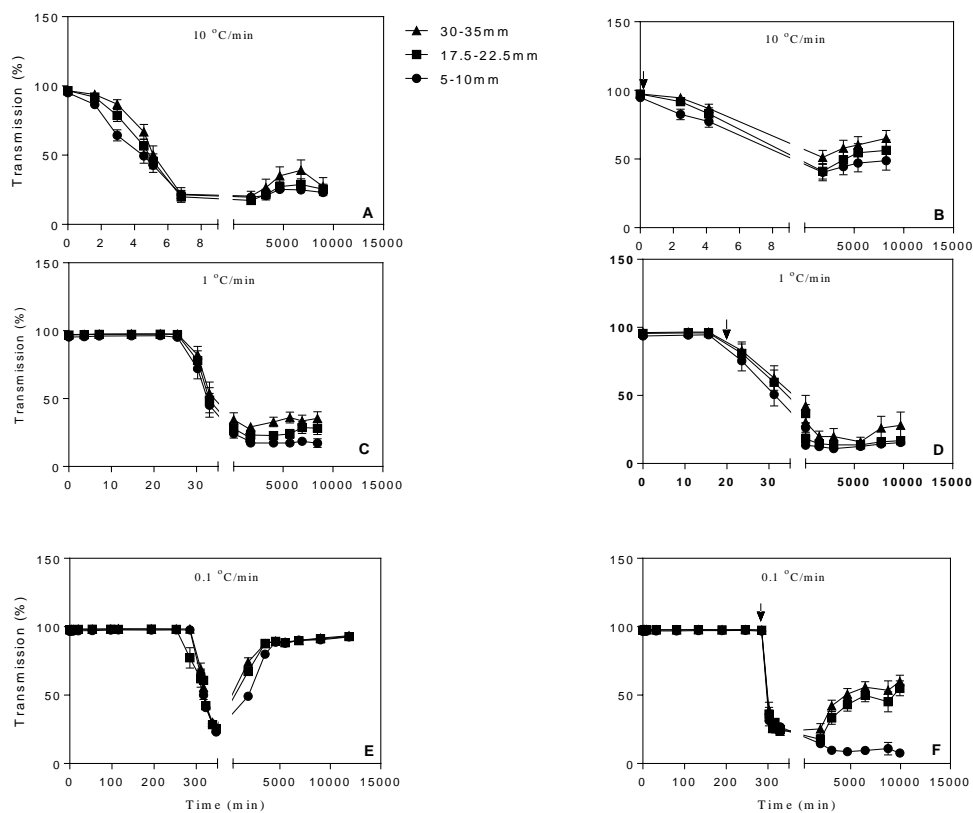


Figure 4-1. Transmission measurements of 0.5% BW in soybean oil crystallized at 25 °C for 7 days using different cooling rates (0.1, 1 and 10 °C/min) without (left column) and with (right column) HIU. Figures A and B = 10 °C/min, Figures C and D = 1 °C/min, Figures E and F = 0.1 °C/min. Transmission measurements were performed at the bottom of the tube (5-10 mm from the bottom, filled circles), at the middle of the tube (17.5-22.5 mm, filled squares), and at the top of the tube (30-35 mm, filled triangles). The arrow (right column) indicates the moment at which HIU was applied. 100% transmission of light indicates there is no turbidity and 0% transmission indicates that the assay tubes are completely turbid.

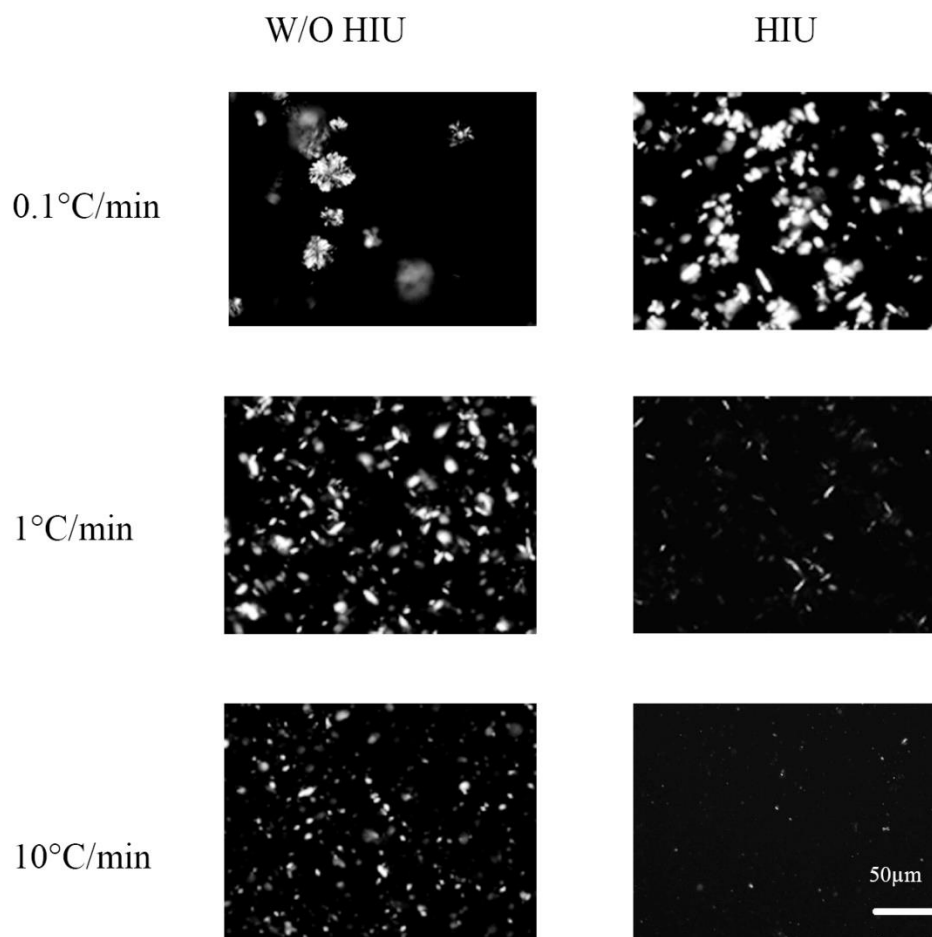


Figure 4-2. Morphology of crystals obtained when 0.5% BW in SBO is crystallized at 25 °C for 7 days at different cooling rates (0.1, 1 and 10 °C/min) without (left column) and with (right column) HIU. Crystal pictures were taken at 20X magnification under Polarized Light Microscopy. The white bar corresponds to 50 µm.

As expected, bigger crystals were obtained when samples were crystallized at slow cooling rates. Previous research has reported the increase in crystal size when lipids are crystallized using slow cooling rates.²² In addition; this figure shows that HIU reduced crystal sizes and morphologies, especially for the BW crystallized at slow cooling rates: big spherulites are observed in the sample crystallized without the use of HIU, and smaller crystals are observed when HIU was used.

The experiments performed in Figures 4-1 and 4-2 were repeated using a BW concentration of 1% to evaluate the effect of cooling rate and sonication when a higher wax concentration is used. Figure 4-3 shows the transmission measurements for these samples.

All of the crystallization conditions remained constant except the timing of the ultrasound application. HIU was applied at 5 h, 15 min, and 1.5 min for 0.1, 1, and 10 °C/min, respectively. This change was performed so that HIU could be applied at the moment when the first crystals appeared. The higher concentration of BW (1 vs 0.5%) induced crystallization, and therefore HIU was applied sooner. Figure 4-3 shows that no phase separation was observed in the samples crystallized at intermediate (1 °C/min) and fast cooling rates (10 °C/min) with transmission values of 5 ± 0 and $7 \pm 2\%$, respectively (Figure 4-3, panels A and C, respectively). Some degree of phase separation was observed in samples crystallized at the slow cooling rate with transmission values of $90 \pm 2\%$ at the top of the tube and $31 \pm 8\%$ at the bottom of the tube (Figure 4-3F).

The use of HIU did not affect the final transmission value of the samples crystallized at 1 and 10 °C/min (Figure 4-3B,D) but significantly affected transmission values and therefore phase separation of samples crystallized at slow cooling rates (Figure 4-3F). The transmission values for these samples decreased to $52 \pm 10\%$ at the top of the tube and $19 \pm 7\%$ at the bottom of the tube. Similarly to the results reported for the 0.5% samples, these results show that HIU delayed phase separation during storage. Figure 4-4 shows the morphology of crystals obtained for the samples discussed in Figure 4-3 after 7 days of storage at 25 °C. Even though a slight decrease in the crystal size is observed as a consequence of sonication, the effects are not as evident as the ones observed for the 0.5% BW in soybean oil samples (Figure 4-2). Figure 4-4 shows that the morphology of the BW crystals cooled at 0.1 °C/min is not changed as a consequence of sonication as reported for the 0.5% BW samples.

Results reported in Figures 4-1–4-4 suggests that a significant phase separation occurs when 0.5 and 1% of BW is crystallized at the slow cooling rate (0.1 °C/min) in soybean oil and that this phase separation can be delayed using HIU. Previous research on natural waxes with soybean oil was done by Hwang et al.^{14,15} and suggested that sunflower wax works best toward crystallization and cooling rate in a concentration range of 0.5– 10%. Dassanayake et al.¹² evaluated the crystallization behavior of rice bran, carnauba, and candelilla wax in olive oil and salad oil (50% canola + 50% soybean oil) and suggested that the long, thin, needle-shaped crystal structures formed by rice bran wax in the above oils might be responsible for the good gelling properties of this wax.

Similar to our data, Toro-Vazquez et al.⁵ showed that 1% candelilla wax crystallized in safflower oil showed phase separation during storage for 3 months. Even though some wax/oil combinations have been studied as discussed above, it is not clear how the type of oil affects the crystallization of waxes. However, the existing literature and our data agree on the fact that wax concentration and cooling rate have a direct impact on wax crystallization. Therefore, the next step in our research is to evaluate if the crystallization of BW is affected by the type of oil used when crystallized at 0.1 °C/min.

Effect of Oil Type and Sonication on BW Crystallization:

Table 4-1 shows the fatty acid composition of the oils used in this research. These oils were chosen to include different and typical chemical compositions found in vegetable oils.

For example, canola and sunflower oils have approximately 62% of oleic acid (C18:1), whereas olive and safflower oils have higher contents of oleic acid (approximately 73 and 76%, respectively). On the other hand, corn and soybean oils have lower contents of oleic acid with values of approximately 29 and 23%, respectively.

Figure 4-5 shows the crystallization behavior of 0.5% BW in different vegetable oils cooled at 0.1 °C/min. Phase separation was observed in 0.5% BW samples crystallized in all of the oils tested (canola, corn, olive, safflower, and sunflower) when stored. It is interesting to note that the crystallization behavior of the 0.5% BW solutions is significantly affected by the type of oils used.

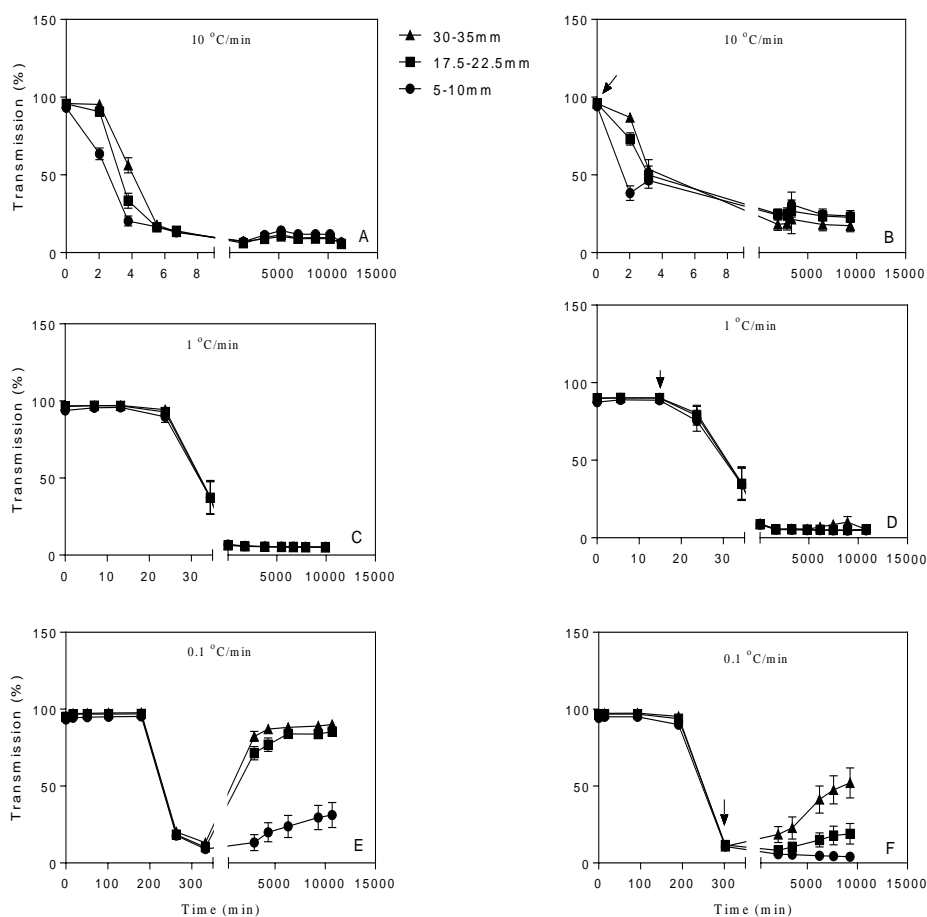


Figure 4-3. Transmission measurements of 1% BW in soybean oil crystallized at 25 °C for 7 days using different cooling rates (0.1, 1 and 10 °C/min) without (left column) and with (right column) HIU. Figures A and B = 10 °C/min, Figures C and D = 1 °C/min, Figures E and F = 0.1 °C/min. Transmission measurements were performed at the bottom of the tube (5-10 mm from the bottom, filled circles), at the middle of the tube (17.5-22.5 mm, filled squares), and at the top of the tube (30-35 mm, filled triangles). The arrow (right column) indicates the moment at which HIU was applied. 100% transmission of light indicates there is no turbidity and 0% transmission indicates that the assay tubes are completely turbid.

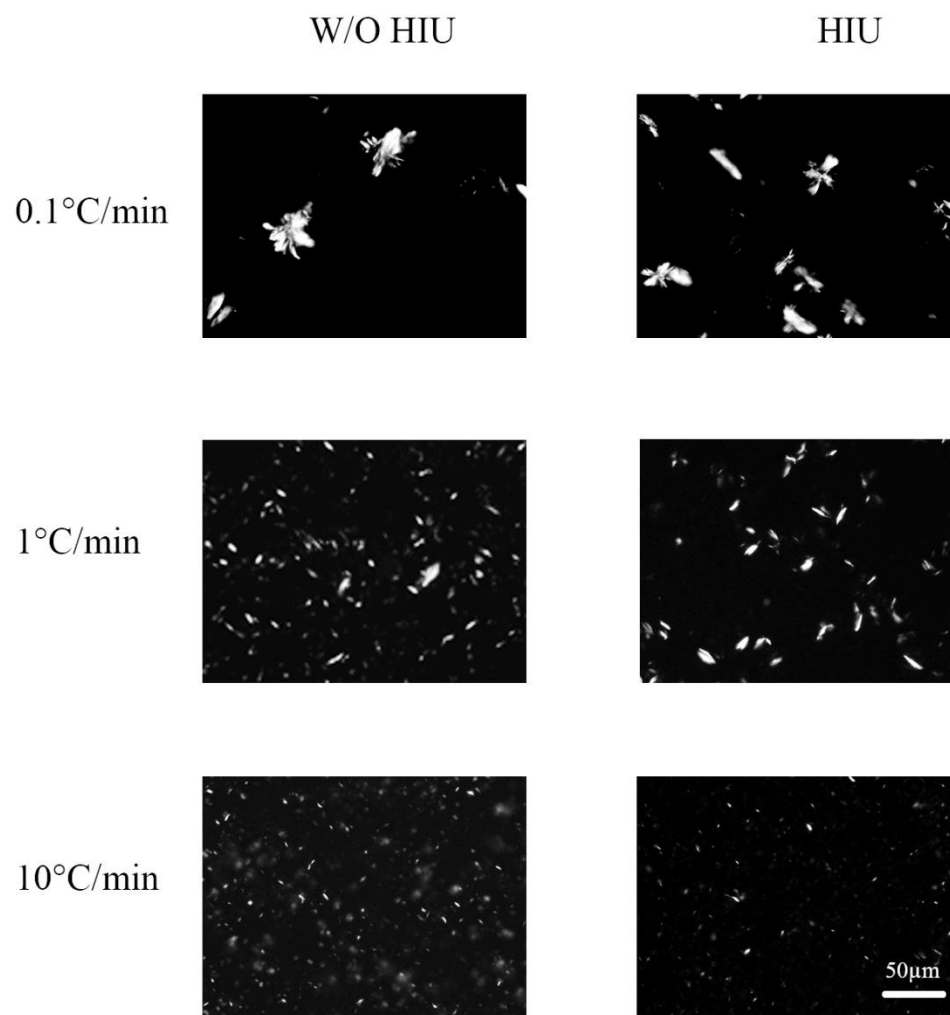


Figure 4-4. Morphology of crystals obtained when 1% BW in SBO is crystallized at 25 °C for 7 days at different cooling rates (0.1, 1 and 10 °C/min) without (left column) and with (right column) HIU. Crystal pictures were taken at 20X magnification under Polarized Light Microscopy. The white bar corresponds to 50 μm .

For example, when BW is crystallized in soybean oil, the sample starts crystallizing at approximately 300 min (Figure 4-1E). The onset of crystallization is lower for canola, corn, olive, safflower, and sunflower with an onset of crystallization of approximately 200 min for canola and sunflower and 250 min for corn, olive, and safflower (Figure 4-5A,C,E,G,I).

As previously discussed, phase separation was very marked when 0.5% BW was crystallized in soybean oil (Figure 4-1E). Phase separation was observed in all the other samples but to a lower degree. When 0.5% BW was crystallized in canola oil (Figure 4-5A), the sample remained turbid at the bottom of the tube even after 5000 min (~ 3.5 days) of storage with transmission values of $22 \pm 1\%$. However, some degree of phase separation is present after the first day of storage, which is evidenced by higher transmission values observed at the top of the tube ($50 \pm 4\%$). This phase separation becomes more evident at approximately 3500 min (~ 2.5 days), when the transmission increased to $61 \pm 5\%$ at the top of the tube and to $33 \pm 3\%$ in the middle of the tube.

The use of HIU in this sample inhibited crystallization, and lower values of transmission were observed ($60 \pm 15\%$ at the bottom of the tube at 1500 min). These transmission values remained constant during storage, indicating that phase separation was delayed due to the use of HIU. When 0.5% BW was crystallized in corn oil (Figure 4-5C), the sample shows more turbidity ($24 \pm 7\%$) at the bottom after 5000 min of storage compared to the middle ($39.6 \pm 5.3\%$) and top ($51 \pm 7\%$) of the tube.

Table 4-1. Fatty acid composition of the oils used in this research. Mean values are standard deviation of 2 replicates are reported. Fatty acids present at levels below 0.5% are not reported.

| Fatty Acids | Canola | Corn | Olive | Soybean | Sunflower | Safflower |
|-----------------------------|---------------|-------------|--------------|----------------|------------------|------------------|
| C16:0 | 4.4±0.0 | 11.9±0.3 | 11.8±0.1 | 11.1±0.1 | 4.4±0.6 | 4.9±0.2 |
| C18:0 | 2.0±0.1 | 1.8±0.2 | 2.5±0.0 | 4.4±0.0 | 3.4±0.1 | 1.4±0.7 |
| C18:1 | 63.9±5.4 | 29.9±2.7 | 73.8±1.1 | 23.9±2.7 | 63.6±2.0 | 80.4±3.3 |
| C18:2 c9 c12 | 19.8±0.0 | 55.4±1.8 | 11.2±0.8 | 53.6±0.2 | 28.3±0.2 | 12.6±0.2 |
| C18:3 c9 c12 c15 | 9.8±0.7 | 0.9±0.2 | 0.6±0.2 | 7.0±0.3 | 0.3±0.0 | 0.6±0.3 |
| SFA | 6.5 | 13.7 | 14.3 | 15.5 | 7.8 | 6.4 |
| UFA | 93.5 | 86.2 | 85.6 | 84.5 | 92.2 | 93.6 |
| MUFA | 63.9 | 29.9 | 73.8 | 23.9 | 63.6 | 80.4 |
| PUFA | 29.5 | 56.4 | 11.8 | 60.6 | 28.6 | 13.2 |
| Total | 100.0 | 100.0 | 100.0 | 100.0 | 100.0 | 100.0 |

HIU application (Figure 4-5D) made the transmission values approximately similar at the bottom ($29 \pm 10\%$), middle ($32 \pm 11\%$), and top ($32 \pm 11\%$) of the tube, suggesting the lack of phase separation. The transmission at the bottom part of 0.5% olive oil (Figure 4-5E) was low ($42 \pm 7\%$) up to 4200 min and then increased over time.

Similar results were observed at the middle ($65 \pm 5\%$) and top ($73 \pm 2\%$) of the tube. When HIU was used (Figure 4-5F), transmission levels were lower at the bottom ($22 \pm 6\%$), middle ($45 \pm 9\%$), and top ($46 \pm 8\%$) part of the tube after 4700 min. In transmission values were observed when HIU was applied (Figure 4-5H) with approximately the same turbidity obtained throughout all levels of the tube (transmission at bottom, $63 \pm 2\%$; middle, $69 \pm 1\%$; and top, $70 \pm 1.6\%$) after 5000 min. When 0.5% BW was crystallized in sunflower oil, the transmission at the bottom after 5000 min was

$59 \pm 3\%$ and the transmissions in the middle and top portions were 64 ± 3 and $69 \pm 3\%$, respectively. The transmission through sunflower oil (Figure 4-5J) shows more turbidity with HIU application after 5000 min at all levels of the tube. The bottom part reached a transmission value of $20 \pm 6\%$, and the middle and top reached 30 ± 6 and $49 \pm 7\%$, respectively.

Overall, the stability toward phase separation increased in the order soybean oil < olive oil < sunflower oil < canola oil < safflower oil < corn oil. These results suggest that (a) for the same type and amount of wax, the type of oil used affects the degree of phase separation and (b) HIU can help p in the delay of phase separation to different degrees depending on the oil used. However, it is not clear how the type of oil affects BW crystallization. For example, corn oil and soybean oil have both very similar fatty acid compositions (Table 4-1, 29.9 vs 23.9% of oleic acid), and the crystallization behavior of BW and phase separation observed are significantly different (Figures 4-1E and 4-5C) where more phase separation is observed in the soybean oil samples and a greater effect of sonication is observed in the corn oil samples (Figures 4-1F and 4-5D). It is possible that the differences observed are a consequence of the C18:3 content because the value observed in soybean oil is approximately 87% higher than in corn oil.

Similarly, Figure 4-6 shows the crystallization behavior of 1% BW in different vegetable oils cooled at $0.1\text{ }^{\circ}\text{C}/\text{min}$. Phase separation was observed in 1% BW samples crystallized in all of the oils tested (canola, corn, olive, safflower, and sunflower) when stored and was affected by the type of oil used.

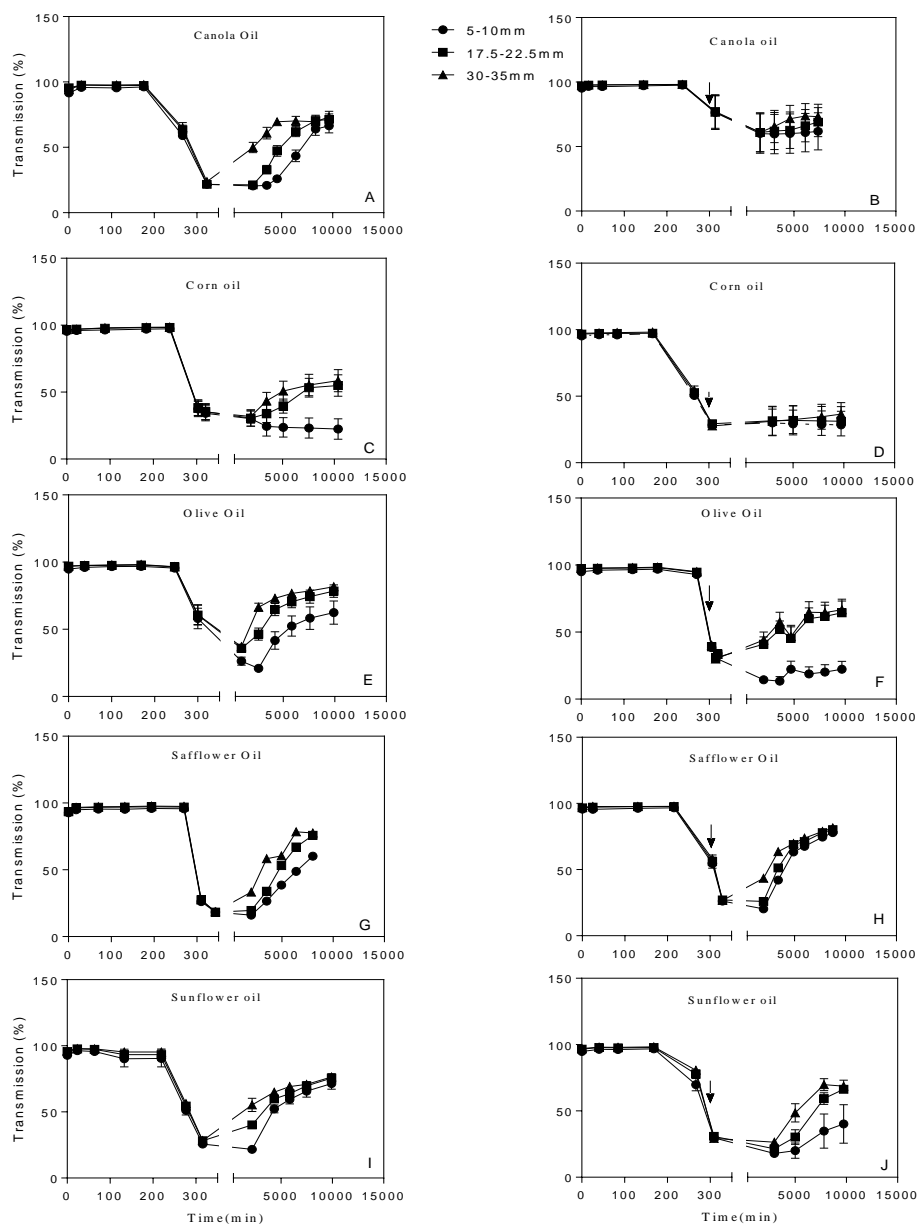


Figure 4-5. Transmission measurements of 0.5% BW in different edible oils crystallized at 25 °C for 7 days using slow cooling rate 0.1 °C/min without (left column) and with (right column) HIU. Figures A and B = canola oil, Figures C and D = corn oil, Figures E and F = olive oil, Figures G and H = safflower oil, Figures I and J = sunflower oil. The arrow shows the time of HIU application i.e.; 300 min after starting the experiment.

When 1% BW samples were crystallized in canola oil (Figure 4-6A), the sample remains more turbid at the bottom ($18 \pm 7\%$) after 5000 min and the transmissions at the middle and top parts were 25 ± 8 and $42 \pm 8\%$, respectively. At 340 min the transmissions in all three levels were the same for 1% BW samples in canola oil (almost 11%). When HIU (Figure 4-6B) was applied in 1% BW in canola oil sample, the transmission at the top level after 6000 min was $15 \pm 5\%$ and the transmissions at bottom and middle of the tube after 6000 min were 12 ± 4 and $12 \pm 4\%$, respectively.

This low value of transmission suggests that HIU decreases phase separation of 1% BW in canola oil. When 1% BW samples were crystallized in corn oil (Figure 4-6C), the contents at the top ($80 \pm 3\%$) and middle ($67 \pm 7\%$) of the tube were more transparent than that at the bottom part after 4500 min kept at 25 °C. Data collected from 1% BW sample with HIU application (Figure 4-6D) show no different transmission pattern (top level, $82 \pm 5\%$; middle, $78 \pm 6\%$; and bottom, $11 \pm 5.4\%$) in all levels of transmission after 6500 min of storage at 25 °C compared to the sample crystallized without HIU (Figure 4-6C). Previous research in our laboratory in anhydrous milk fat showed that the effect of HIU is less effective in samples crystallized under high driving forces.¹⁹

In this case, the higher concentration of wax (1 vs 0.5%) might create a high enough driving force that inhibits the effect of sonication to some degree. When 1% BW is crystallized in olive oil (Figure 4-6E), more turbidity at the bottom of the tube ($13 \pm 6\%$) is observed compared to the turbidity at the middle and top (50 ± 10.5 and $76 \pm 3\%$, respectively).

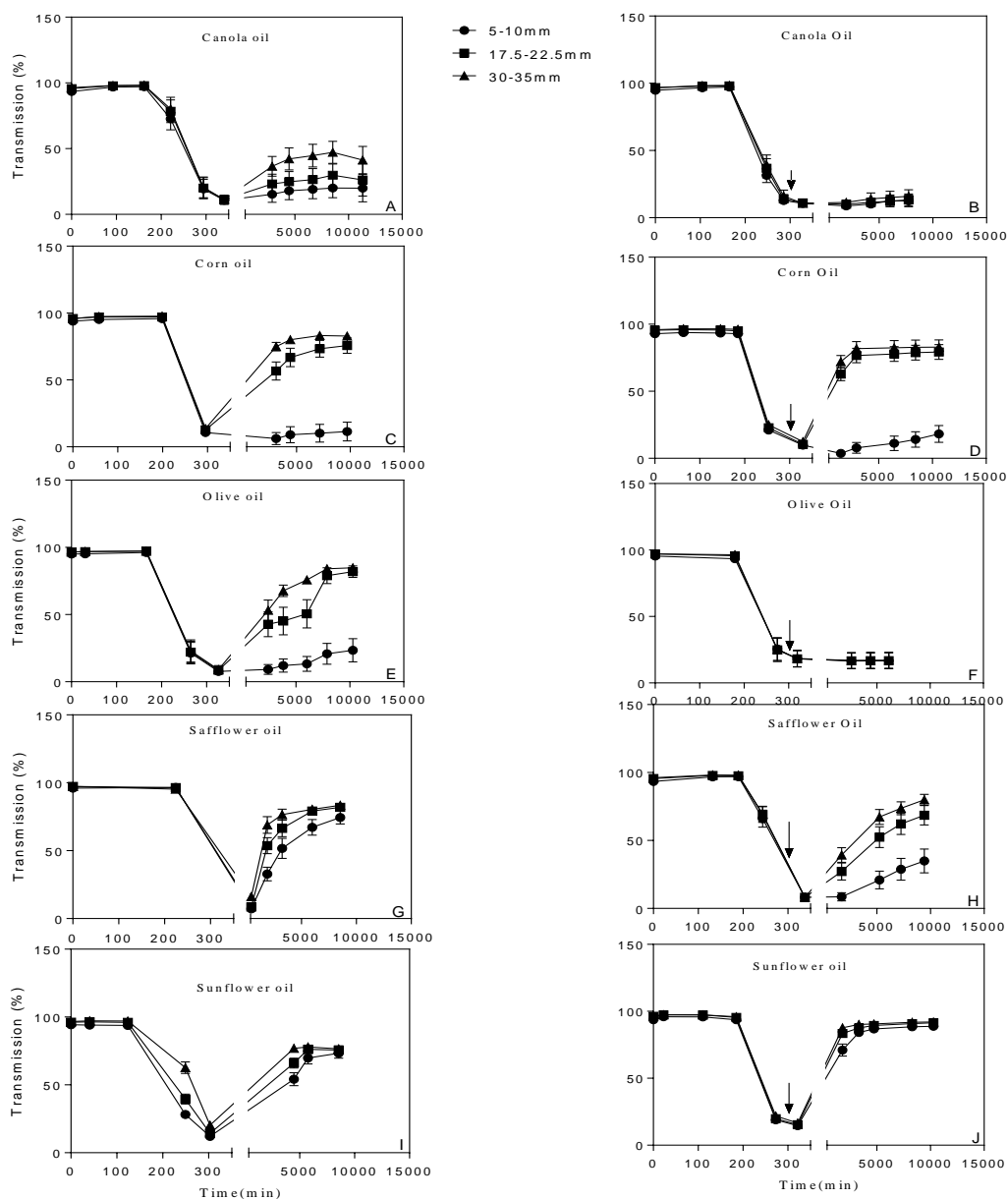


Figure 4-6. Transmission measurements of 1% BW in different edible oils crystallized at 25 °C for 7 days using slow cooling rate 0.1 °C/min without (left column) and with (right column) HIU. Figures A and B = canola oil, Figures C and D = corn oil, Figures E and F = olive oil, Figures G and H = safflower oil, Figures I and J = sunflower oil. The arrow shows the time of HIU application i.e; 300 min after starting the experiment.

The transmissions obtained for 1% BW samples crystallized with HIU (Figure 4-6F) were similar for the entire tube length. The bottom part shows $17 \pm 6\%$ transmission, the middle part shows $17 \pm 6\%$ transmission, and the top part shows $17 \pm 6\%$ transmission. Similar to the results shown for 1% BW crystallized in canola oil, HIU inhibited phase separation for a period of 7 days.

When 1% BW samples were crystallized in safflower oil (Figure 4-6G), phase separation was observed with transmission values of $80 \pm 2\%$ at the top, $79 \pm 3\%$ in the middle, and $67 \pm 6\%$ at the bottom after 6000 min of storage. When HIU was applied (Figure 4-6H), the transmission after 5200 min at the bottom was $21 \pm 6.5\%$. Lower transmission values were also obtained in sonicated samples in the middle ($52 \pm 8\%$) and in the top ($67 \pm 6\%$) sections of the tube. These results suggest that HIU helped delay phase separation in 1% BW crystallized in safflower oil.

When 1% BW was crystallized in sunflower oil (Figure 4-6I), there was a difference in transmission in the three sections of the tube after 4500 min; the contents in the bottom section are more turbid ($54 \pm 5\%$ transmission) than those in the middle ($66 \pm 4\%$) and top ($77 \pm 3\%$) sections. When HIU was applied in that sample (Figure 4-6J), transmission values through all sections of the tubes remained almost similar to the ones obtained without the use of HIU. Transmission values were $87 \pm 2\%$ at the bottom, $90 \pm 2\%$ in the middle, and $91 \pm 1\%$ at the top.

Figures 4-5 and 4-6 show that the degree of phase separation is not related to wax concentration and that the effect of HIU toward the delay of phase separation at both wax

concentrations (0.5 and 1%) highly depends on the type of oil used. The stability toward phase separation observed at 0.5% BW does not correlate with stability observed at 1% BW. For example, BW/corn oil samples are the most stable toward phase separation when used at a 0.5% level, whereas BW/ canola oil is the most stable when used at 1%.

Data reported in Figure 4-6 show that the stability toward phase separation increases in the following order: safflower oil < sunflower oil < soybean oil < corn oil < olive oil < canola oil. These data suggest that phase separation is probably related to the content of saturated fatty acids (SFA), where a higher content of SFA in the vegetable oil results in less phase separation. Table 4-1 shows that soybean, corn, and olive oils have a higher amount of SFA (15.5, 13.7, and 14.3%, respectively), and these oils show the least phase separation (Figures 4-1 and 4-6). On the other hand, sunflower and safflower oils have lower SFA contents of 7.8 and 6.4%, respectively, and show more phase separation (Figure 4-6).

The mixture of canola oil/BW seems to be an exception to this hypothesis because this sample is the most stable toward phase separation and has a low content of SFA (Figure 4-6; Table 4-1). It is possible that for a similar content of SFA a higher content of PUFA contributes to the higher stability toward phase separation. This could explain the different behaviors observed for canola oil and safflower oil samples and also for olive oil and corn oil (Table 4-1).

As suggested by Dassanayake et al.,^{12,13} it is likely that the physical characteristics (oleogel formation, phase separation) of the crystallized material are affected by the type

of crystalline network formed. Therefore, to better understand the different crystallization behaviors observed in BW samples crystallized in different oils with and without HIU, we analyzed the morphology of the crystals obtained after 7 days of storage.

Figures 4-7 and 4-8 show the morphology of crystals obtained in 0.5 and 1% BW, respectively, crystallized in different oils with and without HIU at 0.1 °C/min and stored at 25 °C for 7 days. Crystal morphology significantly changed depending on the type of oil used. When 0.5% BW was crystallized in canola oil without the use of HIU, big spherulites similar to the ones found in soybean oil were observed (Figures 4-2 and 4-7). This type of morphology was also observed in the BW crystallized in sunflower oil, although the spherulites were not as well formed as the ones observed in canola and soybean oils. Spherulite morphologies were maintained in BW crystallized in canola oil with the use of HIU but was not observed in BW crystallized in soybean and sunflower oils with HIU. Spherulites were also observed when 1% BW was crystallized in all of the vegetable oils but breaks down the spherulites, and small needle-like crystals are observed. We hypothesize that these needle-like crystals can interact more readily with each other, allowing for more oil entrapment and therefore delaying phase separation.

Figure 4-9 shows crystal average areas of samples crystallized with and without the use of HIU. It can be observed that HIU generated significantly smaller ($\alpha = 0.05$) crystals in 0.5% BW in all oils with the exception of safflower and soybean oils (Figure 4-9A). These two oils were the ones on which HIU had the least effects on decreasing the degree of phase separation (Figure 4-5G–J). The effect of HIU in reducing crystal size in the 1% BW solutions was not as evident as the one observed in the 0.5% BW solutions.

HIU reduced crystal areas in 1% BW in corn and sunflower oils ($p < 0.05$), whereas no significant effect was observed in the other oils (Figure 4-9B).

It is interesting to note that even though no significant differences were found in crystal areas in some of these samples, HIU was still effective at delaying phase separation. These results suggest that the effect of crystal area is less important in stabilizing the crystalline network at higher concentrations.

Further analysis on the characteristics of the crystals formed in BW/vegetable oil systems was performed using DSC. Table 4-2 illustrates onset and peak temperatures of crystals obtained from 0.5 and 1% BW crystallized in different oils (canola, corn, olive, safflower, sunflower, and soybean) at 0.1 °C/min with and without HIU application after 7 days of storage. The melting behavior of the wax crystals obtained from the different wax/oil combinations was very similar with T_{on} values between 38 and 41 °C for the 0.5% samples and between 38 and 45 °C for the 1% samples.

In general, the use of HIU resulted in a narrower melting profile as evidenced by either higher T_{on} values or lower T_p values in the sonicated samples. It is likely that the effect of HIU in delaying phase separation is related to the generation of a less fractionated crystalline network where similar molecules can interact strongly among them, entrapping more oil.

Overall, this study shows that several processing conditions can affect phase separation in wax/oil systems. Cooling rate, wax concentration, and type of oil play important roles in the crystallization behavior of waxes,

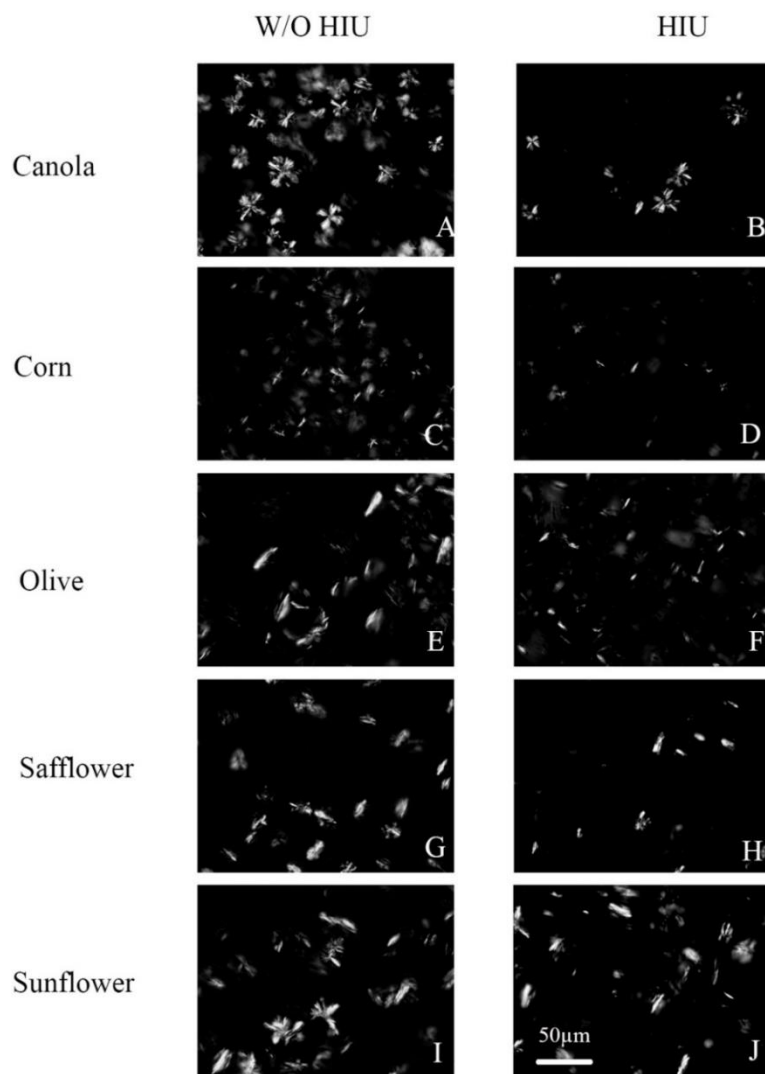


Figure 4-7. Morphology of crystals obtained when 0.5% BW is crystallized in different edible oils at slow cooling rate (0.1 °C/min) without (left column) and with (right column) HIU after 7 days of storage at 25 °C. Figures A and B = canola oil, Figures C and D = corn oil, Figures E and F = olive oil, Figures G and H = safflower oil, Figures I and J = sunflower oil. Crystal pictures were taken at 20X magnification under Polarized Light Microscopy. The white bar corresponds to 50 µm.

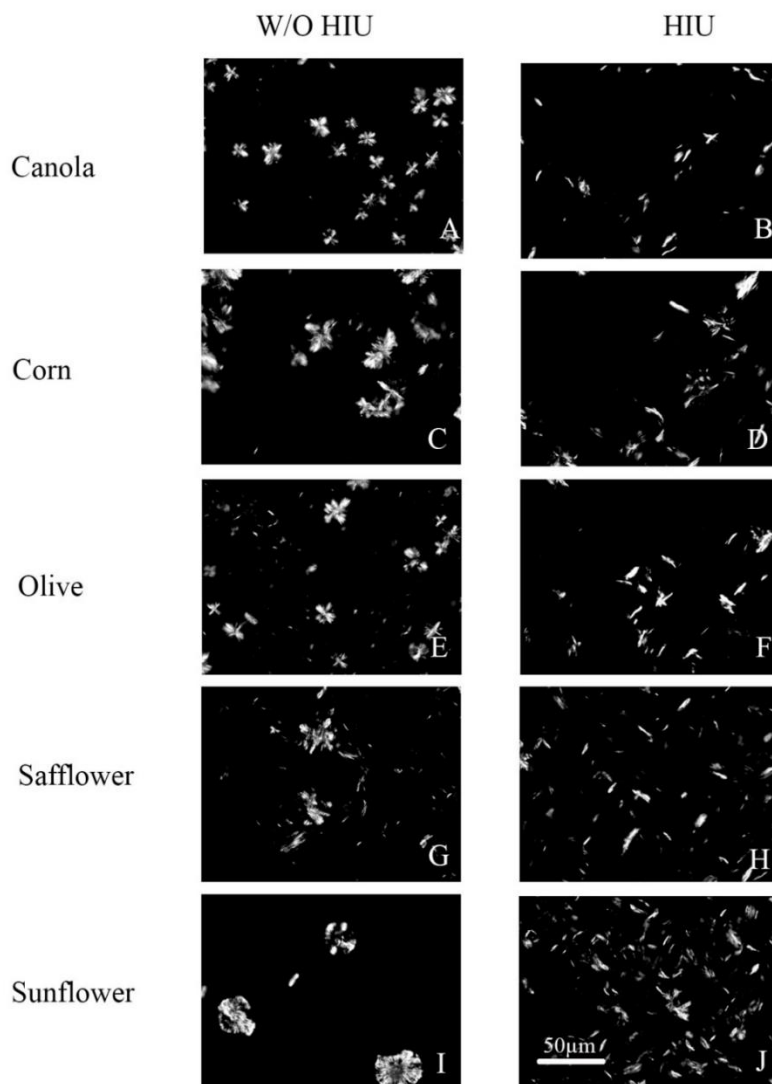


Figure 4-8. Morphology of crystals obtained when 1% BW is crystallized in different edible oils at slow cooling rate (0.1 °C/min) without (left column) and with (right column) HIU after 7 days of storage at 25 °C. Figures A and B = canola oil, Figures C and D = corn oil, Figures E and F = olive oil, Figures G and H = safflower oil, Figures I and J = sunflower oil. Crystal pictures were taken at 20X magnification under Polarized Light Microscopy. The white bar corresponds to 50 µm.

which can also be controlled by using HIU. It is still not clear how the different types of oils affect the crystallization of waxes, but this research suggests that crystal morphology might play an important role in phase separation.

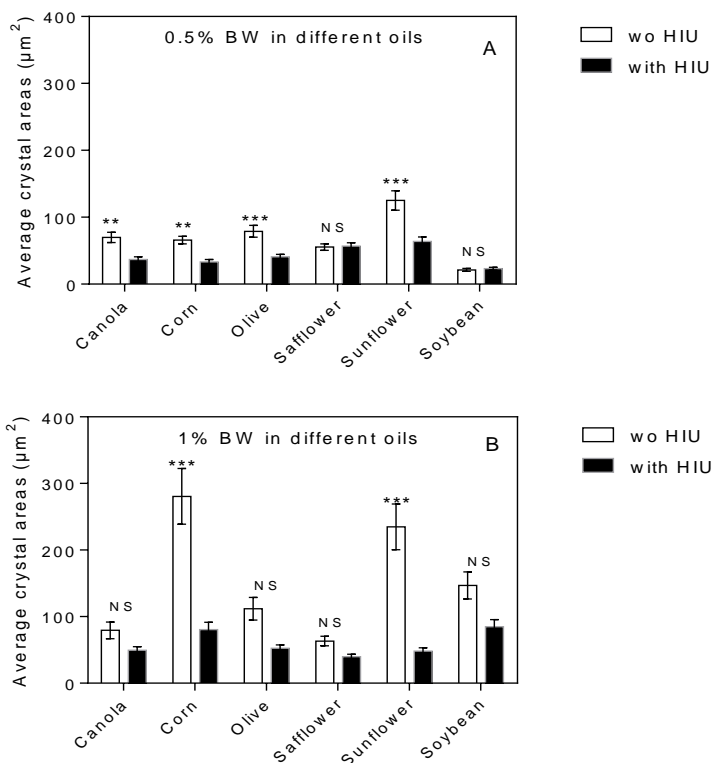


Figure 4-9. Mean crystal area (μm^2) of crystals obtained when 0.5% (A) and 1% (B) BW is crystallized in different vegetable oils (canola, corn, olive, safflower, sunflower, and soybean) at $0.1\text{ }^\circ\text{C}/\text{min}$ after 7 days of storage at $25\text{ }^\circ\text{C}$. Mean values and standard errors are reported. * $p < 0.05$, ** $p < 0.01$, *** $p < 0.001$, NS means non-significant ($\alpha = 0.05$). Minimum count of the crystals taken was 200 in all the cases.

Table 4-2. Onset (T_{on}) and peak (T_p) temperatures of crystals obtained from 0.5% BW and 1% BW crystallized in different edible oils (canola, corn, olive, safflower, sunflower, and soybean) at 0.1 °C/min without and with HIU after 7 days at 25 °C. Mean values and standard deviation of 2 independent runs are reported. NS means that T_{on} or T_p within each BW/oil samples are not significantly different ($\alpha = 0.05$). * means $p < 0.05$; ** means $p < 0.01$, *** means $p < 0.001$

| | | 0.5% BW | | | 1% BW | | |
|------------------------|------------------------------------|------------|------------|------|------------|------------|------|
| | | W/O | HIU | Sign | W/O HIU | HIU | Sign |
| | | HIU | | | | | |
| BW in Canola | T_{on} (°C) | 41.2 ± 0.0 | 40.7 ± 0.5 | NS | 38.0 ± 0.4 | 40.6 ± 1.4 | NS |
| | T_p (°C) | 53.8 ± 0.0 | 51.3 ± 0.5 | *** | 50.3 ± 1.9 | 52.2 ± 1.9 | NS |
| BW in Corn | T_{on} (°C) | 39.9 ± 0.3 | 39.2 ± 0.6 | NS | 41.3 ± 0.1 | 40.9 ± 0.9 | NS |
| | T_p (°C) | 50.4 ± 0.5 | 47.0 ± 0.4 | *** | 50.8 ± 0.5 | 51.8 ± 0.5 | NS |
| BW in Olive | T_{on} (°C) | 39.1 ± 0.3 | 40.7 ± 0.1 | NS | 37.9 ± 0.4 | 43.1 ± 0.9 | * |
| | T_p (°C) | 50.1 ± 0.5 | 52.1 ± 0.2 | ** | 47.4 ± 0.0 | 54.1 ± 0.7 | * |
| BW in Safflower | T_{on} (°C) | 40.3 ± 0.1 | 42.2 ± 0.4 | * | 44.0 ± 1.0 | 44.1 ± 1.1 | NS |
| | T_p (°C) | 52.2 ± 0.7 | 54.6 ± 0.6 | ** | 57.8 ± 0.8 | 54.1 ± 2.0 | * |
| BW in Sunflower | T_{on} (°C) | 41.0 ± 0.9 | 41.5 ± 0.7 | NS | 47.0 ± 0.1 | 48.9 ± 2.2 | NS |
| | T_p (°C) | 52.4 ± 0.5 | 53.2 ± 0.6 | NS | 57.4 ± 0.9 | 58.7 ± 0.9 | NS |
| BW in Soybean | T_{on} (°C) | 38.8 ± 1.1 | 40.5 ± 0.1 | * | 42.5 ± 0.1 | 38.3 ± 1.4 | * |
| | T_p (°C) | 50.9 ± 0.2 | 51.8 ± 0.5 | NS | 53.8 ± 0.4 | 51.7 ± 0.0 | NS |

Other factors such as the presence of minor components and the solubility of wax in the different oils might also play an important role in the crystallization behavior of these molecular entities and therefore on the phase separation observed during storage.

Results presented in this study suggest that HIU can be used to delay phase separation in wax/oil systems that have the potential to be used as *trans*-fat replacements in food products.

References

- (1) Shi, R.; Zhang, Q.; Vrieskoop, F.; Yuan, Q.; Liang, H. Preparation of organogel with tea polyphenols complex for enhancing the antioxidation properties of edible oil. *J. Agric. Food Chem.* 2014, 62, 8379–8384.
- (2) Sawalha, H.; den Adel, R.; Venema, P.; Bot, A.; Flöter, E.; van der Linden, E. Organogel-emulsions with mixtures of β -sitosterol and γ -oryzanol: influence of water activity and type of oil phase on gelling capability. *J. Agric. Food Chem.* 2012, 60, 3462–3470.
- (3) Jadhav, S. R.; Hwang, H.; Huang, Q.; John, G. Medium-chain sugar amphiphiles: a new family of healthy vegetable oil structuring agents. *J. Agric. Food Chem.* 2013, 61, 12005–12011.
- (4) Kerr, R. M.; Tombakan, X.; Ghosh, S.; Martini, S. Crystallization behavior of anhydrous milk fat-sunflower oil wax blends. *J. Agric. Food Chem.* 2011, 59, 2689–2695.

- (5) Toro-Vazquez, J. F.; Morales-Rueda, J. A.; Dibildox-Alvarado, E.; Charo-Alonso, M.; Alonzo-Macias, M.; Gonzalez-Chavez, M. M. Thermal and textural properties of organogels developed by candelilla wax in safflower oil. *J. Am. Oil Chem. Soc.* 2007, 84, 989–1000.
- (6) Morales-Rueda, J. A.; Dibildox-Alvarado, E.; Charo-Alonso, M. A.; Toro-Vazquez, J. F. Rheological properties of candelilla wax and dotriacontane organogels measured with a true-gap system. *J. Am. Oil Chem. Soc.* 2009, 86, 765–772.
- (7) Morales-Rueda, J. A.; Dibildox-Alvarado, E.; Charo-Alonso, M. A.; Weiss, R. G.; Toro-Vazquez, J. F. Thermo-mechanical properties of candelilla wax and dotriacontane organogels in safflower oil. *Eur. J. Lipid Sci. Technol.* 2009, 111, 207–215.
- (8) Toro-Vazquez, J. F.; Alonzo-Macias, M.; Dibildox-Alvarado, E.; Charo-Alonso, M. A. The effect of tripalmitin crystallization on the thermomechanical properties of candelilla wax organogels. *Food Biophys.* 2009, 4, 199–212.
- (9) Toro-Vazquez, J. F.; Morales-Rueda, J.; Mallia, V. A.; Weiss, R. G. Relationship between molecular structure and thermo-mechanical properties of candelilla wax and amides derived from (R)-12-hydroxystearic acid as gelators of safflower oil. *Food Biophys.* 2010, 5, 193–202.
- (10) Chopin-Doroteo, M.; Morales-Rueda, J. A.; Dibildox-Alvarado, E.; Charo-Alonso, M. A.; de la Peña-Gil, A.; Toro-Vazquez, J. F. The effect of shearing in the thermo-mechanical properties of candelilla wax and candelilla wax-tripalmitin organogels. *Food Biophys.* 2011, 6, 359–376.

- (11) Alvarez-Mitre, F. M.; Morales-Rueda, J. A.; Dibildox-Alvarado, E.; Charo-Alonso, M. A.; Toro-Vazquez, J. F. Shearing as a variable to engineer the rheology of candelilla wax organogels. *Food Res. Int.* 2012, 49, 580–587.
- (12) Dassanayake, L. S. K.; Kodali, D. R.; Ueno, S.; Sato, K. Physical properties of ricebran wax in bulk and organogels. *J. Am. Oil Chem. Soc.* 2009, 86, 1163–1173.
- (13) Dassanayake, L. S.; Kodali, D. R.; Ueno, S.; Sato, K. Crystallization kinetics of organogels prepared by rice bran wax and vegetable oils. *J. Oleo Sci.* 2012, 61, 1–9.
- (14) Hwang, H. S.; Kim, S.; Singh, M.; Winkler-Moser, J. K.; Liu, S. X. Organogel formation of soybean oil with waxes. *J. Am. Oil Chem. Soc.* 2012, 89, 639–647.
- (15) Hwang, H. S.; Singh, M.; Bakota, E. L.; Winkler-Moser, J. K.; Kim, S.; Liu, S. X. Margarine from Organogels of plant wax and soybean oil. *J. Am. Oil Chem. Soc.* 2013, 90, 1705–1712.
- (16) Blake, A. I.; Co, E. D.; Marangoni, A. G. Structure and physical properties of plan wax crystal networks and their relationship to oil binding capacity. *J. Am. Oil Chem. Soc.* 2014, 91, 885–903.
- (17) Yilmaz, E.; Ögütçü, M. Properties and stability of hazelnut oil organogels with beeswax and monoglyceride. *J. Am. Oil Chem. Soc.* 2014, 91, 1007–1017.
- (18) Dassanayake, L. S.; Kodali, D. R.; Ueno, S. Formation of oleogels based on edible lipid materials. *Curr. Opin. Colloid Interface Sci.* 2011, 16, 432–439.

(19) U.S. Food and Drug Administration. Food Additive Status List,

<http://www.fda.gov/Food/IngredientsPackagingLabeling/>

FoodAdditivesIngredients/ucm091048.htm (accessed June 2014).

(20) Ye, Y.; Wagh, A.; Martini, S. Using high intensity ultrasound as a tool to change the functional properties of interesterified soybean oil. *J. Agric. Food Chem.* 2011, 59, 10712–10722.

(21) Martini, S.; Tippetts, M. Effect of processing conditions on the crystallization behavior and destabilization kinetics of oil-in-water emulsions. *J. Am. Oil Chem. Soc.* 2008, 85, 119–128.

(22) Martini, S.; Herrera, M. L.; Hartel, R. W. Effect of cooling rate on crystallization behavior of milk fat fraction/sunflower oil blends. *J. Am. Oil Chem. Soc.* 2002, 79, 1055–1062.

CHAPTER 5

VISCOELASTIC PROPERTIES OF WAX/OIL CRYSTALLINE NETWORKS²

Abstract

The objective of this research is to evaluate the viscoelastic properties of three different waxes such as sunflower, paraffin and beeswax in different vegetable oils (soybean, canola, corn, sunflower, safflower and olive oil) at different concentrations such as 1, 2.5, 5 and 10%. In general it was observed that amount of wax increase in wax/oil system increases elastic modulus G' . When SFW was used in wax/oil system G' values show significant differences in different oils. Higher G' values were observed when SFW was used in the system (2 to 6×10^6 Pa) compared to BW and PW in different oils. BW samples resulted in significantly higher ($P < 0.05$) G' values in the 5% and 10% samples with values of 3.9×10^6 and 6.1×10^5 Pa for 10% BW and PW, respectively.

Introduction

The ability of a wax/oil system to form a crystalline network with specific characteristics such as texture and melting behavior depends on the concentration of the wax used and on the types of wax and oil used. Hwang and others (2013) showed that the firmness of wax/oil crystalline networks was affected by the type of wax and by the source of the wax. For example, sunflower

² Partially adapted with permission from Martini, S.; Tan, C. Y.; Jana, S. Physical Characterization of Wax/Oil Crystalline Networks. *Journal of Food Science*. Vol.80, Nr.5, 2015 (C989- C997). © 2015 Institute of Food Technologists.

waxes created the firmest crystalline network, followed by candelilla waxes, whereas rice bran waxes created the least firm networks. Toro-Vazquez and others (2007) reported that a minimum of 2% wax is necessary to form a well-structured three-dimensional network that does not flow upon inversion of the container.

Similarly, Hwang and others (2012) reported that sunflower waxes can form a gel-like structure at concentrations as low as 0.5%. These authors also evaluated the crystallization behavior of candelilla wax and rice bran wax in soybean oil and explained that longer wax esters have a better crystallization behavior. But there is no systematic approach taken towards finding of the characterization of wax/oil system using different chemical composition of waxes in different oils at different wax concentrations.

Viscoelastic properties play a major role in wax/oil crystalline network formation as sensory properties of the final products are dependent on it. Therefore the objective of this research was to characterize the visco-elastic properties of 3 waxes of different chemical composition: sunflower oil wax (66-69% was ester, 6-7% hydrocarbon, 12-16% free fatty acids, 11-13% fatty alcohol), beeswax (35% wax ester, 24% hydroxyl ester, 14% hydrocarbon, 12% free fatty acids, 12% di-esters), and paraffin wax (100% hydrocarbon) in different vegetable oils: soybean, canola, corn, sunflower, safflower, and olive oil. Wax concentrations of 1%, 2.5%, 5%, and 10% were used in this study.

Materials and methods

Commercial vegetable oils (soybeanoil [SBO; WesternFamily], canola [CAO; Kroger], corn [CO; Kroger], sunflower [SFO; Antoine & Muse], safflower [SAFO;

LouAnna], and oliveoil [OO; Great Value]) were used in this study. Three different waxes (sunflowerwax [SFOW], beeswax [BW], and paraffinwax [PW]) were added to the vegetable oils at different concentrations (1%, 2.5%, 5%, and 10%). All waxes were purchased from Koster Keunen, Inc. (Watertown, Conn., U.S.A.). As previously reported by Hwang and others (2012), SFOW is composed of approximately 70% wax esters (long-chain saturated alcohols esterified to long-chain saturated fatty acids), 15% fatty acids, 10% fatty alcohols, and 5% n-alkanes. BW is composed of approximately 35% wax esters, 24% hydroxyl esters, 14% n-alkanes, 12% diesters, and 12% free acids. Finally, PW is a mixture of n-alkanes (C₂₀ to C₄₀). These waxes were chosen to evaluate the effect of chemical composition on their crystallization behavior in different vegetable oils.

Preparation of wax/oil samples

Mixtures of 1%, 2.5%, 5%, and 10% (wt. basis) of waxes in vegetable oil were prepared in a beaker (50 g total). The wax/oil samples were placed in an oven at 100 to 120 °C for 30 min, stirred with a glass pipette, and left in the oven for another 15 min. This thermal treatment was performed to allow for a complete melting of the sample. Melted samples were then stirred and placed in an incubator at 25 °C for 24 h to allow complete crystallization. Crystal morphology, melting behavior, and rheology measurements were performed after storage at 25 °C for 24 h.

Viscoelastic properties of wax/oil samples

A TA Instruments AR-G2 Magnetic Bearing Rheometer was used to evaluate the viscoelastic properties of the material. Oscillatory tests were performed at 25 °C by a strain sweep step to obtain storage modulus (G'). Concentric cylinder geometry was used for the 1% concentration. A 10-mL pipette was used to transfer the crystallized sample from the beaker to the rheometer cylinder which was kept at 25 °C. A 40-mm-diameter parallel-plate geometry was used for the 2.5%, 5%, and 10% concentrations. A spoon was used to transfer the samples from the 2.5% and 5% samples to the rheometer plates, whereas 10% samples were crystallized directly in 40-mm-diameter molds that were held at 25 °C in a water bath for 24 h. For each concentration of waxes and respective oil combination, there were 2 replicates and 2 rheology measurements taken from each replicate. Therefore, a total 4 measurements were taken for each wax/oil mixture.

Results and discussion

Viscoelastic Properties

In general, the crystallization behavior of lipids and the type of microstructure generated affect the viscoelastic properties of the crystalline network formed. The viscoelastic properties of the wax/oil systems were quantified using the elastic modulus (G') which represents the solid-like behavior, or elasticity, of the material.

Figure 5-1 summarizes the G' values obtained for samples crystallized at 25 °C as a function of wax content, and wax and oil type. As expected, G' values increased with wax concentration with values as low as 5 Pa for the 1% samples to approximately 1×10^7

for the 10% samples. However, the rate of G' increase as a function of wax concentration was affected by wax and oil type. When lower concentrations of waxes (1% and 2.5%) are used, crystalline networks formed with SFOW had higher G' values compared with materials formulated with PW and BW for all the oils tested. However, the elasticity of BW samples increased for the 5% and 10% samples reaching similar values to the ones observed for the SFOW samples. Crystalline networks formulated with PW remained with a low elasticity value compared to SFOW and BW samples. G' values of the wax/oil samples were different from the ones observed for pure waxes, where the highest G' values were observed for PW ($3.0 \times 10^8 \pm 4.7 \times 10^7$ Pa) followed by SFOW ($1.6 \times 10^8 \pm 2.1 \times 10^6$ Pa) and the lowest value was obtained for BW ($8.0 \times 10^7 \pm 6.4 \times 10^6$). It is evident from Figure 5-1 that G' values were significantly affected, in some cases by the type of oils used.

Figure 5-1 A shows the G' values obtained for wax/oils samples crystallized at 1%. The crystalline networks obtained with BW had the lowest G' value followed by PW samples and finally by SFOW samples. No significant differences were observed in G' values of the BW samples crystallized in different oils, however some differences were observed for the SFOW and the PW samples. The highest G' values in PW were observed for samples crystallized in SFO and CO, whereas the highest G' values obtained for SFOW samples were observed in SBO samples. Similarly to the results described for the 1% samples, BW samples crystallized at 2.5% concentration had the lowest G' values and these were not affected by the type of oil used (Figure 5-1 B).

These values were not significantly different from the ones obtained for PW samples and were significantly lower than the ones obtained for SFOW. The highest G' values obtained for SFOW samples crystallized at 2.5% were observed for SFO, CAO, and OO. G' values obtained for 5% samples of BW were significantly higher than the ones observed for PW.

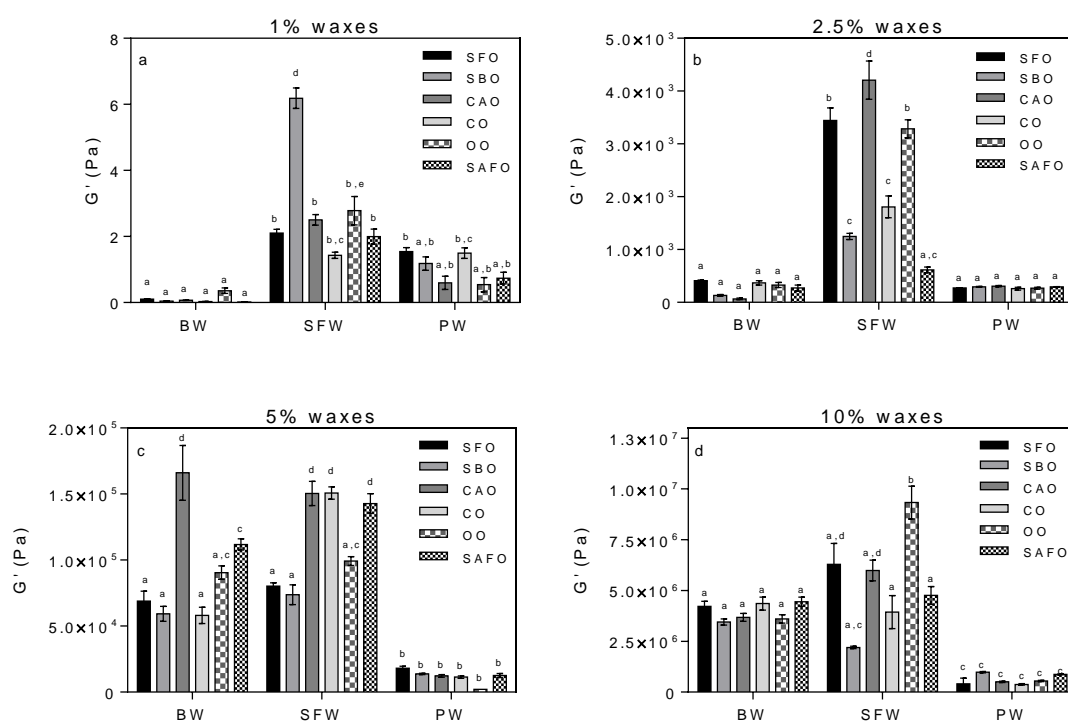


Figure 5-1. Viscoelastic properties of wax/oil systems crystallized at 1, 2.5, 5, and 10% concentrations (a-d, respectively) after 24 h incubation at 25°C. Within each wax concentration, same letters indicate that values are not significantly different ($\alpha = 0.05$).

The highest G' value observed for 5% BW was obtained for the sample crystallized in CAO and SAFO (Figure 5-1 C). G' values obtained for BW at this concentration were similar to the ones obtained for SFOW, where the highest values were obtained for SFOW crystallized in CAO, CO, and SAFO. As previously mentioned, G' values for PW remained lower than the ones obtained for BW and SFOW when samples were crystallized at 10% concentration (Figure 5-1 D).

Similar to the results reported for the 5% samples, BW G' values were similar to the ones observed for the SFOW samples; however, in this case, the type of oil used did not affect the G' values of BW samples, where as it significantly affected the G' value of SFOW samples with higher values obtained for the samples crystallized in OO.

Conclusion

This study shows that elastic modulus G' increases as wax amount increases in wax/oil system; type of wax did not make any difference. Changes in G' values did not show any significant differences when PW was used in all the oils at 2.5, 5 and 10% concentrations. Similar results were found when BW was used in different oils but at concentrations of 1, 2.5 and 10%. But there were significant differences in G' values observed when SFW was used in all the oils in different wax concentrations. No particular reason can be made to explain this difference but wax solubility could play a role in this difference. Amount of wax ester presence in waxes drives G' values. SFW with higher wax ester compared to BW shows highest G' values followed by BW and PW with no wax ester presence shows lowest G' values.

References

1. Hwang H, Singh M, Bakota EL, Winkler-Moser JK, Kim S, Liu SX. 2013. Margarine from organogels of plant wax and soybean oil. *J Am Oil Chem Soc* 90:1705–12.
2. Toro-Vazquez JF, Morales-Rueda JA, Dibilidox-Alvarado E, Charo-Alonso M, Alonzo-Macias M, Gonzalez-Chavez MM. 2007. Thermal and textural properties of organogels developed by candelilla wax safflower oil. *J Am Oil Chem Soc* 84:989–1000.
3. Hwang H, Kim S, Singh M, Winkler-Moser JK, Liu S. 2012. Organogel formation of soybean oil with waxes. *J Am Oil Chem Soc* 89:639–47.

CHAPTER 6
PHASE BEHAVIOR OF BINARY BLENDS OF FOUR
DIFFERENT WAXES³

Abstract

The objective of this study was to investigate the phase behavior of binary blends of four waxes—beeswax (BW), paraffin wax (PW), sunflower wax (SFW), and rice bran wax (RBW)—using differential scanning calorimetry (DSC) and polarized light microscopy (PLM). Blends of BW/PW, RBW/PW, SFW/PW, SFW/RBW, SFW/BW, and RBW/BW were crystallized in a DSC, and their melting behavior was used to build binary phase diagrams. The microstructure of the crystalline networks formed in these blends was analyzed using PLM. BW/PW, SFW/PW, SFW/BW, and RBW/BW blends showed eutectic phase behavior, while RBW/SFW showed continuous solid solution and the RBW/PW blend showed monotectic behavior. Results from the box-counting fractal dimension (D_b) measurement of crystal morphology showed higher D_b values for the 20 and 80 % wax blends, irrespective of crystallization temperature or wax type. D_b values of single waxes decrease as temperature increases.

³ Reprinted with permission from (Jana, S.; Martini, S. Phase Behavior of Binary Blends of Four Different Waxes. *J Am Oil Chem Soc* DOI 10.1007/s11746-016-2789-6) License Number: 3824981256921 © American Oil Chemists' Society (2016)

Introduction

Waxes have recently been used by food researchers to entrap vegetable oil and create semi-solid materials that can be used as a replacement for *trans*-fat in food products such as margarine, ice-cream, and shortening [1–12]. The physical properties of waxes, including hardness, viscoelasticity, smoothness, and encapsulation efficiency, are driven by the molecular composition and molecular interactions that occur during crystallization. Waxes such as sunflower wax (SFW), beeswax (BW), and rice bran wax (RBW) in particular have garnered attention within the food industries, given the natural origin of these materials and the possibility of including them in clean-label products. However, the crystallization behavior—and therefore the functional properties—of these materials differ significantly due to differences in their chemical composition. For example, paraffin wax (PW) is formed mainly of high molecular weight n-alkanes, and RBW consists mainly of long-chain aliphatic esters, while SFW and BW are a mixture of n-alkanes, esters, free fatty acids, and aliphatic alcohols. Despite a significant amount of research dedicated to evaluating the phase behavior of natural waxes [2, 4, 5, 8, 10–16], none of these studies have evaluated the phase behavior of wax mixtures. Using combinations of different waxes can help in designing wax materials with specific physical properties for various food applications.

The phase behavior of binary systems can be investigated using phase diagrams. A phase diagram shows the different phases (solid, liquid, or gas) of materials at equilibrium as a function of temperature and composition, and sometimes of pressure. This diagram helps to determine the total amount of material that can be crystallized

under any given condition. Binary phase diagrams are typically constructed by blending different proportions of two pure components. Natural waxes, however, are mixtures of different molecular entities [17], and phase diagrams constructed for these types of materials are usually referred to as pseudo-phase diagrams [18]. The use of phase and pseudo-phase diagrams in food systems has been reported by several researchers [19–24]. Mixtures of pure triacylglycerols [21, 25, 26], fatty acids [17, 20], and monoacylglycerols [23] were studied using phase diagrams, while pseudo-phase diagrams were reported for confectionery fats such as cocoa butter and anhydrous milk fat [19, 27]. Pseudo-phase diagrams have become an important tool in the confectionery industry for identifying fats that are compatible with cocoa butter and that will not form eutectics [19, 27]. Eutectic formation between fats and cocoa butter result in a softer material that significantly affects product quality and shelf life.

Pseudo-phase diagrams can be used to understand the phase behavior of binary wax systems. These diagrams can also be helpful in evaluating the effect of different molecular entities present in natural waxes on the crystallization behavior of the system. It is also important to characterize the types of crystalline networks formed in terms of crystal morphology, as this will significantly affect the physical property of the material. Therefore, the objective of the present study was to evaluate the phase behavior of four different waxes (BW, PW, SFW, and RBW) and their binary mixtures using differential scanning calorimetry and polarized light microscopy.

Experimental procedures

Materials and Sample Preparation:

Beeswax (BW) and rice bran (RBW), sunflower (SFW), and paraffin (PW) waxes were supplied by Koster Keunen, LLC (Watertown, CT, USA). The chemical composition [17] and melting points of the waxes are presented in Table 6-1. Binary systems were prepared by mixing these waxes (PW/BW, PW/RBW, PW/SFW, RBW/BW, RBW/SFW, and SFW/ BW) in different proportions from 0 to 100 % in 10 % increments. The binary systems were prepared by placing specific amounts of the waxes in 17×60 -mm² (8 ml) vials to reach 1 g of solids. Approximately 7 ml of hexane was added to the vial, which was then closed with an appropriate lid.

Vials were placed in a sonication water bath for 5–10 min and on a vortex mixer for 1–2 min to allow for complete dissolution of the waxes in the hexane. The vial lids were then loosened, and the vials placed under the airflow of a thin-wall fume hood for 1 week to evaporate the hexane. The remaining solid was utilized to obtain the phase diagrams using differential scanning calorimetry and to evaluate crystal morphology by polarized light microscopy.

Differential Scanning Calorimetry (DSC):

The melting profiles of the different samples were measured using differential scanning calorimetry (DSC 2910 Modulated DSC; TA Instruments - Waters LLC, New Castle, DE, USA). The DSC baseline and temperature was calibrated with a pure indium standard.

Table 6-1. Typical chemical composition of waxes used in this study as previously reported by Hwang et al.[17]. Melting points of waxes used in this study measured by DSC. Melting points are the representation of T_p values in duplicates.

| Chemical Composition | Beeswax | Rice bran Wax | Sunflower Wax | Paraffin Wax |
|---------------------------------------|----------------|----------------------------|--------------------------------|------------------|
| Wax Esters | 35% C50 | 100% (C44 – C64 saturated) | 66 – 69% (C38 – C54 saturated) | -- |
| Hydroxyl Esters | 24% | -- | -- | -- |
| Hydrocarbons | 14% | -- | 6 – 7% | 100% (C20 – C40) |
| Free Fatty Acids | 12% | -- | 12 – 16% | -- |
| Di Esters | 12% | -- | -- | -- |
| Fatty Alcohols | -- | -- | 11-13% | -- |
| Unidentified Compounds | 6% | -- | -- | -- |
| Melting Points ($^{\circ}\text{C}$) | 60.5 ± 3.0 | 80.8 ± 0.8 | 75.5 ± 0.0 | 60.5 ± 0.2 |

Approximately 10–15 mg of wax crystals was placed in hermetic aluminum pans, covered with a hermetic aluminum lid, and sealed. Samples were equilibrated at 100 $^{\circ}\text{C}$ and kept isothermal for 15 min to allow for complete melting of the sample. This step

was followed by a ramp of $-0.5\text{ }^{\circ}\text{C}/\text{min}$ to reach $25\text{ }^{\circ}\text{C}$ in order to evaluate the crystallization behavior of the sample, and then by an isothermal step for 90 min.

Lastly, a ramp of $0.5\text{ }^{\circ}\text{C}/\text{min}$ was used to heat the sample to $100\text{ }^{\circ}\text{C}$ to analyze its melting behavior. DSC runs were performed in duplicate. Slow cooling and heating rates were used in these experiments to allow phase transitions to occur close to equilibrium. TA Universal Analysis software was used to analyze the melting onset (T_{on}) and peak (T_{p}) temperatures and melting enthalpies (ΔH).

Experimental Pseudo-Phase Diagram:

Experimental pseudo-phase diagrams were constructed from the melting curves obtained from the DSC. Phase diagrams were constructed using the onset temperature (T_{on}) of the lowest melting peak and the peak temperature (T_{p}) of the highest melting peak to represent an approximation of the onset and completion of the melting process [23]. These values were plotted as a function of the composition of the binary mixture.

Crystal Morphology:

Vials with the binary wax systems were placed in an oven set at $85\text{--}90\text{ }^{\circ}\text{C}$ for at least 30 min. A small amount of molten sample was gently placed on a glass microscope slide and covered with a glass-covered slip. This operation was performed with all the materials placed in the oven and working with the doors open to avoid wax crystallization during the process. After slides were prepared, they were rapidly transferred to a temperature-controlled stage (STC200; Instec Inc., Boulder, CO, USA) set at $90\text{ }^{\circ}\text{C}$. Samples were then cooled to $25\text{ }^{\circ}\text{C}$ (room temperature) and $50\text{ }^{\circ}\text{C}$ using the same

temperature profile as that for the DSC experiments ($-0.5\text{ }^{\circ}\text{C}/\text{min}$) and WINTEMP MFC Application Software (Instec Inc.). This experiment was carried out in duplicate, and images were obtained in duplicate from each slide. The objective in using these two crystallization temperatures was to evaluate crystal morphologies of solid materials obtained at different points in the phase diagrams. Crystal morphologies were evaluated for 0, 20, 80 and 100 % mixtures of all binary systems. Crystals obtained were observed using a polarized light microscope (PLM, Olympus BX41; Olympus Optical Co., Tokyo, Japan). Digital images were captured using Lumenera's INFINITY2-2 (Lumenera Corporation, Nepean, Canada).

Box - Counting Fractal Dimension Measurements:

All morphology images (grayscale) were processed for the box-counting method using Benoit 1.3 software (Tru- Soft Int'l Inc., St. Petersburg, FL, USA). Fractal dimension (D_b) values at all concentrations tested (0, 20, 80 and 100 %) were measured and compared. The microscopic images were set to its threshold level using Adobe Photoshop CS2 (Adobe Systems Inc., San Jose, CA, USA), and the images were then processed using Benoit software. The box-counting fractal dimension, D_b , was calculated as the negative of the slope of the linear regression curve of the log-log plot of the number of occupied boxes N_b vs. the side length l_b [29–31]. D_b values were calculated for two images, and the mean value and standard deviations are reported. Significant differences were tested using two-way ANOVA and Tukey's post hoc test ($\alpha = 0.05$).

Results and discussion

Melting Behavior:

Figure 6-1 shows the DSC melting profiles of all binary systems tested in this study. Figure 6-1a depicts the melting profile of the BW/PW mixtures. The melting profile of 100 % PW is characterized by two peaks at 44.7 and 60.5 °C, while the melting profile of 100 % BW is characterized by two peaks at approximately 52.1 and 60.5 °C. The BW/PW blends at 10–50 % concentration show melting profiles similar to those observed for 100 % PW (0 % BW), with only two melting peaks observed. The melting peak that appears at lower temperatures in PW mixtures remains constant for all concentrations of the BW/PW mixture. The second peak of PW merges with BW peaks at 40 % BW/ PW concentration, but still only two peaks are observed for 40 and 50 % BW/PW samples. Based on the T_p values of these peaks, it is very likely that the first peak of these samples is associated with the melting of PW, while the second peak is the combination of PW and BW peaks. Three melting peaks are observed for the 60–90 % BW/PW samples. Similar to that previously discussed, the first peak of these concentrations corresponds to the first peak of PW.

It is possible that the second peak is the combination of the second peak of PW and the first peak of BW, while the third peak is a combination of the second peak of PW and the second peak of BW. These DSC melting profiles suggest that the presence of BW affects the melting behavior of PW, indicating some degree of co-crystallization of these two systems. This effect will be discussed later with specific phase diagrams.

Figure 6-1b shows the melting profile of mixtures of RBW/PW at different relative concentrations of each component. RBW has only one peak at approximately 80.8 °C. At 0 % RBW/PW (i.e. 100 % PW), two melting peaks are observed. For samples of 10–90 % RBW/PW concentration, three melting peaks are observed. Based on the T_p values of 100 % of the components, the first two melting peaks (those at lower temperatures) correspond to PW, and the third peak corresponds to the RBW.

In these cases, it is possible that RBW did not affect the melting behavior of PW, suggesting that RBW did not co-crystallize with PW, and melting peaks originating from each type of wax were thus easily identifiable.

Figure 6-1c shows the melting profile of the SFW/ PW blends. SFW has only one melting peak, at approximately 75.5 °C, and as previously discussed, PW has two melting peaks. The first melting peak (observed at lower temperatures) of PW remains approximately constant and is not affected by the presence of the second component in the mixture for samples composed of 0 % SFW/PW (i.e. 100 % PW) to 90 % SFW/PW concentrations. The second peak of PW remains approximately constant for samples composed of 0–80 % SFW/PW concentration. However, a third melting peak is observed at higher temperatures in samples with 60–80 % SFW/PW binary mixture. Based on the T_p of the melting peak of 100 % SFW, it is very likely that this third peak is associated with the melting of SFW components. The absence of the third peak in samples with 10–50 % SFW suggests that SFW components co-crystallize with PW when mixed at these proportions.

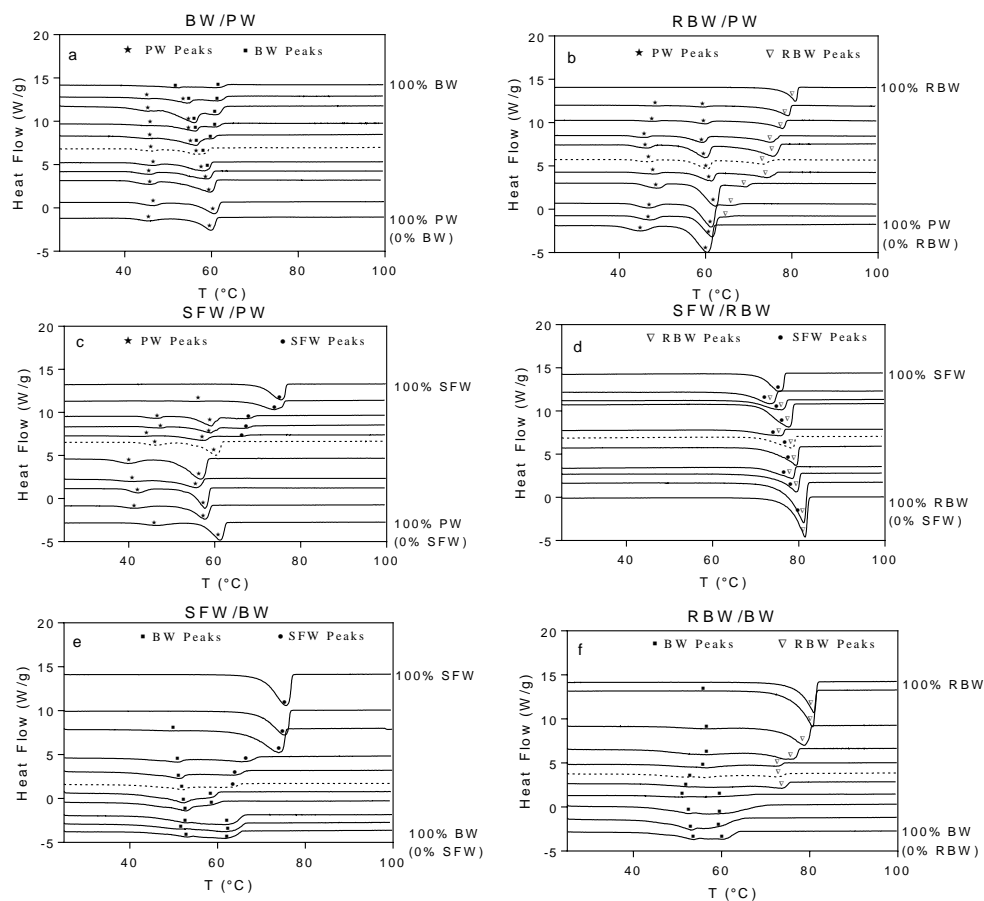


Figure 6-1. DSC melting profile of binary blends of waxes. Melting profiles for BW/PW, RBW/PW, SFW/PW, SFW/RBW, SFW/BW, and RBW/BW are shown in a, b, c, d, e, and f, respectively. From the bottom to the top lines represent the melting behavior of binary wax mixtures at 10% interval increases of the first component. The first line from the bottom represents the DSC melting profile of the second wax component of the blend (100%) and the top line represents the melting profile of the first wax component of the blend (100%). The dotted line represents 50% of the binary wax blend. Peaks associated with each wax type are indicated with different symbols.

It is interesting to note that although RBW and SFW have a similar melting temperature (Table 6-1), the binary mixtures with PW show very different behavior, where RBW does not seem to co-crystallize with PW, while partial co-crystallization seems to occur with SFW and PW.

Figure 6-1d shows the melting profile of SFW/RBW binary wax systems. SFW and RBW have similar melting temperatures (75.1 °C for SFW and 80.9 °C for RBW), and a single peak is observed for all SFW/RBW concentrations tested. These waxes co-crystallize, showing only one melting peak for all proportions of SFW in RBW, perhaps indicating that there should be a continuous solid system in the binary wax mixture.

Figure 6-1e shows the melting profile of SFW/BW binary wax mixtures. As previously described, SFW has only one melting peak (75.1 °C), whereas BW has two. The addition of SFW to BW changes the crystallization behavior of BW for samples composed of 10–80 % SFW/BW. The first peak of BW remains approximately constant for samples composed of 0 % SFW/BW (i.e. 100 % BW) to 80 % SFW/BW concentration; however, the T_p of the second BW melting peak decreases, reaching a minimum for the 40 % SFW/ BW sample. From 50 to 80 % of the SFW/BW mixture, the T_p of the second peak observed in the melting profiles increases, reaching values similar to those observed for the 100 % SFW. Similar to the behavior described for the BW/ PW and SFW/PW, the presence of SFW affects the melting behavior of BW, suggesting some degree of co-crystallization in the system.

Figure 6-1f shows the melting profile of RBW/BW. Similar to the melting profile observed for SFW, RBW has only one peak. The melting profile of RBW/BW would be expected to be similar to that of SFW/BW (Fig. 6-1e); however, slight differences can be observed. Even though the number of peaks across concentrations is the same as in the SFW/BW melting profiles, the two BW peaks remain in the same position from 0 to 30 % RBW/BW. Only one peak is observed for the 40 % RBW/BW at lower temperatures. This single peak may result from the co-crystallization between the BW and RBW molecules. This low-temperature peak continues to appear up to the 90 % RBW/ BW mixture. An additional peak is observed at higher temperatures for the 40 % RBW/BW samples up to the 90 % blend. Similar to that discussed above, this peak could be a consequence of the melting of BW crystals or, more likely, the melting of molecular compounds formed between RBW and BW molecules. Since a third melting peak is not observed in this binary mixture, it is very likely that molecules present in the BW and RBW partially co-crystallize. Again, keeping BW constant for SFW and RBW, the new wax blends do not follow a similar melting peak formation pattern. In the case of SFW/BW, the first melting peak of BW remains at its original position from 100 to 80 % SFW/ BW, but the RBW/BW blend shows that the first melting peak is displaced from its original position beyond the 50 % RBW/BW mixture.

Pseudo-Phase Diagrams:

Figure 6-2 shows the pseudo-phase diagrams obtained from the melting profiles presented in Fig. 6-1. We refer to these as pseudo-phase diagrams because they are formed by waxes that are not pure components, but a mixture of different molecular

entities. Pseudo-phase diagrams are constructed by plotting the T_{on} of the lowest melting peak and the T_p of the highest melting peak as a function of the composition of the binary mixture. If a single melting peak is obtained, T_{on} and T_p of that single peak are then reported. The lines connecting T_{on} and T_p values are used as best approximation to represent the solidus and liquidus lines, respectively.

The solidus line represents the solid/liquid boundary below which all material is solid, while the liquidus line represents the solid/liquid boundary above which all material is liquid [19].

Figure 6-2 shows that blend containing BW (BW/PW, SFW/BW, and RBW/BW) showed eutectic behavior, with eutectic points at 41.3, 47, and 46.9 °C at 50 % BW/PW, 40 % SFW/BW, and 40 % RBW/BW blends, respectively.

SFW/PW blends also showed eutectic behavior, with a eutectic point at 38.2 °C at the 60 % SFW/PW blend. Similar eutectic behavior was observed in the most stable β form of an LLL/MMM TAG binary system reported by Takeuchi et al. [26] and in PPP/StStSt, POSt/POP, and StOSt/StStO reported by Timms [19] (where L is lauric acid, M is myristic acid, P is palmitic acid, St is stearic acid, and O is oleic acid). However, RBW/SFW formed solid solutions, while RBW/PW showed monotectic behavior. Timms et al. [19] reported that TAGs (PPP/StOSt and PPP/POP) with melting points differing by 20 °C showed monotectic behavior. Different behavior was observed for RBW/SFW mixtures which formed a continuous solid solution (Fig. 6-2d), where both waxes were completely mutually soluble over the entire range of concentrations.

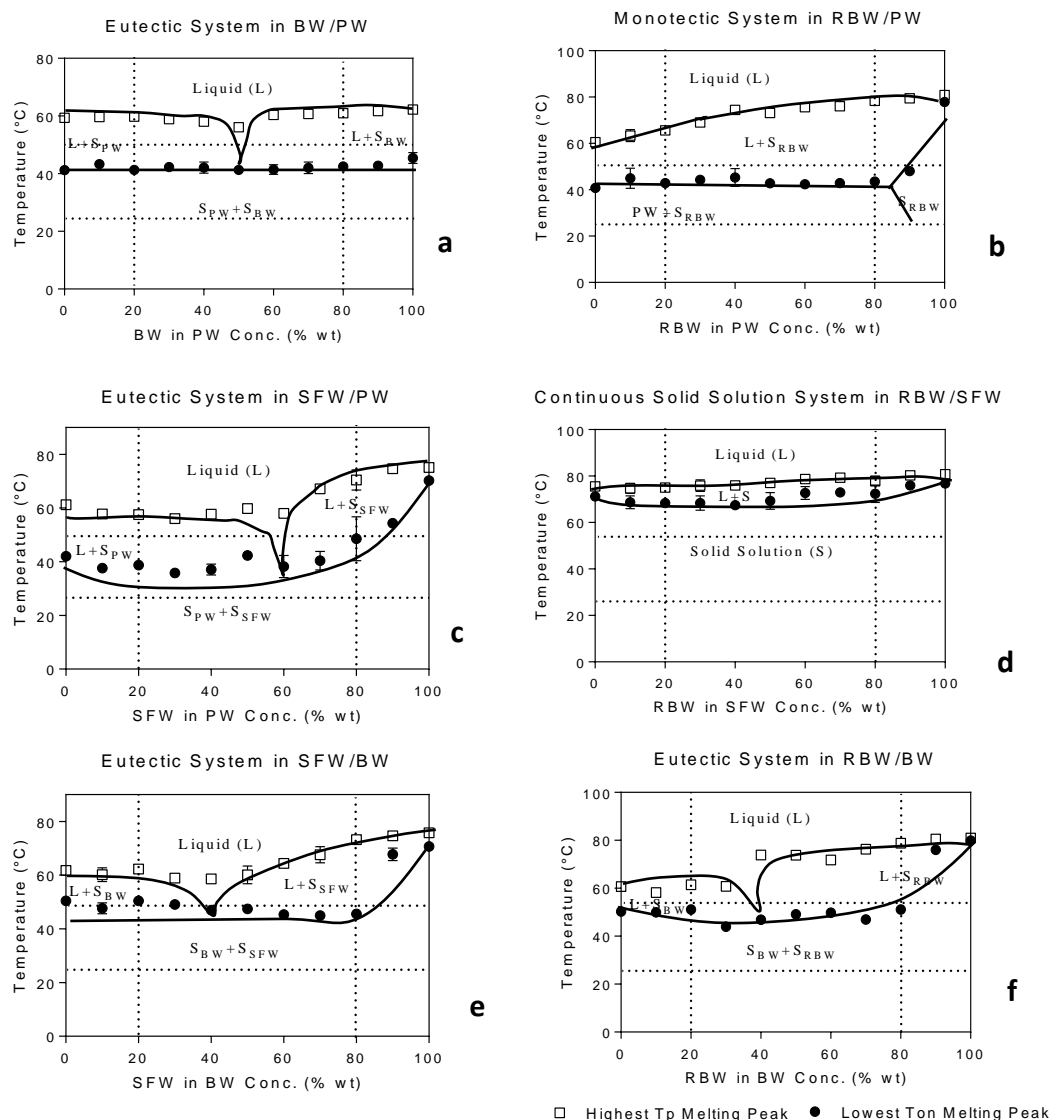


Figure 6-2. Pseudo-phase diagrams of binary wax blends for BW/PW, RBW/PW, SFW/PW, SFW/RBW, SFW/BW, and RBW/BW in a, b, c, d, e, and f, respectively. The line formed by T_p values (open squares) is called the liquidus line above which everything is liquid. The line formed by T_{on} values (filled circle) is called the solidus line below which everything is solid. There is an intermediate phase formed inside liquidus and solidus line where solid and liquid phases are in equilibrium.

This pattern is often found when two molecules or elements have very similar characteristics. Timms [19] reported a similar system for binary TAGs POS_t/StOS_t and StStSt/StStE (where E is elaidic acid).

The melting profile of the 50 % BW/PW blend in Fig. 6-1a shows only two melting peaks, indicating that both waxes co-crystallize at that particular concentration, and that the crystallization of one component is affected by the presence of the other component forming a solid solution, the composition of which changes as a function of the composition of the initial mixture. When the sample is cooled below the liquidus temperature, solid solutions predominant in PW (S_{PW}) or BW (S_{BW}) are formed and are in equilibrium with the liquid phase (Figure 6-2a). The type of solid solution formed depends on the composition of the initial material. If the sample is further cooled below the eutectic temperature (41.3 °C), only mixed crystals predominant in PW (S_{PW}) or BW (S_{BW}) are formed. Figure 6-2b suggests monotectic phase behavior of the RBW/PW blends. PW was kept constant, and RBW was chosen instead of BW. In this scenario, crystals predominant in RBW (S_{RBW}) crystallize first when the binary mixture of RBW/PW is cooled in its liquid state. In this process, the PW concentration increases in the liquid phase with RBW in its solid state, inducing the crystallization of 100 % PW. This is the case for the RBW/ PW system, where the melting point of RBW is 80.9 °C and the melting point of PW is 60.5 °C. RBW is composed of 100 % wax esters, and PW of 100 % n-alkanes (Table 6-1). The chemical composition of both waxes suggests that the n-alkanes present in PW do not interact completely with the esters in RBW, leading to a binary wax mixture with partial co-crystallization forming a monotectic system.

Although Fig. 6-1b suggests that RBW and PW did not co-crystallize, a careful analysis of the melting enthalpies of the samples (data not shown) indicates that some degree of partial co-crystallization occurred in this system, which supports the monotectic behavior depicted in Fig. 6-2b. If we compare the previous two types of diagrams, binary wax-based product formulation can be easily understood. From the eutectic diagram, the lowest-temperature liquid composition within the binary composition range can be predicted from the eutectic point, whereas from the monotectic diagram, the immiscible region of the binary composition can be studied in the liquid phase. In the crystallization study, eutectic diagrams will be more favorable than monotectic diagrams, due to the co-crystallization advantages of binary wax composition at a lower temperature over the higher individual melting temperatures. There is a small difference in the eutectic phase diagram in Fig. 6-2c compared to 6-2a. The solidus line in this eutectic diagram is curved upwards towards a higher percentage of SFW/PW. This surge is due to the higher melting temperature of the SFW content. At temperatures below the eutectic point, solid solutions predominant in PW (S_{PW}) and SFW (S_{SFW}) are formed. SFW comprises mainly wax esters, and also contains free fatty acids, fatty alcohols, and n-alkanes (Table 6-1). It is very likely that the presence of these minor components aids in the co-crystallization of SFW and PW, forming a eutectic system. The chemical composition of RBW and SFW is very similar, as they are mainly composed of wax esters (Table 6-1). As such, neither component is subject to freezing point depression, because neither component crystallizes as a pure compound. In addition, the melting temperatures of these two waxes are very close, with a difference of only 5 °C (Table 6-1). When PW is constant in RBW/PW and

SFW/ PW binary mixtures, Fig. 6-2b and c are formed. Therefore, a continuous solid solution in a binary mixture of RBW/ SFW explains how the hydrocarbon binding mechanism with wax esters affects phase diagrams, as a 66–69 % wax ester presence in SFW formed a eutectic diagram when the SFW/PW mixture was formed, but 100 % wax ester in RBW resulted a monotectic diagram.

The eutectic formation in SFW/BW (Fig. 6-2e) suggests that BW partially co-crystallized with SFW, forming a solid solution, whose composition was determined by the initial composition of the liquid. BW and SFW are similar in chemical composition, except that BW has fewer esters and no long-chain fatty alcohols (Table 6-1). When samples are cooled below the solidus line, mixed crystals predominant in SFW (S_{SFW}) or BW (S_{BW}) are formed.

Similarly, Fig. 6-2f shows the phase diagram of RBW/BW systems with a eutectic formation at 40 % RBW/BW and 46.9 °C. Similar to the previous description of eutectic systems, RBW and BW co-crystallize, forming solid solutions whose composition is dependent on the chemical composition of the liquid phase with the formation of mixed crystals predominant in RBW (S_{RBW}) or BW (S_{BW}). When BW was kept constant, both the SFW and RBW binary mixture with BW resulted in a eutectic phase diagram. Results from the phase diagrams suggest that the chemical composition of the waxes plays an important role in the crystallization behavior of their binary mixtures. Therefore, when waxes with differing chemical composition such as RBW and PW are blended, very little co-crystallization occurs, due to the poor molecular organization and lack of interaction between the n-alkanes and the esters present in these types of waxes. However, when

polar components such as free alcohols and free fatty acids are present in the samples, these molecules are able to align and partially co-crystallize. This alignment is likely driven by the formation of hydrogen bonds between the functional bonds in the esters, alcohols, and free fatty acids. Crystalline networks formed upon cooling are characterized by specific crystal morphologies, which ultimately affect the physical properties of the material. Some of the important physical properties include the texture, structural organization, and strength of the crystalline network formed [13–16]. These are important in the pharmaceutical, chemical, and food industries for providing products with appropriate quality characteristics such as drug delivery, material structure or hardness, and mouthfeel and flavor. Therefore, it is important to evaluate the effect of the composition of wax systems on the morphology of the crystals formed.

Crystal Morphology:

Figure 6-3 shows the crystal morphologies of the waxes and their binary combinations obtained when crystallized at 25 °C at a slow cooling rate (0.5 °C/min). The crystal structures change as the proportion of wax changes in the binary blends. String-like crystals forming a junction point in the shape of a knot (Fig. 6-3a) for 0 % BW/PW (100 % PW) change to blunt needles for 20 % BW/PW (Fig. 6-3b). Similar morphology is observed for the 80 % BW/PW (Fig. 6-3c), but the crystals are thinner and smaller than those observed for the 20 % BW/PW samples. The 100 % BW/PW (100 % BW) shows larger, bifurcated needle-like crystals. Other authors have reported similar 100 % BW crystal morphology [16, 17].

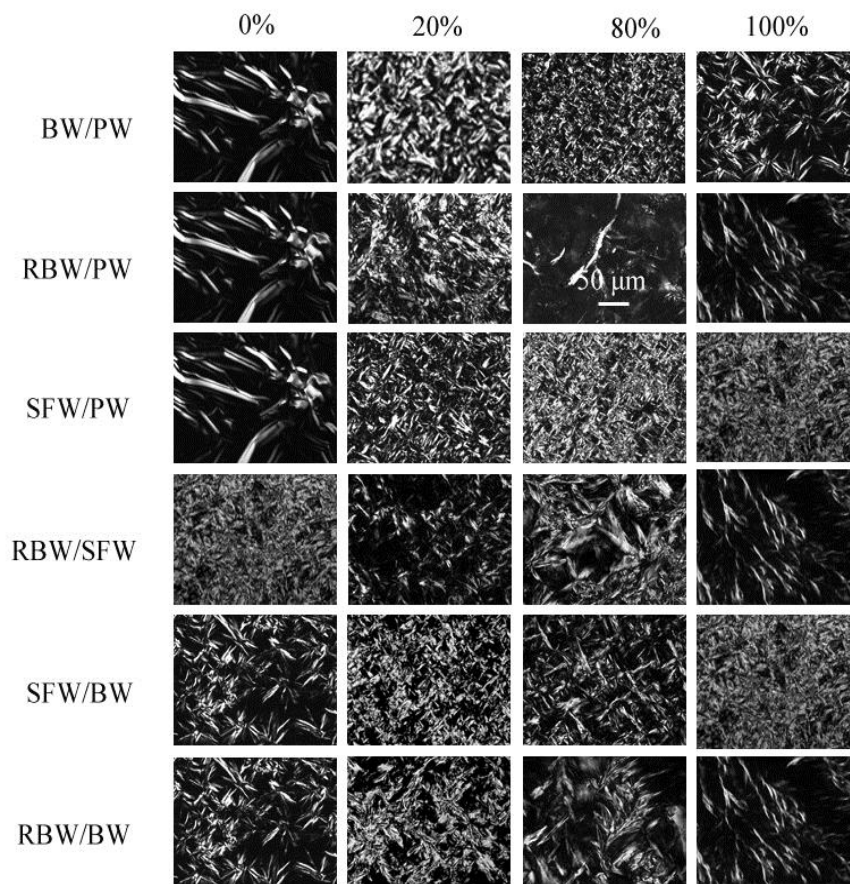


Figure 6-3. Crystal morphology of binary blends of waxes crystallized at 25 °C (20X magnification) at slow cooling rate (0.5 °C/min). The first column shows crystals obtained for 0% of the first wax component. Increasing levels (20, 80 and 100%) of the first component of the mixture is shown in the second, third, and fourth columns, respectively. White bar indicates 50 μ m.

It is very likely that these differences in crystal morphology are related to the phase diagrams shown in Fig. 6-2. For example, crystals observed in the 20 % BW/ PW are formed by partial co-crystallization of molecules present in BW and PW, but more

predominant in PW, and therefore a more open structure with larger crystals, more like that obtained in 100 % PW crystals. Similarly, crystals observed in the 80 % BW/PW sample are smaller and tighter, with characteristics more like those observed for 100 % BW. A small addition of a different wax to 100 % paraffin wax changes the binary blend morphology in relation to the different proportions of wax added. This was observed when the morphology of the BW/PW blend was discussed. But there is no specific trend for predicting the structural changes in crystal morphology as the proportion of binary waxes is changed.

The addition of 20 % of RBW to PW (Fig. 6-2f) generates a crystalline network characterized by highly interconnected crystals with the appearance of a rough gravel surface. RBW/PW shows monotectic behavior, and when mixtures of RBW/PW are crystallized at 25 °C 100 %, crystals of PW and solid solutions of RBW and PW are formed. The highly dense microstructure observed for the 20 % RBW/PW results from the promotion of crystallization of PW due to a concentration effect produced by the formation of S_{RBW} , as described in Fig. 6-2b. However, the highly interconnected structure in 20 % is lost in the 80 % RBW/PW samples (Fig. 6-3g), where the crystalline structure is very different, showing mainly a molten sample with a couple of stripes or even platelet-like shapes. When the amount of RBW increases to 80 %, the crystalline structure is driven by S_{RBW} crystals which are predominant in RBW molecular entities, and therefore the crystalline structures look more like those observed for 100 % RBW crystals.

Figure 6-3i-l shows crystal morphologies of the SFW/PW samples as a function of the addition of SFW. The type of crystals observed correlate well with the amount of SFW added to the mixture, meaning that the higher the amount of SFW added, the denser the crystalline network becomes. From the phase diagram (Fig. 6-2c), we can observe that the morphology images taken in Fig. 6-3i-l fall below the solidus line, which indicates that these crystals are mainly of $S_{PW} + S_{SFW}$ composition. Crystals observed in 20 % RBW/SFW do not form a tight crystalline network with long granules as observed in the more SFW-rich samples (80 % RBW/SFW in Fig. 6-3o). As was described previously, this combination of waxes forms a solid solution where RBW and SFW are completely soluble at all proportions (Fig. 6-2d). Although the solid formed at temperatures below the solidus line has a constant composition, the crystal morphology of this solid appears to be affected by the initial composition of the melt (Fig. 6-3m-p). Crystals shown in Fig. 6-3q-t represent crystalline structures from S_{SFW} and S_{BW} solid solutions depicted in Fig. 6-2e. The addition of 20 % of SFW (Fig. 6-3r) results in a crystalline network characterized by smaller blunt-needle structures. Figure 6-3s shows 80 % of SFW/BW crystals, and these crystals look like needles but are arranged in a different pattern and are larger than the 20 % SFW crystals observed in Fig. 6-3r. In this binary system, both 100 % waxes (BW and SFW) form needle-like structures, with a small difference in that the 100 % BW crystals are less dense than the SFW crystals and are oriented radially. Crystals shown in Fig. 6-3u-x represent crystalline structures from $SRBW$ and SBW solid solutions presented in Fig. 6-2f. The addition of 20 % RBW results in a crystalline network that looks much like the 100 % BW, but with a higher

concentration of crystalline material (Fig. 6-3v). However, when 80 % of RBW is added to BW, the morphology of the crystalline network changes significantly (Fig. 6-3w), with crystals showing a highly branched conformation resembling the shape of wheat. A comparison of 20 % RBW/BW crystals with 100 % BW and 100 % RBW reveals that blends with higher BW content (20 % RBW/BW) have a crystalline structure similar to that in 100 % BW, while crystals obtained in blends with higher RBW content (80 % RBW/ BW) are more similar to those obtained for 100 % RBW samples.

Eutectic formation in binary wax blends shows a trend when just 20 and 80 % of their blends are compared, and a close relationship is observed between their structures and crystal density. Monotectic formation in RBW/PW may be explained by the marked change in crystal morphology observed in 20 and 80 % blends. Comparing all of the 20 % binary wax composition (vertically, Fig. 6-3b–v), we can observe that they possess a symmetrical structure. In contrast to the 20 % blends (vertically), the 80 % blends are visibly different, and the RBW/PW can be spotted as out of place. Eutectic formation of BW/PW and SFW/PW shows smaller crystals at 80 %, but other eutectic formation of SFW/BW and RBW/BW shows noticeably larger crystals in comparison. RBW/SFW (80 %) crystals show similarity to 80 % RBW/BW crystals.

Crystal structure trends cannot be predicted based only on increasing or decreasing wax proportion in binary blends. Crystal structures are also affected by the temperature at which the crystals are formed, individual melting temperatures of the waxes, chemical composition, and molecular interactions. Figure 6-4 shows morphologies of wax crystals and their binary combinations when crystallized at 50 °C using slow cooling (0.5 °C/min)

from 90 to 50 °C. The crystal morphologies in Fig. 6-3 were obtained when samples were crystallized at 25 °C, and show the crystalline structure of solids obtained below the solidus line in the phase diagrams (Fig. 6-2).

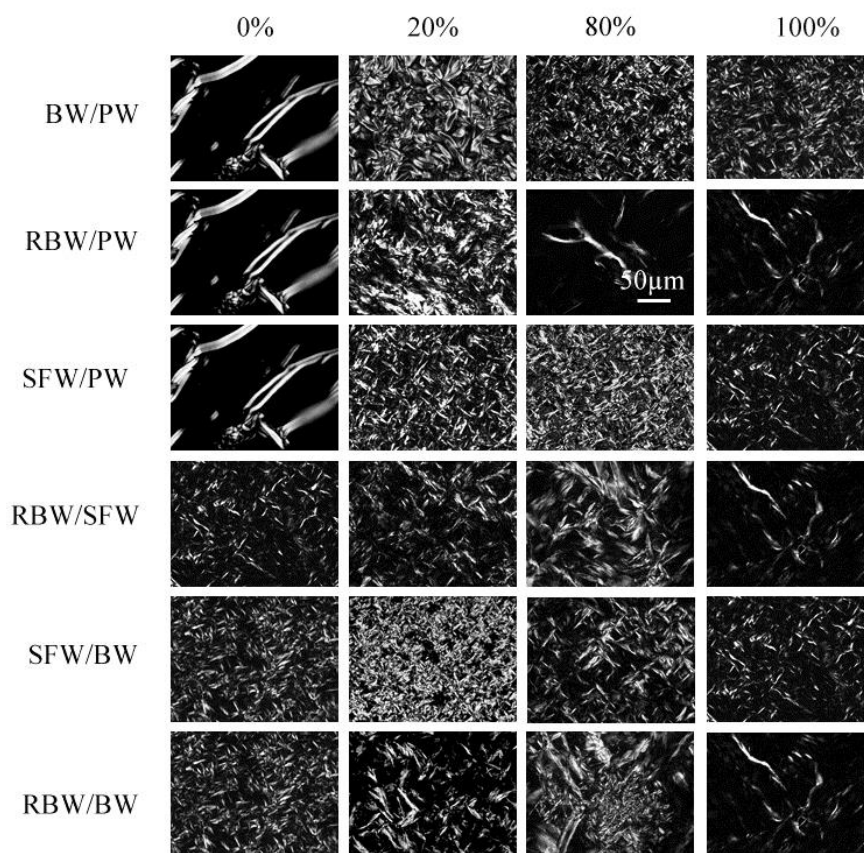


Figure 6-4. Crystal morphology of binary blends of waxes crystallized at 50° C (20X magnification) at slow cooling rate (0.5° C/min). The first column shows crystals obtained for 0% of the first wax component. Increasing levels (20, 80 and 100%) of the first component of the mixture is shown in the second, third, and fourth columns, respectively. White bar indicates 50µm.

The objective in measuring crystal morphology at 50 °C is to evaluate crystalline structure where the solid is in equilibrium with the liquid. This is the case for all the binary systems tested in this study, with the exception of the RBW/SFW blend, where the liquidus and solidus lines are close together, and no liquid phase is observed when samples are crystallized at 50 °C.

Super-cooling, the difference between crystallization and melting temperatures, constitutes the driving force in lipid nucleation [33]. Therefore, differences in crystalline morphologies observed between samples crystallized at 50 and 25 °C are likely due to the differences in the supercooling of the system. Crystalline networks obtained at 50 °C (Fig. 6-4) were similar to those shown in Fig. 6-3, but they were characterized by a more open structure, with fewer crystals, due to the lower super-cooling. In addition, crystal morphologies reported for the 20 and 80 % blends represent the crystalline network of the solid that is in equilibrium with the liquid for a particular blend. For example, crystal morphologies shown in Fig. 6-4b represent the crystal morphology of SPW formed during crystallization of this blend and which is in equilibrium with the liquid phase, while Fig. 6-4c represent the crystal morphology of SBW.

In order to quantify the morphology of the crystals shown in Figs. 6-3 and 6-4, fractal dimension analysis was performed. The fractal dimension of a lipid crystal network is obtained from microscopy images of lipid crystals. The fractal dimension of lipid crystalline structures has been previously evaluated using the box-counting method [35–39], and research has suggested that the mass fractal dimension technique (box-counting method) is suitable for a two-dimensional Euclidean space when the sample is

small and thin [29]. The box-counting fractal dimension is largely affected by three microstructural factors—crystal shape, size, and area fraction—and the interaction of these factors [30, 31].

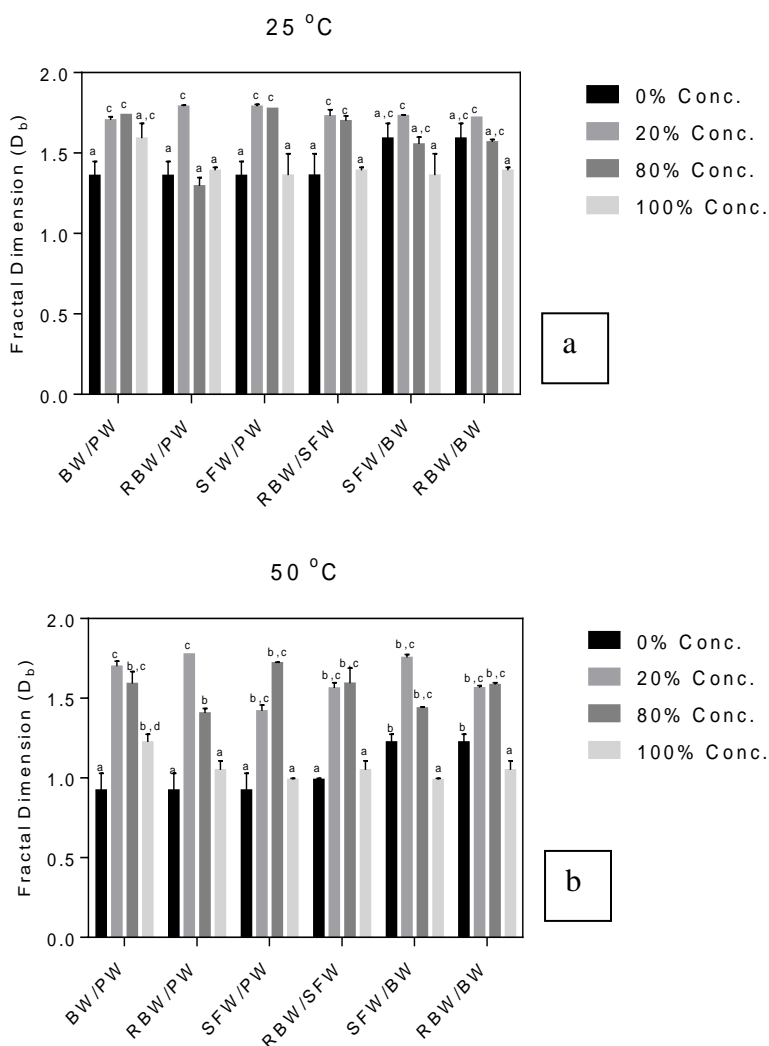


Figure 6-5. Box-counting fractal dimension (D_b) values obtained for samples crystallized at (a) 25 °C and (b) 50 °C. Columns with the same letter are no significantly different ($\alpha = 0.05$)

Figure 6-5a delineates the multiple comparisons of fractal dimension values (D_b) obtained using the box-counting method for the binary wax systems of different concentrations at 25 °C. In the BW/PW binary system, the combination of waxes results in higher D_b values than those of 100 % BW or PW waxes, although the D_b value of 100 % PW is significantly lower than that of 100 % BW. In addition, no significant ($\alpha = 0.05$) difference in D_b values is observed among 20, 80 and 100 % BW/PW (or 100 % BW) systems. These results suggest that a higher degree of filling (or area fraction) is observed as the content of BW in the blend increases. This statement is supported by the crystal morphology previously discussed in Fig. 6-3a–d.

The RBW/PW binary system shows no significant difference in D_b values obtained for any of the RBW/PW mixtures, with the exception of the 20 % RBW/PW sample. The crystal sizes and shapes for RBW/PW 0, 80 and 100 % are similar, as shown in Fig. 6-3e, g, and h, respectively, leading to similar fractal dimension values. The D_b value obtained for the 20 % blend of RBW/PW is significantly higher ($\alpha = 0.05$) than the D_b values obtained for the other blends. This 20 % blend shows completely different crystal morphology, and even the area of fraction is higher (Fig. 6-3f). The fractal dimension value of 100 % SFW is not significantly different ($\alpha = 0.05$) from D_b values of 100 % PW; however, a significant ($\alpha = 0.05$) increase in D_b values is observed when SFW and PW are mixed to form 20 and 80 % binary systems, with no significant difference ($\alpha = 0.05$) in D_b values of these two samples.

The crystal sizes of the 20 and 80 % SFW/PW blends show that there is an increase in area fraction as any amount of SFW is added, which explains the significantly higher

D_b value (Fig. 6-3j, k). The crystal morphology images show that 100 % PW has a low area fraction, which would result in a lower D_b ; however, a high D_b value is observed, similar to that obtained for 100 % SFW, which is characterized by a high area fraction. It is important to note that 100 % PW is characterized by long and large crystals, which explains a high D_b value [30, 31, 34, 35] (Fig. 6-3i, l), and thus explains why 100 % PW and 100 % SFW have statistically the same D_b value but significantly different microstructures.

D_b values for the RBW/SFW binary system are similar to those described previously for SFW/PW. Similar to the previous discussion, 100 % RBW and 100 % SFW had similar D_b values but significantly different microstructures. The larger crystalline structures observed in the 100 % RBW are responsible for a high D_b value in this sample, with low area fraction (Fig. 6-3m, p). The 20 and 80 % concentrations of RBW/ SFW show a significant ($\alpha = 0.05$) increase in D_b values compared to those obtained for the 100 % waxes, and these values (D_b values for 20 and 80 % RBW/SFW blends) are not significantly different from each other ($\alpha = 0.05$). The increase in D_b values can be explained by the crystal morphology, where size, shape, and area fraction must be considered (Fig. 6-3n, o). The lowest D_b value for the SFW/BW blends was obtained for 100 % SFW, but this value was not significantly different ($\alpha = 0.05$) from that obtained for 0 and 80 % SFW/BW blends. These D_b values can be explained by the crystal morphologies observed in Fig. 6-3q, s, and t, where no differences are observed between 0 and 80 % SFW/BW.

Although the area fraction for the 100 % SFW is greater than that for the other blends, the size and shape of the crystals reduces the D_b value (Fig. 6-3q, s, t). The highest ($\alpha = 0.05$) D_b value was observed for 20 % SFW/BW, which can be explained by the high area fraction observed in this sample (Fig. 6-3r). The RBW/BW binary system follows the same pattern as SFW/BW at 25 °C when D_b values are plotted. RBW/BW blends also behave similarly to SFW/BW as far as crystal morphology is concerned, except that the 100 % RBW crystal size, shape, and area fraction are different from those of the 100 % SFW. In this scenario, the area fraction of the crystals leads to a higher D_b value due to the longer crystals of RBW (Fig. 6-3u-x). Here it is important to note that the addition of BW in any wax material studied in this research (PW, SFW, and RBW) increased either by increasing the area fraction or by decreasing crystal size. Table 6-1 helps explain this phenomenon to some extent. The 100 % BW is a mixture of wax esters, n-alkanes, free fatty acids, and alcohols, whereas other waxes comprise mostly wax ester or n-alkanes. We hypothesize that molecules present in BW promote the formation of molecular compounds by creating van der Waals interactions and/or hydrogen bonds.

This could also explain the eutectic formation in BW-containing blends. An overall look at Fig. 6-5a shows that there is no significant difference at the 20 % blend across all binary systems (BW/PW, RBW/PW, SFW/PW, RBW/SFW, SFW/BW, and RBW/BW). The same behavior is observed with the 80 % blends, with the exception of RBW/PW. It is also interesting to note that all 20 and 80 % blends of all binary systems show higher D_b values than their 100 % waxes.

Figure 6-5b shows the multiple comparisons of fractal dimension values (D_b) obtained using the box-counting method for the binary wax systems at different concentrations at 50 °C. There is no significant difference ($\alpha = 0.05$) between 20 and 80 % of the BW/PW system. When this blend is compared at 25 °C (Fig. 6-5a), D_b values obtained for both BW and PW are lower at a higher temperature (<1 for PW; <1.5 for BW).

The crystal size, shape, and area fraction are the cause of this change in D_b values from 25 to 50 °C (Figs. 6-3a–d, 4a–d). There is no significant difference observed in the 20 and 80 % blends at a higher temperature. No significant differences ($\alpha = 0.05$) are observed in D_b values of 100 % RBW and 100 % PW. The 20 % blend of RBW/PW has a significantly higher D_b value ($\alpha = 0.05$) than 100 % RBW, 100 % PW, and 80 % of the RBW/PW system. There is a significant increase in D_b value at 80 % RBW/PW from 100 % RBW and 100 % PW. These results are supported by the microstructures presented in Fig. 6-4e–h. SFW D_b values were not significantly different ($\alpha = 0.05$) from those obtained for PW. No significant difference ($\alpha = 0.05$) in D_b values was observed for 20 and 80 % SFW/ PW binary waxes, but these values are significantly higher ($\alpha = 0.05$) than 100 % SFW and 100 % PW D_b values. Similar to that discussed above, D_b values for 100 % RBW and 100 % SFW blends were not significantly different ($\alpha = 0.05$), but significantly higher ($\alpha = 0.05$) D_b values were observed for the 20 and 80 % RBW/SFW blends. This is an interesting result, since the area fraction of the 20 and 80 % RBW/SFW samples is not significantly different from that of the 100 % waxes. Differences in D_b values may be a consequence of the smaller crystals observed in the 20 and 80 % blends

(Fig. 6-4m–p). The behavior of D_b values observed for SFW/BW and RBW/BW samples is similar to that as described above for RBW/SFW, where higher area fractions and smaller crystals are obtained in the mixtures compared to the 100 % waxes (Fig. 6-4q–x).

Conclusion

The pseudo-phase diagram and microstructure of binary waxes at different concentrations aids in understanding crystalline network formation and in developing new products for all types of industry. Results from this study have shown that molecular entities present in natural waxes significantly affect their crystallization behavior and the morphology of crystals formed. The addition of as little as 20 % of one component over another can dramatically alter phase behavior. Waxes with similar chemical composition can co-crystallize, forming ideal solid solutions, while waxes with significantly different chemical composition can show either eutectic or monotectic behavior. These differences in phase behavior are reflected in the morphology of the crystals formed, where smaller crystals that cover a larger area fraction are usually observed in the mixed blends.

Changes in the phase behavior and microstructure of these binary systems will have a direct impact on the functional and physical properties of these systems. More research is needed in this area to tailor the functional and physical properties of these materials for specific food and non-food applications.

References

1. Hughes NE, Marangoni AG, Wright AJ, Rogers MA, Rush JWE (2009) Potential food applications of edible oil organogels. *Trends in Food Sci Technol* 20:470–480

2. Hwang KS, Singh M, Bakota EL, Winkler-Moser JK, Kim S, Liu SX (2013) Margarine from organogels of plant wax and soybean oil. *J Am Oil Chem Soc* 90:1705–1712
3. Aguilar F, Crebelli R, Dusemund B, Galtier P, Gott D, Gundert- Remy U, König J, Lambré C, Leblanc JC, Mortensen A, Mosesso P, Parent-Massin D, Stankovic I, Tobback P, Waalkens- Berendsen I, Woutersen RA, Wright M (2012) Scientific opinion on the re-evaluation of carnauba wax (E 903) as a food additive. *EFSA J* 10(10):2880
4. Toro-Vazquez JF, Morales-Rueda JA, Dibildox-Alvarado E, Charo´-Alonso M, Alonzo-Macias M, Gonzalez-Chavez MM (2007) Thermal and textural properties of organogels developed by candelilla wax in safflower oil. *J Am Oil Chem Soc* 84:989–1000
5. Blake AI, Co ED, Marangoni AG (2014) Structure and physical properties of plan wax crystal networks and their relationship to oil binding capacity. *J Am Oil Chem Soc* 91:885–903
6. Rogers MA (2009) Novel structuring strategies for unsaturated fats—Meeting the zero-trans, zero-saturated fat challenge: a review. *Food Res. Intl* 42:747–753
7. Daniel Co E, Marangoni AG (2012) Organogels: an alternative edible oil-structuring method. *J Am Oil Chem Soc* 89:749–780

8. Daniel J, Rajasekharan R (2003) Organogelation of Plant oils and hydrocarbons by long-chain saturated FA, fatty alcohols, wax esters, and dicarboxylic acids. *J Am Oil Chem Soc* 80:417–421
9. Botega DCJ, Marangoni AG, Smith AK, Goff HD (2013) The potential application of rice bran wax oleogel to replace solid fat and enhance unsaturated fat content in ice cream. *J Food Sci* 78:1334–1339
10. Blake AI, Daniel Co E, Marangoni AG (2014) Structure and physical properties of plant wax crystal networks and their relationship to oil binding capacity. *J Am Oil Chem Soc* 91:885–903
11. Yilmaz E, Öğütçü M (2014) Comparative analysis of olive oil organogels containing beeswax and sunflower wax with breakfast margarine 79:1732–1738
12. Jang A, Bae W, Hwang HS, Lee HG, Lee S (2015) Evaluation of canola oil oleogels with candelilla wax as an alternative to shortening in baked goods. *Food Chem* 187:525–529
13. Blake AI, Daniel Co E, Marangoni AG (2014) Structure and physical properties of plant wax crystal networks and their relationship to oil binding capacity. *J Am Oil Chem Soc* 91:885–903
14. Martini S, Carelli AA, Lee J (2008) Effect of the addition of waxes on the crystallization behavior of anhydrous milk fat. *J Am Oil Chem Soc* 85:1097–1104

15. Martini S, Tan CY, Jana S (2015) Physical characterization of wax/oil crystalline networks. *J Food Sci* 5:989–997
16. Jana S, Martini S (2014) Effect of high-intensity ultrasound and cooling rate on the crystallization behavior of beeswax in edible oils. *J Agric Food Chem* 62:10192–10202
17. Hwang HS, Kim S, Singh M, Winkler-Moser JK, Liu SX (2012) Organogel formation of soybean oil with waxes. *J Am Oil Chem Soc* 89:639–647
18. Zantl R, Baicu L, Artzner F, Sprenger I, Rapp G, Rädler JO (1999) Thermotropic phase behavior of cationic lipid-DNA complexes compared to binary lipid mixtures. *J Phys Chem B* 103:10300–10310
19. Timms RE (1984) Phase behavior of fats and their mixtures. *Prog Lipid Res* 23:1–38
20. Koch JR, Hable GJ, Wrangell L (1938) Melting point studies of binary and trinary mixtures of commercial waxes. *Ind Eng Chem Anal Ed* 10:166–168
21. Knoester M, De Bruijne P, Van Den Tempel M (1972) The solid–liquid equilibrium of binary mixtures of triglycerides with palmitic and stearic chains. *Chem Phys Lipids* 9:309–319
22. Inoue T, Hisatsugu Y, Yamamoto R, Suzuki M (2004) Solid–liquid phase behavior of binary fatty acid mixtures 1. Oleic acid/ stearic acid and oleic acid/behenic acid mixtures. *Chem Phys Lipids* 127:143–152
23. Craven RJ, Lenki RW (2011) Binary phase behavior of diacid 1, 3-diacylglycerols. *J Am Oil Chem Soc* 88:1125–1134

24. Inoue T, Hisatsugu Y, Suzuki M, Wang ZN, Zheng LQ (2004) Solid–liquid phase behavior of binary fatty acid mixtures 3. Mixtures of oleic acid with capric acid (decanoic acid) and caprylic acid (octanoic acid). *Chem Phys Lipids* 132:225–234
25. Takeuchi M, Ueno S, Flöter E, Sato K (2002) Binary phase behavior of 1, 3-distearoyl-2-oleoyl-sn-glycerol (SOS) and 1, 3-distearoyl-2-linoleoyl-sn-glycerol (SLS). *J Am Oil Chem Soc* 79:627–632
26. Takeuchi M, Ueno S, Sato K (2003) Synchrotron radiation SAXS/WAXS study of polymorph-dependent phase behavior of binary mixtures of saturated monoacid triacylglycerols. *Cryst Growth Des* 3:369–374
27. Timms RE (1981) Phase behavior of fats and mixtures of fats. Oral Presentation at Palm Oil Research Institute of Malaysia
28. Timms RE (1983) In fats for the future. In: Brooker SG, Renwick A, Hannan SF, Eyres L (eds) *The Proceedings of the International Conference on oils, fats and waxes*. Duromark Publishing, Auckland, pp 25–28
29. Marangoni AG (2002) The nature of fractality in fat crystal networks. *Trends Food Sci Technol* 13:37–47
30. Tang D, Marangoni AG (2006) Microstructure and fractal analysis of fat crystal networks. *J Am Oil Chem Soc* 83:377–388
31. Tang D, Marangoni AG (2006) Quantitative study on the microstructure of colloidal fat crystal networks and fractal dimensions. *Adv Colloid Interface Sci* 128–130:257–265

32. Dassanayake LSK, Kodali DR, Ueno S, Sato K (2009) Physical properties of rice bran wax in bulk and organogels. *J Am Oil Chem Soc* 86:1163–1173
33. Hartel RW (2013) In crystallization in Foods, Chap. 5. Aspen Publishers, Gaithersburg, pp 145–188
34. Tang D, Marangoni AG (2006) Computer simulation of fractal dimensions of fat crystal networks. *J Am Oil Chem Soc* 83:309–314
35. Campos R (2005) In fat crystal networks. In: Marangoni AG (ed) Chapter 9. Marcel Dekker, New York, pp 320–326
36. Awad TS, Marangoni AG (2005) In fat crystal networks. In: Marangoni AG (ed) Chapter 11. Marcel Dekker, New York, pp 394–408
37. Alvarado ED, Rodrigues JN, Gioielli LA, Toro-Vazquez JF, Marangoni AG (2004) Effects of crystalline microstructure on oil migration in a semisolid fat matrix. *Cryst Growth Des* 4:731–736
38. Marangoni AG, McGauley SE (2003) Relationship between crystallization behavior and structure in cocoa butter. *Cryst Growth Des* 3:95–108
39. Batte HD, Marangoni AG (2005) Fractal growth of milk fat crystals is unaffected by microstructural confinement. *Cryst Growth Des* 5:1703–1705

CHAPTER 7

**PHYSICAL CHARACTERIZATION OF CRYSTALLINE NETWORKS
FORMED BY BINARY BLENDS OF WAXES IN SOYBEAN OIL**

Abstract

The objective of this study is to analyze the crystallization behavior of 2.5% binary wax blends consisting of beeswax (BW), rice bran wax (RBW), and sunflower wax (SFW) in soybean oil (SBO) using differential scanning calorimetry (DSC), pulsed nuclear magnetic resonance (p-NMR), magnetic bearing rheometer, and polarized light microscopy (PLM). Melting behavior of binary waxes was significantly affected by the type and proportion of wax used. Melting T_{on} and T_p for RBW/SFW and RBW/BW blends were significantly higher than those observed for SFW/BW. Enthalpy values suggest that different molecules present in the wax affect intermolecular interactions in the binary blends.

A wider solid fat content curve is observed in all the RBW/SFW blends compared to the SFW/BW and RBW/BW blends. Iso-solid diagrams show that there is certainly a softening effect in RBW/BW and SFW/BW systems. Viscoelastic parameters (G' , G'') analyzed in SBO at 2.5% of waxes shows that RBW has the highest G' value (31360.0 ± 973.3 Pa) followed by SFW (26702.5 ± 2177.2 Pa) and BW having the lowest (90.7 ± 74.4 Pa). A higher G' value in RBW/SFW binary system in SBO indicates significantly more solid-like behavior than any other combinations. Crystal morphology pictures show no

significant difference in crystals except for the 50% RBW/SFW blend when analyzed by fractal dimension (D_b).

In general, the addition of RBW or SFW to BW increased T_p , T_{on} , enthalpy values, SFC and G' values with no significant effect on microstructure. The addition of RBW to SFW also increased T_p , T_{on} , enthalpy values but to a lower extent. In addition, SFC was not affected in the RBW/SFW blends and only minor changes were observed for G' values.

Introduction

Wax in oil systems has been popular for their potential use as *trans*-fat and saturated fat replacers. High melting waxes crystallized in low melting oils form a crystalline network that entraps oil forming semi solid materials. Several studies have been performed on natural waxes such as beeswax (BW), sunflower wax (SFW), candelilla wax (CW), and rice bran wax (RBW) and different edible oils (Hwang et al., 2012, Toro-Vazquez et al., 2007, Dassanayake et al., 2009, Jana et al., 2014, and Martini et al. 2015). In addition, the use of wax/oil systems in a number of food products has been explored (Hwang et al., 2013, Yilmaz et al., 2014 & 2015, Jang et al., 2015 and Patel et al., 2014).

These studies showed that crystallization behavior and physical properties of the different natural waxes used for food application strongly depends on the type of wax (Dassanayake et al., 2009, Martini et al., 2015, and Hwang et al., 2013) and oil (Dassanayake et al., 2009, Jana et al., 2014 and Lupi et al., 2013) used. Martini et al. (2015) and others (Lupi et al., 2013, Hwang et al., 2012, and Martini et al., 2008)

confirmed that concentration of wax used in the oil also has an effect when structuring wax/oil systems. The crystallization behavior and the functional properties of the wax materials differ significantly due to their different chemical composition. For example, paraffin wax (PW) is formed mainly of high molecular weight n-alkanes; RBW consists mainly of long chain aliphatic esters, while SFW and BW are a mixture of n-alkanes, esters, free fatty acids, and aliphatic alcohols.

Waxes are high melting point materials ($T_m = 50\text{--}80\text{ }^\circ\text{C}$) and have low solubility in vegetable oils and therefore crystallize rapidly when placed at room temperature. Toro-Vazquez et al. (2007) studied thermal and physical characteristics of candelilla wax (2% wt. basis) in safflower oil which forms gel upon crystallization. They concluded that structural organization of organogel is dependent on the cooling rate, thermodynamic driving force, and gel setting temperature. They also mentioned that chemical composition in oil and wax provides a structure-function relationship associated with gelling properties. Similarly, Dassanayake et al. (2009) studied rice bran wax and carnauba wax in olive and salad oil (canola: soy bean oil = 50:50). This research group has shown that different types of waxes are responsible for different hardness and viscosity and those parameters are explained by crystallization behavior and thermal kinetics. These researchers confirm that analysis of different physical properties is needed for better understanding on the crystalline network formed in wax/oil system.

Considering that waxes have different melting temperatures and that they generate a range of physical properties when crystallized in an oil our hypothesis is that we can broaden the physical properties of these wax/oil systems by using wax mixtures. BW,

RBW, and SFW are popular natural waxes with significantly different chemical compositions. Moreover, these waxes are being used in different applications in food industry. Therefore, the objective of this research is to characterize physical properties of binary wax/oil systems. BW, RBW, and SFW are used as waxes and SBO is used as oil in the wax/oil system. A concentration of 2.5% (% wt. basis) of binary wax (0, 20, 50, 80, and 100%) in SBO is used based on preliminary data in our laboratory. Thermal properties such as melting temperatures (onset [T_{on}] and peak [T_p]) and enthalpies, viscoelastic properties such as storage modulus (G'), loss modulus (G''), solid fat content (SFC), and crystal morphology were measured.

Materials and methods

Materials and Sample Preparation

Beeswax, sunflower wax, and rice bran wax were supplied by Koster Keunen LLC (Watertown, CT, USA). Pure Wesson soybean oil was purchased from local supermarket. Chemical compositions and melting temperatures (T_m) of the waxes have been previously reported (Hwang et al. 2012, and Jana & Martini 2016). In short, BW ($T_m = 60.5 \pm 3.0$ °C) is composed of wax esters, hydroxyl esters, hydrocarbon, free fatty acids, and di-esters. RBW ($T_m = 80.8 \pm 0.8$ °C) is composed only by saturated wax esters. Lastly, SFW ($T_m = 75.5 \pm 0.0$ °C) is composed of wax esters, hydrocarbons, free fatty acids, and fatty alcohols. Binary wax systems were prepared by mixing BW, RBW, and SFW waxes in different proportions, from 0-100% in 10% intervals. The binary systems (RBW/BW, RBW/SFW, and SFW/BW) were prepared by placing a specific amount of waxes in 17 x

60 mm² (8 ml) vials to reach 1 g of solids. Approximately 7 ml of hexane was added to the vial and closed with an appropriate lid. Vials were then placed in a sonication water bath for 5 – 10 min and placed on a vortex mixer for 1-2 min to allow for complete dissolution of the waxes in the hexane. The vial lids were then loosened and placed under airflow thin-wall fume hood for a week to evaporate the hexane. Samples of 2.5% (wt. basis) of the binary waxes in soybean oil (SBO) were used in this study. Binary wax (2.5% wt. basis) in soybean oil is optimized to organogel formation based on thermal stability, viscosity-temperature relationship and visual observation compared to 1, 5 and 10% (wt. basis). Binary waxes were mixed with the oil and heated to 100 °C in an oven to allow for complete melting and dissolution of the wax blends in the oil. Then the samples were incubated at 25 °C for 24 h.

Differential Scanning Calorimeter (DSC)

Samples were crystallized at 25 °C in a water-bath for 24 h and the melting profile was measured at this point using DSC (TA Instruments DSC model Q20 1963 with RCS cooling system, New Castle, DE, USA). The DSC baseline and temperature were calibrated with a pure indium standard. Approximately 10 mg of the sample were placed in Tzero aluminum pans, covered and sealed with Tzero aluminum lids. The samples were heated from 25 °C to 100 °C at 5 °C/min to analyze the melting profile of the samples. TA Universal Analysis software was used to analyze the melting onset (T_{on}), melting peak temperatures (T_p), and melting enthalpy (ΔH).

Theoretical Enthalpy Calculation

Theoretical enthalpies were calculated using enthalpy values of each single wax component in the blend using the following equation.

$$\Delta H^{A}_{th} = \frac{\Delta H^{A}_{exp} \times P}{100}$$

Where ΔH^{A}_{th} is the theoretical enthalpy in the binary mixture from component A, ΔH^{A}_{exp} is the experimental enthalpy of component A when presented at 100%, and P is the percentage of component A in the blend. For a wax blend composed of A and B waxes, the total theoretical enthalpy is given by the following equation:

$$\Delta H^{T}_{th} = \Delta H^{A}_{th} + \Delta H^{B}_{th}$$

Solid Fat Content

A pulsed nuclear magnetic resonance (p-NMR) instrument (Bruker mq 20 Minispec, with a 0.47-T magnetic field operating at a resonance frequency of 20 MHz) was used to determine the solid fat content (SFC) of the samples. Samples were placed in NMR tubes (180 × 10 mm) and kept at 10 °C to 70 °C in 5 °C intervals for 24 h in a water-bath. SFC values were determined as a function of temperature from 10 °C up to 70 °C. Triplicate runs were performed for each set of samples, and three tubes were measured in each run.

Rheology Measurements

A TA Instruments AR-G2 Magnetic Bearing Rheometer was used to evaluate the viscoelastic properties of the material. Oscillatory tests were performed at 25 °C by a strain sweep step to obtain storage modulus (G').

A TA Instruments AR-G2 Magnetic Bearing Rheometer was used to evaluate the viscoelastic properties of the material. Oscillatory tests were performed at 25 °C after 24 h of storage by a strain sweep step to obtain storage (G') and loss (G'') moduli. A 40-mm-diameter parallel-plate geometry was used for the samples. A plastic spoon was used to transfer the samples to the rheometer plates. For each type of wax blends and soybean oil combination, 3 experimental replicates were performed and 3 rheology measurements were taken from each replicate. Therefore, a total 9 measurements were taken for each wax/oil mixture.

Crystal Morphology

After 24 h of storage in a water-bath at 25 °C, crystals present in the samples were evaluated. The crystals were observed using a polarized light microscope (Olympus BX41, Olympus Optical Co., Tokyo, Japan). A small amount of sample containing crystals was placed on a glass microscope slide and covered gently with a glass cover slip. Digital images of the polarized specimens were captured using Lumenera's Infinity 2 (Lumenera Corp., Nepean, Canada). The crystal pictures were taken at 20X magnification.

Statistical Analysis

Data are reported as mean values and standard deviations of replicated experiments. Two-way ANOVA was used to test significant differences between treatments using a level of significance of 0.05. Statistical analyses were performed using GraphPad Prism (Prism 6.01; GraphPad Software Inc., La Jolla, Calif., U.S.A.).

Results & discussion

Melting Behavior

Figure 7-1 shows the DSC melting profiles of all the binary waxes (2.5% wt. basis) in SBO tested in this study. A single melting peak is observed for all binary waxes tested independently from the type or proportion of wax used. Figure 7-1a shows the melting behavior of SFW/BW binary blend in SBO. It is observed that the melting peak is shifted to higher temperatures as the amount of SFW increases in the wax mixture from 0% to 100%. The first melting curve from the top (Figure 7-1a) shows data for the 0% SFW/BW blend in SBO where no SFW is present in the mixture, while the last melting curve from the top shows data for the 100% SFW/BW blend in SBO.

Figure 7-1b shows the melting profile of RBW/BW blends in SBO. Similar to the SFW/BW blends an increasing trend in melting peak temperatures is observed from 0% to 100% blends with a sharper melting peak observed for the 100% RBW/BW melting curve. In addition, sharper melting peaks are observed as the amount of RBW increases in the blend which can be attributed to the homogeneous chemical composition of the sample. In this case, 100% RBW/BW is composed of only wax esters but 100% SFW/BW is composed of wax esters, hydrocarbons, free fatty acids, and fatty alcohols. The presence of these various molecular entities in the SFW/BW blends results in a broader melting profile compared to the RBW/BW ones. SFW/BW or RBW/BW (0%) or 100% BW also show a wide melting peak (Figure 7-1a and Figure 7-1b) since BW is a

mixture of different molecular entities such as wax ester, hydrocarbons, free fatty acids, di-esters, and hydroxyl esters.

Figure 7-1c shows the melting profile of RBW/SFW blends in SBO. The increasing trend in melting peaks is not quickly noticeable like it was observed in Figure 7-1a and 7-1b. In this case, the melting temperatures of both the waxes (RBW and SFW) are close with melting points of 79.8 ± 0.1 °C and 75.8 ± 0.2 °C for RBW and SFW, respectively. Another difference in the RBW/SFW melting curves is the sharp peak formed in all the concentrations except for the 0% RBW/SFW (or 100% SFW) blend in SBO. Because RBW and SFW have wax esters as the major component (above 50% of the total composition), it is very likely that melting curves in RBW/SFW in SBO system are dominated by the wax esters.

In previous research that evaluated phase behavior of binary waxes in the absence of oil (Jana & Martini, 2016) two melting peaks were observed in 100% BW and only one peak in 100% SFW and 100% RBW. As previously discussed in this study, only one peak is observed in BW when crystallized in SBO.

In addition, even if only a single melting peak is observed in SFW and RBW crystallized in the absence or presence of SBO (Jana & Martini, 2016) the melting peaks observed in the presence of SBO appear at lower temperatures. It is likely that the shift towards lower melting temperatures observed when waxes are crystallized in the presence of oil is due to the dissolution of different molecular entities in the oil.

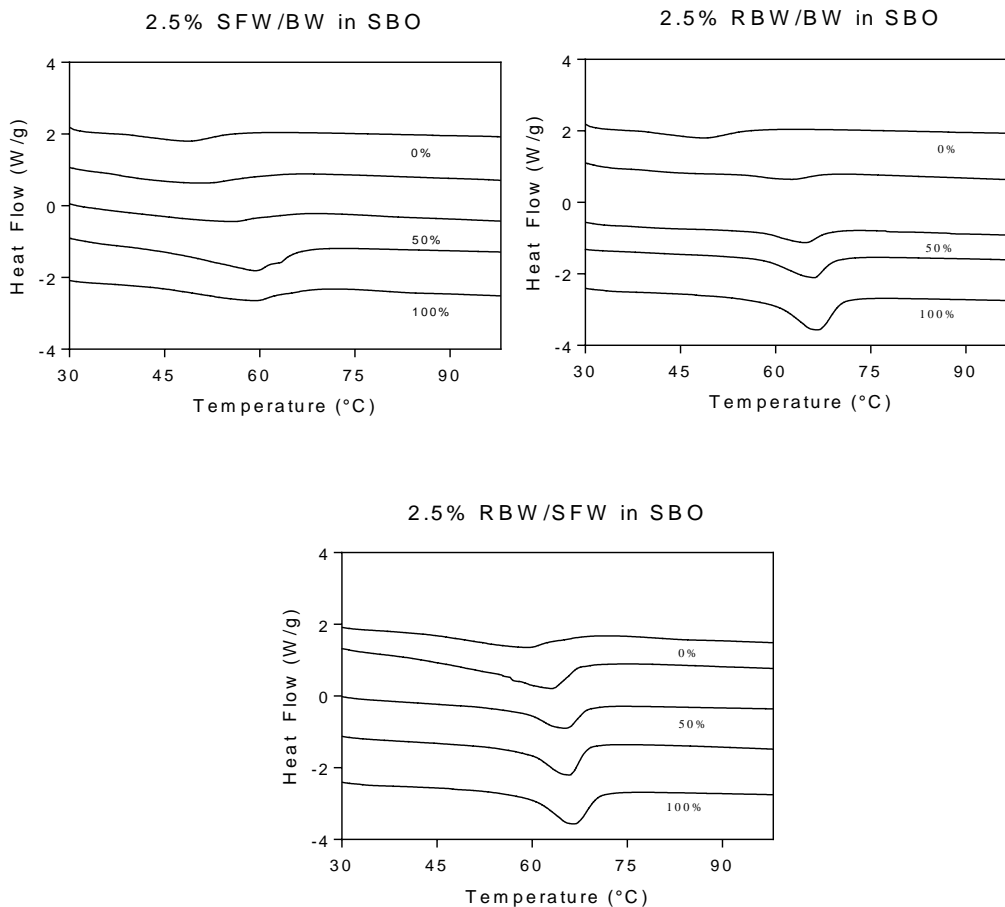


Figure 7-1. DSC melting profile of 2.5% (wt. basis) binary wax in soybean oil (SBO). Binary wax proportions of 0, 20, 50, 80 and 100% are tested. The first melting curve from the top indicates 0% of the first component in the wax mixture and the bottom curve indicates 100% of the first component in the wax mixture. The 3rd line from the top indicates the 50% of the binary wax. Melting profile of SFW/BW, RBW/BW, and RBW/SFW in SBO are shown in A, B, and C respectively.

Similar results regarding the decrease in T_{on} and T_p values with low concentrations of waxes in oil was previously reported (Dassanayake et al., 2009; Martini et al., 2015).

Figure 7-2 shows the comparative data analysis of the melting profile peaks observed in Figure 1. Figure 7-2a shows the melting peak temperatures of all the binary waxes in SBO. The decreasing trend in peak melting temperature from 100% to 0% of all the combinations previously discussed is confirmed by this data analysis. There is a uniform decreasing pattern in SFW/BW blends in SBO. But RBW/BW blend in SBO has a slow decreasing pattern from 100% to 20% and then there is a sharp decline at 0% from 20%. This behavior suggests that the crystallization and therefore the melting behavior of these blends are mainly driven by RBW. RBW/SFW in SBO system follows a similar uniform decreasing trend as SFW/BW; however since RBW and SFW have similar melting points the degree of change is slightly smaller than the one observed for SFW/BW blends.

Figure 7-2b shows the onset temperatures of all the binary waxes in SBO. Onset melting temperature follows similar pattern in all the combinations as peak melting temperature. Figure 7-2c shows a comparative analysis of the enthalpies in all the binary waxes in SBO. The sample composed of 80% SFW/BW blend in SBO shows the highest enthalpy (3.5 ± 0.2 J/g) which decreased significantly ($p < 0.05$) as the content of SFW decreased in the sample. 0% SFW/BW (100% BW) shows the lowest enthalpy of 1.1 ± 0.1 J/g. There is no particular pattern observed in this system. This increase in enthalpy for the 80% SFW/BW blend is unexpected and suggests that the presence of 80% SFW promotes the crystallization in the system. The enthalpies in RBW/BW blend in SBO

shows a rapid decreasing pattern from 100% to 20% and then stay constant even at 0%. No significant difference ($p > 0.05$) is observed in 50, 20, and 0% SFW/BW and RBW/BW in SBO system.

The enthalpy pattern in RBW/SFW blends in SBO smoothly decreases from 100% to 0%. Differences in melting enthalpies observed can be explained by understanding the molecular entities present in each blend. Martini et al. (2015) suggested that enthalpy change in wax/oil system is a function of wax type due to different chemical compositions of the waxes. Majority of wax ester present in SFW and RBW could be a reason of the higher enthalpy values observed in blends containing SFW and RBW compared to enthalpy values obtained for blends with BW which are richer in n-alkanes, free fatty acids, fatty alcohols, and other type of esters.

As the amount of SFW decreases in RBW/SFW mixtures the enthalpy values also decrease. For example, enthalpy values for the 20 and 80% RBW/SFW (80 and 20% of SFW) decreased from 3.8 ± 0.2 to 2.9 ± 0.5 J/g.

In addition, binary wax blends containing BW resulted in lower enthalpy values due to the lower enthalpy associated with this type of wax. It is not clear why enthalpy of 80% SFW/BW is higher. It is likely that in this case, the presence of SFW induces the crystallization of the system resulting in a higher overall enthalpy value. Overall, these results suggest that wax esters in the wax blends are responsible for driving super-saturation of crystals in binary wax/SBO system.

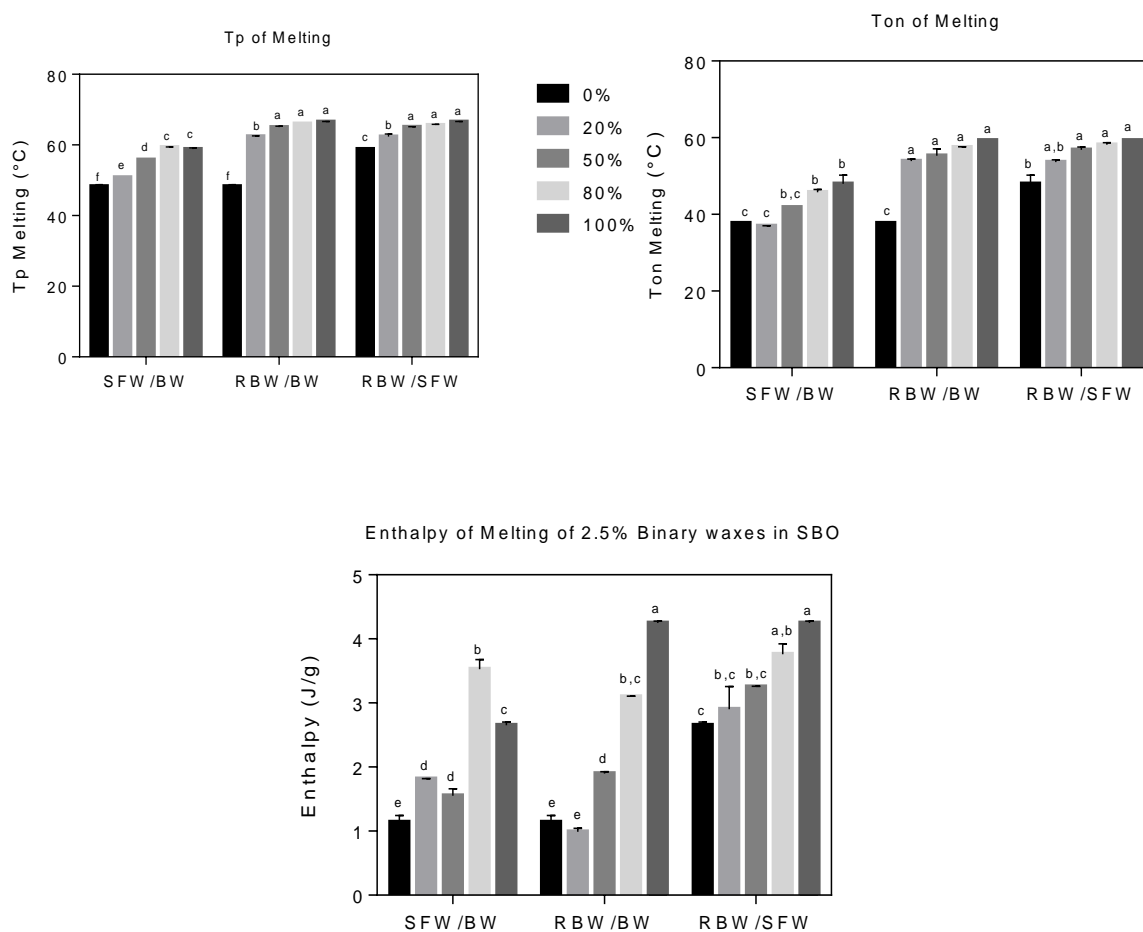


Figure 7-2. Peak melting temperature (T_p), onset melting temperature (T_{on}) and melting enthalpy values are reported in A, B, and C respectively in proportions of 0, 20, 50, 80 and 100%. Columns with same letters indicate that values are not significantly different ($\alpha = 0.05$).

Table 7-1. Melting temperatures (T_p , °C) of binary mixtures used in this study, as reported by Jana and Martini 2016. Two melting values indicate two melting peaks observed.

| Binary Wax Conc. | 0% | 20% | 50% | 80% | 100% |
|---------------------|----------|-----------|----------|-----------|----------|
| SFW/BW | 53.0±0.5 | 52.0±0.6 | 52.1±0.2 | 49.0±0.0 | 75.8±0.2 |
| | 61.2±0.7 | 62.2±0.5 | 60.6±4.0 | 73.2±1.0 | |
| RBW/BW | 53.0±0.5 | 52.1±0.2 | 55.5±0.1 | 53.65±3.4 | 79.8±0.1 |
| | 61.2±0.7 | 60.78±1.0 | 73.8±1.7 | 78.1±0.9 | |
| RBW/SFW | 75.8±0.2 | 75.1±1.3 | 77.0±2.0 | 77.8±2.1 | 79.8±0.1 |

When two components of different chemical composition, and therefore different melting enthalpies, are mixed, one would expect that enthalpy values will change linearly based on the ratio of both components in the blend. This is true if the components are fully miscible and form solid solutions. In order to establish if molecules present in the different waxes are totally miscible or if they partially co-crystallize we decided to compare theoretical and experimental enthalpy values (Figure 7-3). Figure 7-3a shows experimental and theoretical enthalpies in SFW/BW blends in SBO. The linear regression line for experimental enthalpy values in SFW/BW samples (Figure 7-3a) does not follow the theoretical one. In addition, a low R^2 value was obtained ($R^2 = 0.64$) for the

experimental enthalpy regression line. This lack of linearity and the deviation from the theoretical values suggest that SFW and BW are not totally miscible and that only a partial co-crystallization occurs when these two waxes are mixed.

SFW is composed of approximately 70% wax esters and other minor components such as free fatty acids, fatty alcohol and also hydrocarbons (Hwang et al. 2012; Jana & Martini, 2016). These minor components might play an important role in the crystallization behavior of the SFW/BW mixture by promoting intermolecular interactions during crystal formation as evidenced by the broad melting peak observed in Figure 7-1a.

Figure 7-3b and 7-3c show RBW/BW and RBW/SFW enthalpy comparison lines and in both cases linear regression line formed by the experimental data points are parallel to the theoretical data points line. R^2 values are high in both correlations (0.92 and 0.90 in RBW/BW and RBW/SFW, respectively). Although R^2 value is 0.90 in the case of RBW/SFW blend the narrow confidence interval explains how well the experimental data fits the theoretical ones. This suggests that RBW and SFW are fully miscible and behave as solid solutions.

These results corroborate our previous results obtained in binary waxes crystallized without oil (Jana & Martini, 2016). On the contrary, R^2 value of 0.92 for RBW/BW shows a wide confidence interval and the theoretical values fall outside this confidence interval. As previously discussed for the SFW/BW blends these results suggest that

molecular entities present in RBW and BW are not fully miscible and partially co-crystallize affecting each other's crystallization behavior.

Solid Fat Content

Figure 7-4 shows solid fat content (SFC) values as a function of crystallization temperature obtained for the binary wax blends in SBO. The SFC content (%) almost stays constant in all the different concentrations for all combination of waxes in SBO at 10 °C. Figure 7-4a shows the SFC vs. temperature graph of SFW/BW in SBO system. The 0% SFW/BW blend in SBO line decreases sharply from 10 °C to 20 °C and then kept decreasing until 45 °C (% SFC = 0). SFC values as a function of temperature for 100% SFW/BW blend in SBO shows a wider curve, this means that the wax blend remains solid at temperatures as high as 60 °C.

The wider curves become narrower gradually from 100% of the concentration to 0% of the SFW/BW blend. This is expected because SFW in SBO has higher melting temperature and BW in SBO has lower melting temperature. There is a trend observed in SFC content at room temperature (25 °C) that as the amount of SFW is increased, the SFC content increases accordingly.

As SFC content is directly dependent on the amount of crystals formed in the system, the SFC values at room temperature gives an insight to formulate real food products. A similar trend is observed at 35 °C (close to body temperature) indicating wax blends are not fully melted at body temperature and could provide a waxy mouthfeel to the product.

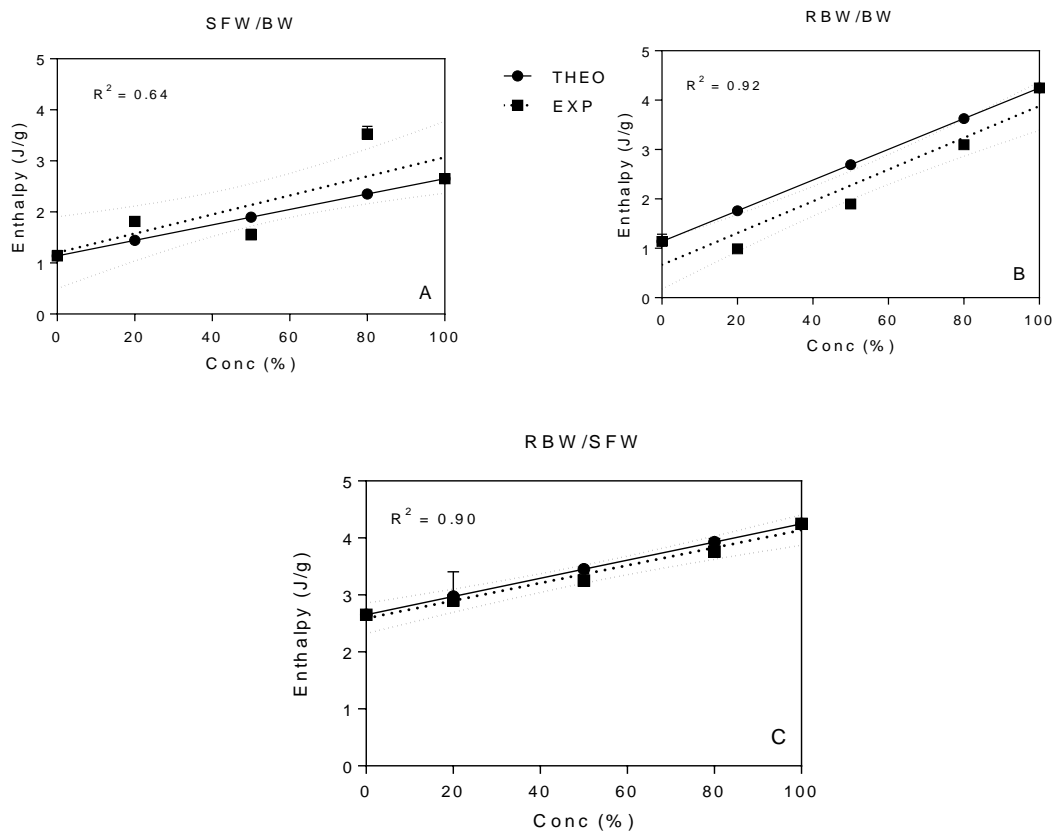


Figure 7-3. Comparison of theoretical (black circle symbol) and experimental (black square symbol) enthalpies for binary wax blends in SBO. The dotted line indicates the linear regression line for experimental enthalpy points. Theoretical and experimental enthalpies of SFW/BW, RBW/BW and RBW/SFW blends in SBO are shown in A, B, and C respectively. Confidence interval (95%) for the experimental data is shown in light dotted hyperbolic lines.

Figure 7-4b shows SFC vs temperature profile for RBW/BW blends in SBO systems. The SFC curve for 100% BW in SBO shows a sharp decline as discussed before but 100% RBW shows a wider curve slightly different than the one observed for SFW with SFC greater than zero for 60 and 65 °C. The difference in SFC content in 100% BW and RBW is by the fact that RBW in SBO has a higher melting temperature than BW in SBO.

The SFC content for 0 and 20% RBW/BW blends at 50 °C is zero but 50, 80 and 100% blends show higher than 0.5% SFC content at that temperature. Similar to the SFW/BW blends, all RBW/BW had SFC > 0 at 35 °C. Figure 7-4c shows SFC vs temperature profile for RBW/SFW blends in SBO systems. There is not significant difference in SFC content at different concentrations. A wider curve is observed in all the RBW/SFW blends compared to the SFW/BW and RBW/BW blends. All the concentration curves stretched flat until 45 °C and then there is a small drop at 50 °C. This indicates that the amount of crystals formed in all the concentrations from 10 °C to 45 °C are close to equal. There is a rapid drop in SFC value (>1.0) for 0 and 20% RBW/SFW between 55 °C and 60 °C. These samples reached SFC values of 0 at 60 °C while the other samples had a SFC of approximately 1 % (Figure 7-4 c).

As previously discussed SFC values at 35 °C for all the blends were not significantly different; however, a significantly lower melting enthalpy ($p < 0.05$) was observed for the 0, 20, and 50% RBW/SFW blends (data not shown). These results suggest that even though a significant amount of wax is still present at body temperature less energy is needed to melt the 0-50% blends and therefore they will melt faster in the mouth.

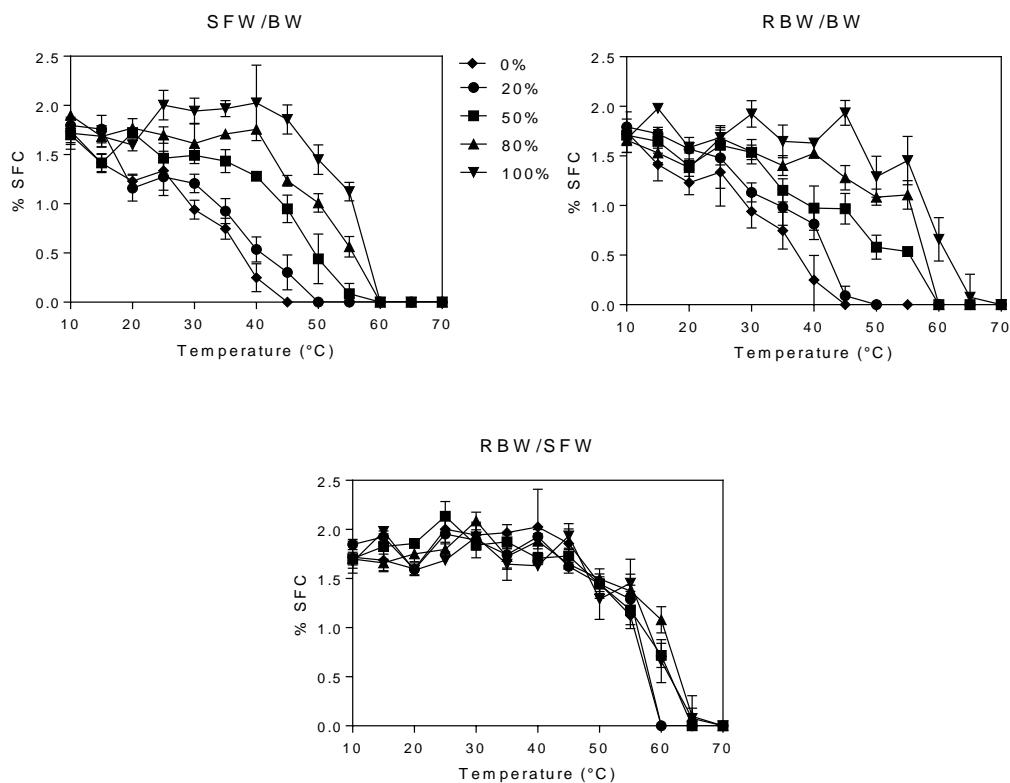


Figure 7-4. Solid Fat Content (SFC) as a function of crystallization temperature for binary wax mixtures in SBO are plotted from temperature-controlled pulse-NMR data. SFC of SFW/BW, RBW/BW, and RBW/SFW blends in SBO are shown in A, B, and C respectively.

Figure 7-5 shows iso-solid diagrams obtained from the SFC data reported in Figure 7-4. These iso-solid diagrams help understand phase behavior of binary mixtures of fats and to evaluate possible softening effects. Iso-solid lines at higher SFC (1.5%) always start from low temperature than other lines in all the binary wax compositions.

RBW/SFW interestingly follows higher temperature (starting at 49 °C for 1.5%) for all the iso-solid lines. This suggests that enthalpies of RBW/SFW blends should be higher than other blends and this pattern is seen in Figure 7-2c. Iso-solid diagrams in Figure 7-5 show a softening effect when SFW and RBW are added to BW. This softening effect is more pronounced at 1.5% SFC and occurs at approximately 50% SFW and 80% RBW addition suggesting a eutectic behavior.

No softening effect was observed for the RBW/SFW blends suggesting that these waxes form solid solutions. These results are in accordance with our previous research on phase transitions of bulk waxes (Jana & Martini, 2016) and suggest that the presence of fatty acids and alcohols in BW help in the co-crystallization of wax esters and alkanes through the formation of hydrogen bonds. This partial co-crystallization is evidenced by a eutectic behavior.

Viscoelastic properties

Viscoelastic properties are affected by the amount of crystalline material and by crystal morphology. Figure 7-6 shows the viscoelastic parameters in all the binary wax in SBO systems at 25 °C. Storage modulus (G') values indicate solid-like behavior of wax/oil system whereas loss modulus (G'') indicates liquid-like behavior.

Figure 7-6a shows G' values of the binary wax in SBO systems at all binary wax proportions. G' value for 100% SFW blend in SBO is significantly higher than 100% BW blend (or 0% SFW/BW in SBO). SFW/BW at 80% blend shows the maximum G' values

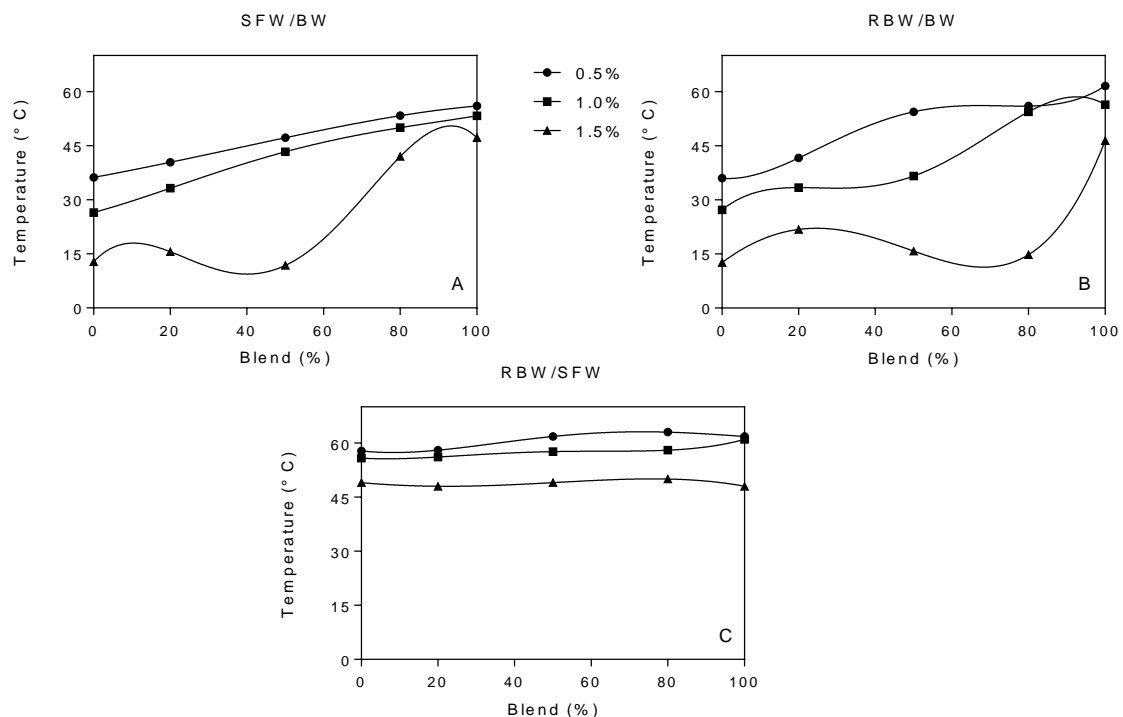


Figure 7-5. Iso-solid lines for the binary mixtures in SBO are drawn using interpolation method from SFC data in Figure 4. Iso-solid lines represent same solid fat content at 0.5, 1, and 1.5%. Iso-solid diagrams of SFW/BW, RBW/BW and RBW/SFW in SBO are shown in A, B, and C respectively.

in the SFW/BW system. This behavior is similar to the one observed for the enthalpy data (Figure 7-2) where 80% SFW/BW composition shows maximum enthalpy. This indicates that 80% composition of SFW/BW in SBO would form the most elastic crystalline network.

As previously discussed it is likely that wax esters present in the 80% SFW/BW mixture are driving the properties of the crystalline network formed. The crystalline

network formed might be richer in wax esters that have a higher enthalpy and that result in a more elastic material while maintaining a constant SFC. SFW/BW of 50% and 20% mixture do not follow significant changes in G' values. All the SFW/BW concentrations pose significantly higher solid-like material than 100% BW (or 0% SFW/BW).

In the RBW/BW system, 100% RBW shows significantly higher G' values than 100% BW. Interestingly, G' values in all the other RBW/BW blends (20, 50 and 80%) are not significantly different. But these values are significantly lower than 100% RBW/BW.

This means that the 100% RBW possess as the most solid-like material than all the other concentrations. These results suggest that RBW is driving the crystallization behavior of RBW/BW blends. 100% RBW and 100% SFW do not show significant difference in G' values but 20%, 50% and 80% of RBW/SFW in SBO system show high G' values than any other concentration mixtures. It is observed that G' values decrease as the amount of RBW increases from 20% to 100% RBW/SFW. Overall, RBW/SFW binary system in SBO shows significantly more solid-like behavior than any other combinations.

Figure 7-6b shows G'' values of the binary wax in SBO systems at all concentrations. It is observed that data presented in Figure 7-6b follows a similar trend to the one presented in Figure 7-6a with lower G'' values observed compared to G' values. This signifies that all the systems analyzed show more solid-like behavior than viscous-like behavior.

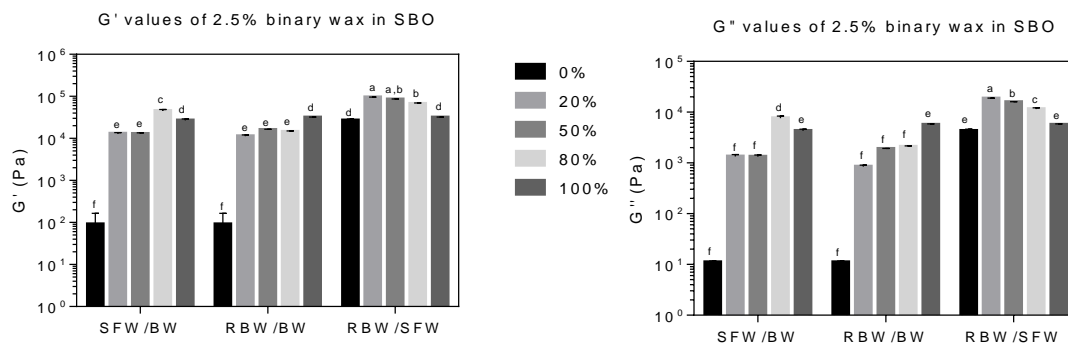


Figure 7-6. Viscoelastic parameters such as storage modulus (G') and loss modulus (G'') measured at 25 °C after 24 h incubation in a water-bath. Y-axis is represented in \log_{10} scale. Columns with same letters indicate that there is no significance difference among others ($\alpha = 0.05$).

Crystal Morphology

Figure 7-7 shows the crystal morphology of 2.5% binary waxes in SBO for all the binary wax blends at 25 °C after 24 h of incubation in a water-bath. All wax mixtures showed needle-shaped crystals. 0% SFW/BW crystals needle-like and seem to be longer than the ones observed in the 20% SFW/BW blends. There is no noticeable difference in the shape of the crystals obtained for the 20% and 80% SFW/BW blends. But crystals of 50% of the SFW/BW blend show a difference in size and arrangement.

Previous research (Jana & Martini, 2016) on SFW/BW crystal morphology at different blend proportions crystallized at 25 °C without oil shows that there are noticeable difference in crystal size, shape and density when compared to the same

blends crystallized in SBO and shown in Figure 7-7. RBW/BW system shows smaller crystals in 50, 80, and 100% RBW/BW blends and crystals observed for the 0% and 20% RBW/BW blends are larger with a less dense crystalline network than the rest of the samples.

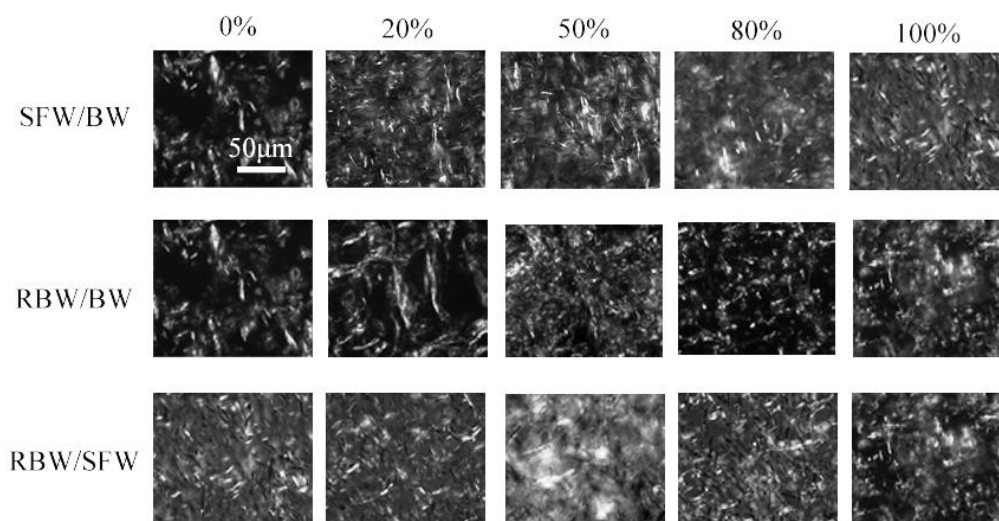


Figure 7-7. Crystal Morphology of 2.5% binary wax in SBO oil at 20X magnification at 25 °C after 24 h of sample incubation in a water-bath. All the binary wax in SBO system crystals are arranged from 0% to 100%. White bar indicates 50 μm .

It is observed that crystal size becomes bigger from 0% to 20% but there is a rapid decrease in crystal size from 20% to 50% of the RBW/BW concentration. Crystal structures in this binary blend too do not show any similarity when compared with the crystals obtained when the bulk blends were crystallized without SBO (Jana & Martini, 2016). 20% of RBW/SFW crystals show similarity in sizes with 0% and 80% of the crystals show same sizes as 100% of RBW/SFW. But crystals in 50% of RBW/SFW are different than all the other crystals where agglomerated structures can be observed (note the large white spots in Figure 7-7). Overall, individual waxes when present in the binary wax blends do not drive any major crystal morphology changes. The ‘white-spots’ observed for the 50% RBW/SFW blend are the indication of densely flocked smaller crystals.

Figure 7-8 shows fractal dimension analysis of the crystal morphology pictures discussed in Figure 7-7. Fractal dimension analysis is performed to quantify the crystal morphology in terms of crystal shape, size, area fraction and the interaction among these three factors. Box counting method is mostly used for lipid fractal dimension and has been previously reported in several studies (Marangoni et al., 2002, Tang et al., 2006a and 2006b). From the multiple comparison analysis done for D_b values from fractal dimension technique, it is observed that there is no significant difference in D_b values among the binary waxes and their different concentrations except for the 50% RBW/SFW. 100% RBW shows no significant difference in D_b values with 50% RBW/SFW. The only significantly higher D_b value observed in 50% RBW/SFW system can be confirmed by the ‘white-spots’ in Figure 7-7. ‘White-spots’ are the indication how

area fraction and size and shape give strongest crystal network. Fractal dimension analysis in Figure 7-7 shows lower values for all the wax blends when compared with the previous research where waxes were crystallized from the melt without SBO (Jana and Martini, 2016).

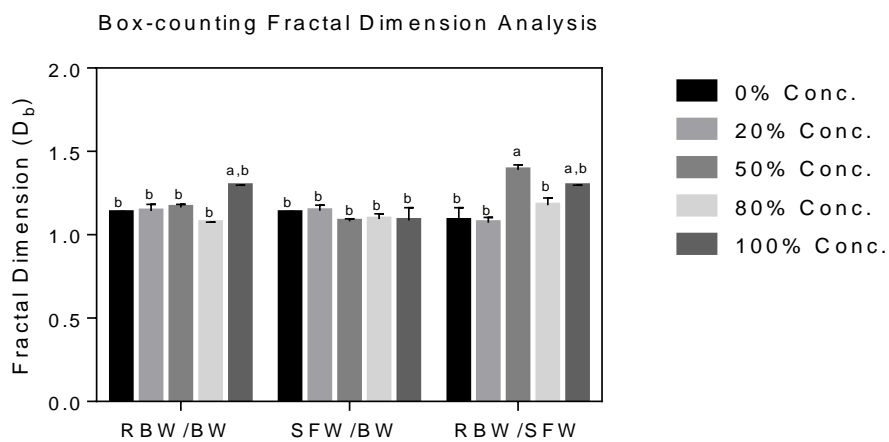


Figure 7-8. Fractal dimension (D_b) of the crystals is analyzed using Box-plot counting technique at different concentrations at 25 °C. Columns with same letters indicate that there is no significance difference among others ($\alpha = 0.05$).

This difference in D_b values is due to the microstructural factors such as crystal size, shape, area fraction and any interaction among these. It likely that wax solubility/supersaturation in the SBO discussed in this study plays an important role in changing crystal morphology compared to waxes crystallized from the melt.

Conclusion

The present study exemplifies how wax chemical composition is responsible for the formation of a crystalline material with particular physical properties. Difference in enthalpy values, solid fat content, and viscoelastic behavior help interpret how different molecular entities in the waxes might affect their crystallization behavior. Our results show that wax esters play a significant role in the crystallization behavior of the binary wax blends. Waxes with similar chemical composition behave as solid solutions while mixtures of waxes with different chemical composition deviate from the ideal behavior. This study shows that blending waxes does not necessarily result in linear changes in physical properties and that inhibition and synergism might occur in the different blends. It is therefore important to characterize these systems to find specific wax combinations that can result in particular physical properties to be used in food applications.

References

1. Dassanayake, L.S.K., Kodali, D.R., Ueno, S., Sato, K. (2009). Physical properties of rice bran wax in bulk and organogels. *Journal of the American Oil Chemists' Society*, 86, 1163–1173.
2. Hwang, H. S., Kim, S., Singh, M., Winkler-Moser, J. K., Liu, S.X. (2012). Organogel formation of soybean oil with waxes. *Journal of the American Oil Chemists' Society*, 89, 639–647.

3. Hwang, H. S., Singh, M., Bakota, E. L., Winkler-Moser, J. K., Kim, S., Liu, S. X. (2013). Margarine from Organogels of plant wax and soybean oil. *Journal of the American Oil Chemists' Society*, 90, 1705–1712.
4. Jana, S., Martini, S. (2014). Effect of High-Intensity Ultrasound and Cooling Rate on the Crystallization Behavior of Beeswax in Edible Oils. *Journal of Agricultural and Food Chemistry*, 62, 10192–10202.
5. Jana, S., Martini, S. (2016). Phase Behavior of Binary Blends of Four Different Waxes. *Journal of the American Oil Chemists' Society*. DOI 10.1007/s11746-016-2789-6.
6. Jang, A., Bae, W., Hwang, H.S., Lee, H.G., Lee, S. (2015). Evaluation of canola oil oleogels with candelilla wax as an alternative to shortening in baked goods. *Food Chemistry*. 187, 525–529.
7. Lupi, F.R., Gabriele, D., Greco, V., Baldino, N., Seta, L., de Cindio, B. (2013). A rheological characterization of an olive oil/fatty alcohols organogel. *Food Research International*, 51, 510–517.
8. Martini, S., Tan, C. Y., Jana, S. (2015). Physical Characterization of Wax/Oil Crystalline Networks. *Journal of Food Science*, 80, 989-997.
9. Martini, S., Carelli, A.A., Lee, J. (2008). Effect of the Addition of Waxes on the Crystallization Behavior of Anhydrous Milk Fat. *J Am Oil Chem. Soc.*,85, 1097–1104.
10. Marangoni, AG. (2002). The nature of fractality in fat crystal networks. *Trends in Food Science & Technology*, 13, 37–47.

11. Patel, A.R., Rajarethinem, P. S., Gredowska, A., Turhan, O., Lesaffer, A., De Vos, W.H., Van de Walle, D., Dewettinck, K. (2014). Edible applications of shellac oleogels: spreads, chocolate paste and cakes. 2014. *Food & Function*, 5, 645–652.
12. Toro-Vazquez, J. F., Morales-Rueda, J. A., Dibildox-Alvarado, E., Charo-Alonso, M., Alonzo-Macias, M., Gonzalez-Chavez, M. M. (2007). Thermal and textural properties of organogels developed by candelilla wax in safflower oil. *Journal of the American Oil Chemists' Society*, 84, 989–1000.
13. Tang, D., Marangoni, AG. (2006a). Microstructure and Fractal Analysis of Fat Crystal Networks. *Journal of the American Oil Chemists' Society*, 83, 377-388.
14. Tang, D., Marangoni, AG. (2006b). Quantitative study on the microstructure of colloidal fat crystal networks and fractal dimensions. *Advances in Colloid and Interface Science*, 128–130, 257–265.
15. Yilmaz, E., Öğütçü, M. (2014). Comparative Analysis of Olive Oil Organogels Containing Beeswax and Sunflower Wax with Breakfast Margarine. *Journal of Food Science*, 79, 1732-1738.
16. Yilmaz, E., Öğütçü, M. (2015). The texture, sensory properties and stability of cookies prepared with wax oleogels. *Food & Function*, 6, 1194-1204.

CHAPTER 8

CONCLUSION

Waxes have been used in various food applications such as food coating, food waxing, gum formulation and gel formation. In addition, waxes have recently been used by food researchers to entrap vegetable oils and create semi-solid materials that can be used as a replacement for partially hydrogenated oil in food products such as margarine, ice-cream and shortening. The physical properties of waxes, including hardness, viscoelasticity, smoothness and encapsulation efficiency, are driven by the molecular composition and molecular interactions that occur during crystallization. A thorough literature review suggests that the rheological and thermal properties of oleogels are driven by the crystallization behavior of the wax, which in turn is affected by the molecular composition of the wax, the type of oil phase used and processing conditions such as shear, temperature and cooling rate.

Overall, the first objective of this study shows that several processing conditions can affect phase separation in wax/oil systems. Cooling rate, wax concentration and type of oil play important roles in the crystallization behavior of waxes, behavior that can also be controlled by using HIU. Higher wax concentration (1% > 0.5%) resulted in faster crystallization (10 °C/min) and more turbidity. When HIU was used in 0.5% BW in SBO, the crystals in the system were fragmented and more and smaller crystals were generated. In this way, a stronger crystalline network was formed, resulting in a less free-flowing oil solution. After analyzing the fatty acid compositions of the oil (Appendix Table 1), there was a trend observed with regard to the stability towards phase separation: soybean oil <

olive oil < sunflower oil < canola oil < safflower oil < corn oil. It was understood that (a) for the same type and amount of wax, the type of oil used affects the degree of phase separation and (b) HIU can help in the delay of phase separation to different degrees, depending on the type of oil used. However, it is not clear how the type of oil affects BW crystallization. The effect of HIU in reducing crystal size in the 1% BW solutions was not as evident as the observed results in the 0.5% BW solutions. The use of HIU resulted in a narrower melting profile, as evidenced by either higher T_{on} values or lower T_p values in the sonicated samples. It is likely that the effect of HIU on delaying phase separation is related to the generation of a less fractionated crystalline network where similar molecules can interact strongly among them, entrapping more oil. HIU can be used to delay phase separation in wax/oil systems that have the potential to be used as *trans*-fat replacements in food products.

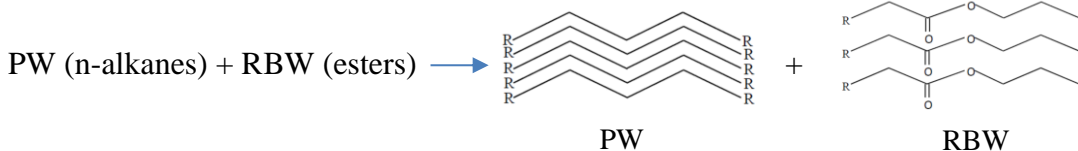
The second objective of this research is to test crystallization behavior of different waxes in different oils at concentrations relevant for food applications (1, 2.5, 5, and 10%). Wax/oil systems formulated with SFOW generated crystalline networks with high G' values (2 to 6×10^6 Pa) compared with the values obtained for BW and PW. BW samples resulted in significantly higher ($P < 0.05$) G' values in the 5% and 10% samples with values of 3.9×10^6 and 6.1×10^5 Pa for 10% BW and PW respectively. In general, the crystallization behavior of lipids and the type of microstructure generated affects the viscoelastic properties of the crystalline network formed (e.g. smaller crystals lead to higher viscosity and vice-versa). It is therefore helpful to understand how waxes and oils

of different chemical compositions exhibit storage modulus (G') at various levels of wax concentration.

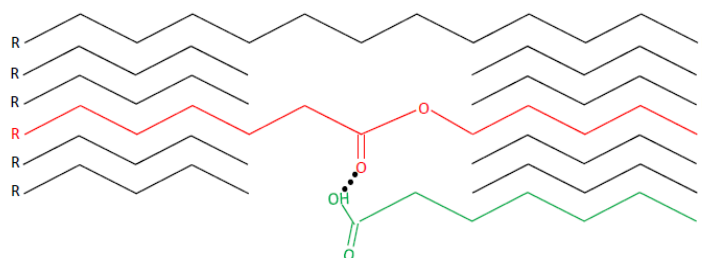
The third objective of this research helps understand the pseudo-phase diagram of binary wax blends and the crystallization behavior of the different molecular entities present in each wax. Pseudo-phase diagrams have become an important tool in the confectionery industry for identifying fats that are compatible with cocoa butter and that will not form eutectics [19, 27]. Changes in the phase behavior and microstructure of these binary wax systems have a direct impact on the functional and physical properties of these systems. Waxes with similar chemical composition can co-crystallize, forming ideal solid solutions (RBW/SFW), while waxes with significantly different chemical composition can show either eutectic or monotectic behavior (RBW/PW) [RBW = 100% wax ester, SFW = 66% wax ester, PW = 100% hydrocarbon]. These differences in phase behavior are reflected in the morphology of the crystals formed. There is still no clear understanding regarding how varying molecules found in natural waxes interact when super-cooled to form a crystal. It is understood from the morphology and pseudo-phase diagrams of binary wax crystals that wax molecular components (alkanes, esters, fatty acids and alcohols), molecular weights (MW), and mole fractions play an important role in wax crystallization. Based on the results obtained in this objective we propose the following crystallization behavior of the wax blends studied.

It is hypothesized that there would be no co-crystallization if alkanes and esters were mixed together (diagram below). Based on that statement, it can also be assumed

that a PW and RBW blend will not show any co-crystallization, a fact also evidenced by our DSC melting profile study.



On the other hand, BW is composed of wax esters (red), fatty acids (green) and n-alkanes (black), and when mixed with PW, there is observed co-crystallization of the molecular entities in the form of hydrogen bond formation (black dots). The figure below is a representation of how we believe wax blend co-crystallization happens at the molecular level.



PW (n-alkanes) + BW (esters, fatty acids, n-alkanes)

The fourth objective of this research is involved with binary wax crystallization in oil and analyzing the physical characteristics of differing oleogel formations. The present study demonstrates how wax chemical composition is responsible for the formation of a crystalline material with particular physical properties. Our results show that wax esters play a significant role in the crystallization behavior of binary wax blends. Waxes with similar chemical composition behave as solid solutions, while mixtures of waxes with differing chemical composition deviate from the ideal behavior. This study shows that

blending waxes could be an appropriate technique to optimize physical properties of wax/oil systems for specific applications.

In summary, the research leading to this dissertation has attempted to prove how molecular entities present in waxes, the types of oil used and processing conditions affect wax crystallization and the physical properties of the materials obtained therefrom. Based on our study, RBW has higher potential to be used as trans-fat replacer in soybean oil at a lowest concentration (as low as 0.5%). The results of this dissertation will shed light on how co-crystallization occurs among varying molecular entities in waxes, and how physical properties of oleogels are driven by the crystallization behavior of the wax, behavior which is, in turn, affected by the molecular composition of the wax, the type of oil phase used and processing conditions such as shear, temperature and cooling rate. Still, further research is needed to analyze why alkanes always form pure crystals when crystallized with esters, in what ways molecular weight and degree of unsaturation affect the type of crystal lattice formed, and how the chemical nature of fatty acids and alcohols affects the molecular interactions that occur upon crystallization. Within the wax/oil system, effects of the minor components in waxes and oils on the crystallization behavior of the system should also be studied further. Differing wax solubility in various oils is another area that should be explored. It is still not clear how the different types of oils and waxes affect the crystallization of the system. Finally, mathematical modeling/simulation is needed to properly analyze 3D structures of the molecular arrangement and how they behave when various co-crystallizations happens.

APPENDICES

Appendix B

Copyright Permissions for Published Papers

RightsLink



Thank You For Your Order!

Dear Mr. SARBOJEET JANA,

Thank you for placing your order through Copyright Clearance Center's RightsLink service. Springer has partnered with RightsLink to license its content. This notice is a confirmation that your order was successful.

Your order details and publisher terms and conditions are available by clicking the link below:
<http://s100.copyright.com/CustomerAdmin/PLF.jsp?ref=3200a5f3-2db3-4269-8e79-0453ac826a2e>

Order Details

Licensee: SARBOJEET JANA
License Date: Mar 9, 2016
License Number: 3824981256921
Publication: Journal of the American Oil Chemists' Society
Title: Phase Behavior of Binary Blends of Four Different Waxes
Type Of Use: Thesis/Dissertation
Total: 0.00 USD

To access your account, please visit <https://myaccount.copyright.com>.

Please note: Online payments are charged immediately after order confirmation; invoices are issued daily and are payable immediately upon receipt.

To ensure that we are continuously improving our services, please take a moment to complete our [customer satisfaction survey](#).

B.1:v4.2

+1-855-239-3415 / Tel: +1-978-646-2777
customercare@copyright.com
<http://www.copyright.com>



 **Copyright Clearance Center** **RightsLink®** [Home](#) [Account Info](#) [Help](#)  **Live Chat**

 **ACS Publications** Most Trusted Most Cited Most Read **Title:** Effect of High-Intensity Ultrasound and Cooling Rate on the Crystallization Behavior of Beeswax in Edible Oils

Author: Sarbojeet Jana, Silvana Martini

Publication: Journal of Agricultural and Food Chemistry

Publisher: American Chemical Society

Date: Oct 1, 2014

Copyright © 2014, American Chemical Society

Logged in as: SARBOJEET JANA
[LOGOUT](#)

PERMISSION/LICENSE IS GRANTED FOR YOUR ORDER AT NO CHARGE

This type of permission/license, instead of the standard Terms & Conditions, is sent to you because no fee is being charged for your order. Please note the following:

- Permission is granted for your request in both print and electronic formats, and translations.
- If figures and/or tables were requested, they may be adapted or used in part.
- Please print this page for your records and send a copy of it to your publisher/graduate school.
- Appropriate credit for the requested material should be given as follows: "Reprinted (adapted) with permission from (COMPLETE REFERENCE CITATION). Copyright (YEAR) American Chemical Society." Insert appropriate information in place of the capitalized words.
- One-time permission is granted only for the use specified in your request. No additional uses are granted (such as derivative works or other editions). For any other uses, please submit a new request.

[BACK](#) [CLOSE WINDOW](#)

Copyright © 2016 [Copyright Clearance Center, Inc.](#) All Rights Reserved. [Privacy statement](#) [Terms and Conditions](#) [Comments?](#) We would like to hear from you. E-mail us at customerscare@copyright.com

CURRICULUM VITAE

Sarbojeet Jana

Sarbojeet.jana@aggiemail.usu.edu**Education**

PhD: Food Science

2012-2016

Utah State University, Logan, UT, USA.

Undergraduate: Agricultural Engineering

2008 – 2012

Tamil Nadu Agricultural University, Coimbatore, India.

OGPA: 8.22/10.00

Experience

- 2012-2015 Graduate Research Assistant, Martini Lab, Department of Nutrition, Dietetics, and Food Sciences, Utah State University.
- 2015-2016 NDFS Food Science Fundraiser.
- 2015 Summer Internship, West Liberty Foods, Tremonton, Utah.
- 2012 Training Program, National Institute of Food Technology Entrepreneurship and Management, Government of India, Sonapat, Haryana, India
- 2011 Training Program, Southern Region Farm Machinery Testing & Training Institute, Government of India, Anantapur, Andhra Pradesh, India.
- 2011 Training Program, Jain Irrigation Systems Ltd. at Jalgaon, Maharashtra, India.
- 2011 Training Program, Indian Institute of Crop Processing Technology (IICPT), Thanjavur, India.
- 2010 Training Program, Central Food Technological Research Institute (CFTRI), Mysore, India.

Honors and Awards

- Gandhi Assistantship, College of Agriculture, Utah State University, 2015-2016
- STEM Fellowship, School of Graduate Studies, Utah State University, 2014-2015
- AOCS 2016 (Salt Lake City, Utah, USA) Travel Award, College of Agriculture & School of Graduate Studies, Utah State University, 2015.
- AOCS 2015 (Orlando, Florida, USA) Travel Award, College of Agriculture & School of Graduate Studies, Utah State University, 2015.
- 2nd Food Structure and Functionality Forum Symposium, (Amsterdam, the Netherlands) Travel Award, School of Graduate Studies, Utah State University, 2014

- AOCS 2014 (San Antonio, Texas, USA) Travel Award, College of Agriculture, Utah State University, 2014.
- Indian Council of Agricultural Research Undergraduate Scholarship, Indian Council of Agricultural Research, 2008-2012

Certification

- HACCP (Hazard Analysis & Critical Control Points), International HACCP Alliance.
- HACCP and GMP in Food Industries and ISO Certification, Indian Institute of Crop Processing Technology, Ministry of Food Processing Industries, Govt. of India.
- Laboratory Quality Management System as per ISO/IEC 17025:2005, Quality Council of India.

Memberships

- AOCS (American Oil Chemists' Society), USA
- IFT (Institute of Food Technologists), USA
- ASABE (American Society of Agricultural and Biological Engineers), USA
- AFSTi (Association of Food scientists and Technologists), India
- ISAE (Indian Society of Agricultural Engineers), India
- IDA (Indian Dairy Association), India
- ISHA (Indian Society of Hill Agriculture), India
- MASU (Madras Agricultural Students' Union), India

Publications

- Jana, S.; Martini, S. (2016). Physical Characterization of Crystalline Networks Formed by Binary Blends of Waxes in Soybean Oil. *Food Research International*. (Submitted)
- Jana, S.; Martini, S. (2016). Phase Behavior of Binary Blends of Four Different Waxes. *Journal of the American Oil Chemists' Society*, Volume 93, Issue 4, pp 543–554.
- Jana, S.; Martini, S. (2014). Effect of High-Intensity Ultrasound and Cooling Rate on the Crystallization Behavior of Beeswax in Edible Oils. *J. Agric. Food Chem.*, 62 (41), pp 10192–10202.
- Martini, S.; Tan, C.Y.; Jana, S. (2015). Physical Characterization of Wax/Oil Crystalline Networks. *Journal of Food Science*, Volume 80, Issue 5, pp C989–C997.